

Height variables in the Abelian sandpile model: scaling fields and correlations

Monwhea Jeng,^{1,2} Geoffroy Piroux,³ and Philippe Ruelle³

¹*Department of Physics, Southern Illinois University Edwardsville, Edwardsville, IL 62025*

²*Department of Physics, Syracuse University, Syracuse, NY 13244*

³*Institut de Physique Théorique, Université catholique de Louvain, B-1348 Louvain-La-Neuve, Belgium*

We compute the lattice 1-site probabilities, on the upper half-plane, of the four height variables in the two-dimensional Abelian sandpile model. We find their exact scaling form when the insertion point is far from the boundary, and when the boundary is either open or closed. Comparing with the predictions of a logarithmic conformal theory with central charge $c = -2$, we find a full compatibility with the following field assignments: the heights 2, 3 and 4 behave like (an unusual realization of) the logarithmic partner of a primary field with scaling dimension 2, the primary field itself being associated with the height 1 variable. Finite size corrections are also computed and successfully compared with numerical simulations. Relying on these field assignments, we formulate a conjecture for the scaling form of the lattice 2-point correlations of the height variables on the plane, which remain as yet unknown. The way conformal invariance is realized in this system points to a local field theory with $c = -2$ which is different from the triplet theory.

PACS numbers: 05.65.+b,45.70.-n

I. INTRODUCTION

Sandpile models are open dynamical systems which generically show a very rich spectrum of critical behaviours, both spatially and temporally. Along with many other models, they are complex critical models. Because of their non-linear dynamics and their non-local features, a fixed external driving can trigger events whose scales follow critical distributions. The references [1, 2, 3] review the ideas and models involved.

One of the simplest and yet most challenging models is the two-dimensional model originally proposed by Bak, Tang and Wiesenfeld [4], now referred to as the BTW model, or the unoriented Abelian sandpile model (ASM) after it was shown by Dhar to possess an Abelian group [5]. It is this model we consider in this article.

The most natural formulation of the ASM is in terms of discrete height variables, taking the four integral values 1 to 4 and located at the sites of a grid. The configuration of the sandpile,

formed by the values of the heights, evolves under a stochastic dynamics, which eventually reaches a stationary regime, where the configurations are weighted according to an invariant measure. Numerical simulations showed that this model has critical properties [4].

The first analytic treatment of the ASM was carried out by Dhar [5], where general and important features of the ASM dynamics were obtained. That work paved the way for numerous exact results. Among these, one can mention the results on correlations of height 1 variables and related clusters (the so-called weakly allowed sub-configurations) [6, 7, 8, 9], on 1-site probabilities of height variables on the whole plane [10], on boundary correlations of height variables [11, 12, 13], on avalanche distributions [14, 15, 16, 17, 18], on specific effects of boundary conditions [19, 20, 21], on finite size corrections [19, 22], and on the insertion of dissipation [8, 12, 20, 21]. Moreover, a number of these references analyze their results in the light of a possible conformal field description. All available results are compatible with such a description, and point to a specific logarithmic conformal field theory, having central charge $c = -2$.

Quite recently, the 1-site probability for the height 2 variable on the upper half-plane, in fact a disguised 2-point correlator, has been computed exactly in the scaling limit, the results having been reported in [23]. It was proved, as had been suspected before, that the height 2 variable behaves logarithmically, unlike the height 1: the height 2 correlations contain logarithms, while those for the height 1 variables are rational functions of the distances. Moreover, numerical simulations suggested that the height 3 and 4 variables have the same behaviour and scale in the same way as the height 2. Finally, the logarithmic conformal field to which these variables converge in the scaling limit was identified, and then used to make predictions for the 2-site bulk correlations of height variables, which, to this date, have not been computed on the lattice (except for height 1). In the logarithmic conformal field theory terminology, the scaling limit of the height 2 (and 3 and 4) is a logarithmic field, which is the partner of the field to which the height 1 scales.

Our purpose in this article is two-fold. First, we want to give the details of the analysis reported in [23]. It involves a lattice part, where the probability of interest is computed in the ASM, and a conformal theory part, where the relevant 4-point correlation function with the intended scaling field is calculated and then compared with the lattice results (and simulations). The details on both, too long and therefore omitted in [23], will be given here. Second, we have extended the analysis to include the height 3 and 4 variables. Our new exact results confirm the behaviour conjectured in [23]. Since the height 3 and 4 variables each scale like linear combinations of the height 1 and 2 variables, any multisite height probability can be reduced, in the scaling limit, to multisite probabilities involving heights 1 and 2 only. These results should close the long chapter

devoted to the height probabilities in the ASM and their description by a field theory¹.

That the critical properties of the ASM can indeed be described by a conformal field theory remains for us a major motivation, for two reasons. First, the description by an underlying conformal field theory can be considered as an actual and explicit solution of the lattice model. Second, the ASM would provide the first instance where the correspondence between a logarithmic conformal field theory and a lattice realization is most clearly exposed. We believe that such a correspondence, so common for usual equilibrium lattice models, should inevitably clarify tricky issues on both sides.

The article is organized as follows. In Section II, we define the sandpile model we consider, review its basic features and recall the elements which prove useful for what follows.

In Sections III and IV, we review the graph theoretic tools used for the derivation of the 1-site height probabilities on the plane, in a way that allows the formalism to be applied to the upper half-plane (UHP). The calculation presented in Section III for the height 2 is identical to that of Priezzhev [10], but our derivation for the height 3 in Section IV is different. The method we use leads to the same results as Priezzhev's but has an interesting corollary, since it leads to an exact relation between the probabilities P_2 and P_3 , a relation unnoticed so far. Moreover, based on very strong numerical evidence, we conjecture exact and simple formulas for P_2 and P_3 , similar to that for P_1 , namely, simple polynomials in $\frac{1}{\pi}$. Although we could not provide a proof for them, we have checked that these formulas are accurate to one part in 10^{12} .

Section V applies the formalism developed in the previous two sections to the upper half-plane, with two homogeneous boundary conditions on the real axis: open and closed. The resulting formulas are then collected in Section VI: the four probabilities $P_2^{\text{cl}}(m)$, $P_3^{\text{cl}}(m)$, $P_2^{\text{op}}(m)$ and $P_3^{\text{op}}(m)$, where m is the distance of the reference site to the boundary, are explicit but complicated expressions, involving multiple integrals and summations.

In Section VII, we proceed to the asymptotic analysis of the integral expressions just derived. These expressions have expansions in inverse powers of m , with coefficients which are polynomials in $\log m$. Anticipating that the scaling fields corresponding to the height variables have dimension 2, we restrict the analysis to the terms of order 2 in m^{-1} . The dominant terms in the probabilities are of order m^{-2} , as expected, and are computed exactly. The final results are summarized in Section VIII. The reader interested in the results, but not in the technical details of the calculations, can

¹ With the usual reservations: we have identified the fields describing the height variables provided that indeed such an identification exists at all, i.e. is compatible with every single lattice joint probability.

safely go straight to Section VIII.

Section IX starts the conformal field theoretic side of our work. In order to assess the effect of a change of boundary condition on the 1-site probabilities, we first compute the correlation function $\langle \mu(z_1)\mu(z_2)\psi(z, \bar{z}) \rangle$ on the UHP, where the μ fields change the boundary condition at two points z_1 and z_2 on the real axis, and where the non-chiral field $\psi(z, \bar{z})$ is supposed to describe the scaling limit of the height variables (2, 3, or 4). The above 3-point field correlator enables us to relate to each other the two UHP 1-point functions $\langle \psi \rangle$ in front of a boundary which is either fully open or fully closed. When ψ is taken to be the logarithmic partner of a dimension 2 primary field ϕ , this relation exactly reproduces the way the probabilities $P_i^{\text{op}}(m)$ and $P_i^{\text{cl}}(m)$ are related on the lattice.

The identification with ψ is further confirmed in Section X, where the finite size corrections predicted by the conformal theory are compared to the results of numerical simulations of the lattice model, showing an excellent agreement.

Section XI reconsiders the field correlation functions established before from a purely conformal field theory point of view. The local logarithmic conformal theory with $c = -2$, believed to be relevant here, has a well-known realization in terms of free symplectic fermions $\theta, \tilde{\theta}$ [24, 25, 26]. The primary field ϕ describing the height 1 variable in the ASM has been well studied and is known to be expressible as a local field in the $\theta, \tilde{\theta}$ theory. We show that the field ψ , corresponding to the heights 2, 3 and 4, has no local realization in the $\theta, \tilde{\theta}$ theory. It follows that the well-studied triplet theory with $c = -2$ [25] is not the appropriate logarithmic conformal field theory to describe the sandpile model.

Finally, relying on the field identifications obtained before, we discuss in Section XII the height joint probabilities on the plane, and formulate conjectures for the 2-site lattice probabilities on the plane, unknown so far. These conjectures compare well with the results obtained from simulations.

II. THE ABELIAN SANDPILE MODEL

We consider a finite, two-dimensional grid \mathcal{L} and attach to each site i a random variable h_i , representing the height of sand at that site and taking integer values 1, 2, 3, ... A configuration \mathcal{C} of the sandpile is the set of values $\{h_i\}$ for all sites. The probability distribution over the height variables or equivalently, over the configurations, evolves dynamically from some initial distribution $P_0(\mathcal{C})$.

The discrete dynamics, itself stochastic, is completely defined in terms of a toppling matrix Δ . This matrix has integral entries, strictly positive on the diagonal, negative or zero off the diagonal,

and moreover satisfies the condition that its row sums $\sum_j \Delta_{ij}$ are non-negative. A configuration is called stable if its height values satisfy $h_i \leq \Delta_{ii}$ for all i .

At time t , the dynamics takes the stable configuration \mathcal{C}_t into a new stable configuration \mathcal{C}_{t+1} as follows. To the configuration \mathcal{C}_t , we first add a grain of sand at a random site i by setting $h_i \rightarrow h_i + 1$ (we assume that the site i is chosen randomly with a uniform distribution on \mathcal{L}). This new configuration, if stable, defines \mathcal{C}_{t+1} . If it is not stable, the site i which has been seeded has now a height $h_i = \Delta_{ii} + 1 > \Delta_{ii}$, and, as consequence, topples: it loses Δ_{ii} grains of sand, the other sites j each receive $-\Delta_{ij}$ grains, and $\sum_j \Delta_{ij}$ grains are dissipated. In other words, when the site i topples, the heights change according to

$$h_j \rightarrow h_j - \Delta_{ij}, \quad \forall j \in \mathcal{L}. \quad (2.1)$$

After the site i has toppled, other sites can be unstable (have heights $h_j > \Delta_{jj}$), in which case they too topple according to the same toppling rule (2.1). Once all unstable sites have been toppled, one is left with a stable configuration, \mathcal{C}_{t+1} . One can show [5] that provided there are dissipative sites in \mathcal{L} (namely, sites k for which $\sum_j \Delta_{kj} > 0$), this dynamics is well-defined: the order in which the unstable sites are toppled does not matter, and the new stable configuration \mathcal{C}_{t+1} is reached after a finite number of topplings.

In the usual BTW model, which we consider here, the grid \mathcal{L} is a rectangular portion of the discrete plane \mathbb{Z}^2 , and Δ is the discrete Laplacian on \mathcal{L} with appropriate boundary conditions on $\partial\mathcal{L}$. Each boundary site k can be either open or closed, depending on whether it is dissipative or not. Explicitly, we take the toppling matrix to be

$$\Delta_{ij} = \begin{cases} z_i & \text{if } i = j \text{ is either a bulk site or a closed boundary site,} \\ 4 & \text{if } i = j \text{ is an open boundary site,} \\ -1 & \text{if } i, j \text{ are nearest neighbours,} \\ 0 & \text{otherwise,} \end{cases} \quad (2.2)$$

where z_i is the coordination number of i in \mathcal{L} , equal to 4 for a bulk site, to 3 for a boundary site and to 2 for a corner site. The toppling rule (2.1) then says that when a bulk or a closed boundary site topples, the sand grains it loses are all transferred to the nearest neighbours, and when an open boundary site topples, it loses 4 grains of sand, z_i of them going to the nearest neighbours, and the others falling off the sandpile. In the latter case, it is convenient to think of the sand grains falling off the pile as being transferred to a sink site, connected to all dissipative sites. Bulk and closed boundary sites are conservative ($\sum_j \Delta_{kj} = 0$), while open boundary sites are dissipative ($\sum_j \Delta_{kj} > 0$).

Because it involves adding a sand grain at a random site, the dynamics is stochastic and can be written in terms of a probability transition matrix p . The matrix p gives rise to a master equation, $P_{t+1}(\mathcal{C}) = \sum_{\mathcal{C}'} p_{\mathcal{C},\mathcal{C}'} P_t(\mathcal{C}')$, which specifies the time evolution of the probability measure on the configurations.

The long-time behaviour of the sandpile is described by the time-invariant probability measures. For the BTW model as defined above, Dhar has shown that there is a unique time-invariant measure $P_{\mathcal{L}}^*$ [5]. This measure assigns all stable configurations their probability of occurrence, when the dynamics has been applied for a sufficiently long time so that the system has set in the stationary regime. The thermodynamic limit of $P_{\mathcal{L}}^*$ is what we want to compare with a conformal field theoretic measure.

The number of stable configurations is $\prod_i \Delta_{ii}$, but only a small fraction of them keep reappearing under the dynamical evolution. The transient configurations are not in the repeated image of the dynamics, and occur only a finite number of times. As a consequence, they all have a zero measure with respect to $P_{\mathcal{L}}^*$. A simple example of a transient configuration is $h_i = 1$ for all i . The non-transient configurations are called recurrent and asymptotically occur with a non-zero probability.

For the BTW model, the recurrent configurations all occur with equal probability under the dynamics [5]. The invariant measure $P_{\mathcal{L}}^*$ is thus a simple uniform distribution, but its support, the set of all recurrent configurations, is not simple, which explains why exact calculations in the ASM are notoriously difficult. On general grounds, it can be shown that the number of recurrent configurations is equal to $\mathcal{N} = \det \Delta$ [5]. For the particular model discussed here, this number is roughly equal to $3.21^{|\mathcal{L}|}$ (up to surface terms), an exponentially small fraction of the $4^{|\mathcal{L}|}$ stable configurations.

Transient and recurrent configurations can be distinguished by a criterion based on forbidden sub-configurations (FSC's): a subset of sites $\mathcal{K} \subset \mathcal{L}$ is said to form a forbidden sub-configuration if $h_i \leq -\sum_{j \in \mathcal{K} \setminus \{i\}} \Delta_{ji} = \#\{\text{neighbours of } i \text{ in } \mathcal{K}\}$, for all sites i of \mathcal{K} . For instance, two neighbour sites with height 1 form an FSC. Then a configuration is recurrent if and only if it contains no FSC [22].

A practical way to test whether a configuration is recurrent or transient is to use the burning algorithm [5]. At time 0, the sink site is the only site to be burnt: we define $\mathcal{K}_0 = \mathcal{L}$ to be the set of unburnt sites at time 0. The sites i of \mathcal{K}_0 such that $h_i > -\sum_{j \in \mathcal{K}_0 \setminus \{i\}} \Delta_{ji} = \#\{\text{neighbours of } i \text{ in } \mathcal{K}_0\}$ are burnable at time 1 (they can only be dissipative sites, namely, open boundary sites). So we burn them, obtaining a set $\mathcal{K}_1 \subseteq \mathcal{K}_0$ of unburnt sites at time 1. Then the sites of \mathcal{K}_1 which are burnable at time 2, *i.e.* those satisfying $h_i > -\sum_{j \in \mathcal{K}_1 \setminus \{i\}} \Delta_{ji} = \#\{\text{neighbours of } i \text{ in } \mathcal{K}_1\}$, are

burnt. This leaves a set $\mathcal{K}_2 \subseteq \mathcal{K}_1$ of unburnt sites at time 2. This burning process is carried on until no more sites are burnable, which means that $\mathcal{K}_{T+1} = \mathcal{K}_T$ for a certain T . Then the configuration is recurrent if and only if all sites of \mathcal{L} have been burnt ($\mathcal{K}_T = \emptyset$). Otherwise \mathcal{K}_T is an FSC, and the configuration is transient.

The burning algorithm allows the definition of a unique rooted spanning tree on a graph \mathcal{L}^* , from the path followed by the fire in the lattice [22]. The graph \mathcal{L}^* has the sites of \mathcal{L} and the sink as vertices, and has links defined by Δ : an off-diagonal entry $\Delta_{ij} = -n$ means there are n bonds connecting the sites i and j , and each site i is connected to the sink by a number of bonds equal to $\sum_{j \in \mathcal{L}} \Delta_{ij} \geq 0$, namely the number of grains dissipated when i topples. At time 0, the sink is the only burnt site and forms the root of the tree. In the next steps, the fire propagates from the sink to those sites which are burnable at time 1, then from the sites which have been burnt at time 1 to those which are burnable at time 2, and so on. If a site burns at time t , it catches fire from one among its neighbours that were burnt at time $t - 1$ (or from the sink site at time 1). In case there are more than one of these, a fixed ordering prescription is used to decide along which bond the fire actually propagates [22]. The collection of all bonds forming the fire path defines a spanning tree, rooted in the sink, and growing towards the interior of the lattice \mathcal{L} . Conversely, to every spanning tree—from Kirchoff's theorem, their number also equals $\mathcal{N} = \det \Delta$ —one can associate a unique recurrent configuration if the ordering prescription mentioned above is known.

Since there is a one-to-one mapping between the recurrent configurations and the spanning trees, the latter provide alternative variables for the description of the ASM. So we trade the random height variables for random spanning trees, on which the invariant measure $P_{\mathcal{L}}^*$ is uniform. Although the local height variables look more natural, they are strongly correlated over the whole lattice, since their values have to make up a recurrent configuration. Their long-range correlations are encoded in the global structure of the spanning trees. Thus height variables are local but constrained while spanning trees are unconstrained but global. For most practical calculations, like those presented here, spanning trees are more convenient.

We want to compute one-site height probabilities, namely the four quantities $P_{\mathcal{L}}^*(h_{i_0} = a)$ for $a = 1, 2, 3, 4$. On a finite grid \mathcal{L} , it amounts to count the recurrent configurations with a height a at position i_0 . As we will use the spanning tree description, the first task is to characterize those spanning trees which correspond to recurrent configurations with a height a at site i_0 . This was done for the first time in [10], and was recently reviewed, with two different derivations, in [12, 13]. That part is not difficult, and we only quote the results.

From the burning algorithm, the spanning tree grows from its root to the open boundary sites

and then towards the interior of \mathcal{L} . A site i is called a predecessor of another site i_0 if the unique path on the spanning tree from i to the root passes through i_0 (equivalently, the fire has propagated from i_0 to i). Then the probabilities that the site i_0 has height a are given by

$$P_{\mathcal{L}}^*(h_{i_0} = a) = P_{\mathcal{L}}^*(h_{i_0} = a - 1) + \frac{X_{a-1}}{(5-a)\mathcal{N}}, \quad a = 1, 2, 3, 4, \quad (2.3)$$

where $P_{\mathcal{L}}^*(h_{i_0} = 0) = 0$ by definition, and where X_k is the number of spanning trees on \mathcal{L} where the site i_0 has exactly k predecessors among its nearest neighbours (so for $k = 0$, i_0 is a leaf of the tree).

While the calculation of X_0 is relatively easy (it was done first in [6] without the spanning tree description), that of the other X_1, X_2 and X_3 is much harder. The basic reason for this is that the spanning trees involved in X_0 are subjected to a local constraint, while those counting for X_k , $k > 0$, must satisfy a global constraint. In the case of X_1 for instance, a spanning tree is counted only if the firepath comes to i_0 , then goes on straight to one neighbour of i_0 but does not eventually come back to another neighbour of i_0 after a long tour through the lattice.

Priezzhev has devised a technique to compute the numbers X_k [10]. It turns out that they can all be expressed—in a complicated way—in terms of entries of the inverse toppling matrix Δ^{-1} , that is, in terms of the discrete Green function on \mathcal{L} for appropriate boundary conditions. The thermodynamic limit of the above probabilities, when the grid \mathcal{L} becomes infinite, then simply corresponds to taking the discrete Green function on the corresponding infinite lattice. For simplicity, we denote the corresponding measure by $P = \lim_{|\mathcal{L}| \rightarrow \infty} P_{\mathcal{L}}^*$.

The calculation of the 1-site probabilities, equivalently of the numbers X_k , was carried out by Priezzhev in the case of the infinite plane $\mathcal{L} \rightarrow \mathbb{Z}^2$, thereby obtaining the 1-site bulk probabilities P_1, P_2, P_3 and P_4 . In the following, we carry out the calculation for the upper half-plane $\mathcal{L} \rightarrow \mathbb{Z}_+ \times \mathbb{Z}$, when the boundary is either fully open or fully closed. The corresponding probabilities $P_a(m)$ depend on the distance m of the reference site i_0 to the boundary. That dependence is precisely what enables us to make the comparison with field theory correlations, and to assess the scaling form of the random height variables $\delta(h_{i_0} - a)$.

III. HEIGHT TWO ON THE PLANE

In this section we review Priezzhev's calculation of the higher height probabilities on the plane, since these calculations are the starting point for our calculations in the UHP [10]. We sketch the key points here; the reader is referred to Priezzhev's original paper for details.

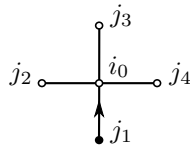


FIG. 1: Labelling of sites.

A. General Methods

Majumdar and Dhar [6] had already shown in 1991 that the height one probability at a site i_0 is given by

$$P_1 = \frac{X_0}{4\mathcal{N}}, \quad (3.1)$$

where X_0 is the number of spanning trees in which the site i_0 is a leaf, and $\mathcal{N} = \det \Delta$ (see Section II).

The restrictions on X_0 are local: a spanning tree is in X_0 if and only if no neighbour of i_0 has an arrow pointing to i_0 . Local restrictions on the spanning tree can be computed as finite-dimensional matrix determinants by the Majumdar-Dhar method. We briefly describe the key points of this method, but the reader is directed to the original paper for a detailed description [6].

The set of spanning trees is characterized by the toppling matrix Δ , which specifies the bonds on the lattice. When we want a subset of spanning trees with local restrictions, those restrictions can be imposed by changes in a finite number of entries of the toppling matrix. For example, to remove the bond between neighbours i and j , we simply change Δ_{ii} and Δ_{jj} to 3, and set Δ_{ij} and Δ_{ji} to 0. Calling the new toppling matrix Δ' , Kirchoff's theorem implies that $\det \Delta'$ is the number of spanning trees on the lattice with the bond ij removed, or equivalently, the number of spanning trees on the original lattice which do not use the bond connecting i and j .

To compute X_0 , we have to count the spanning trees in which i_0 is connected to only one of its neighbours. The simplest way to do this is to remove the three bonds connecting i_0 to three neighbours, say j_2, j_3, j_4 (see Fig. 1) and to define the new matrix $\Delta' = \Delta + B$, with

$$B = \begin{pmatrix} -3 & 1 & 1 & 1 \\ 1 & -1 & 0 & 0 \\ 1 & 0 & -1 & 0 \\ 1 & 0 & 0 & -1 \end{pmatrix}, \quad (3.2)$$

where the rows and columns are labeled by i_0, j_2, j_3, j_4 (all the other entries of B are zero). Then by symmetry, $X_0 = 4 \det \Delta'$.

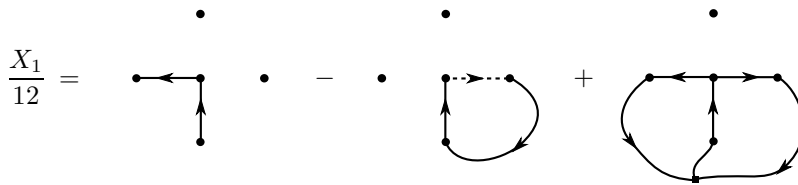


FIG. 2: Breaking X_1 into local, loop, and θ -graph terms.

Δ' is an infinite-dimensional matrix, so its determinant does not make much sense. However the probability P_1 only requires the ratio of two infinite determinants. Noting that B has finite rank, and defining $G \equiv \Delta^{-1}$, one easily sees that

$$P_1 = \frac{\det(\Delta')}{\det(\Delta)} = \det(1 + BG) \quad (3.3)$$

in fact reduces to a 4-by-4 determinant.

It is easy to compute this finite-dimensional determinant. In the limit of an infinite planar lattice, G is the Green matrix of the discrete Laplacian, whose values and properties are well-known [27]. Using them, Majumdar and Dhar were able to show that [6]

$$P_1 = \frac{2(\pi - 2)}{\pi^3} \simeq 0.07363. \quad (3.4)$$

The other X_k for $k > 0$ are much harder to calculate. We discuss X_1 in this Section, and X_2 in Section IV.

B. Decomposition into local, loop, and θ -graphs

Since all four directions are symmetric, to find X_1 , we can, without loss of generality, assume that the single predecessor is the site to the south of i_0 . Fig. 1 shows the labels of the 4 neighbouring sites, with the predecessor site indicated by a large solid circle, and the non-predecessor sites by large open circles. By enumerating possible arrow configurations in X_1 , Priezzhev showed that X_1 can be broken up into the terms in Fig. 2, or the following equation:

$$X_1 = 12 (\mathcal{N}_{\text{local}} - \mathcal{N}_{\text{loop}} + \mathcal{N}_{\theta}), \quad (3.5)$$

where the \mathcal{N} 's are positive (they count certain graphs). The reader is referred to [10] for the derivation of (3.5), or to Section IV for derivations of similar decompositions for X_2 . In this Section, we take the decomposition in Fig. 3.5 as given, and only discuss what the different terms mean, and how to evaluate them.

In the first term in Fig. 2, the arrow from j_1 must point to i_0 , and the arrow from i_0 must point to j_2 , while the sites j_3 and j_4 are disconnected from i_0 . Since the conditions on the spanning tree are local, the size of this set of spanning trees can be calculated with the Majumdar-Dhar method (or Kirchoff's theorem). The B matrix that corresponds to these conditions is

$$B = \begin{matrix} & i_0 & j_3 & j_4 & j_1 & j_1 - \hat{x} & j_1 + \hat{x} & j_1 - \hat{y} \\ \begin{pmatrix} -3 & 1 & 1 & 1 & 0 & 0 & 0 \\ 1 & -1 & 0 & 0 & 0 & 0 & 0 \\ 1 & 0 & -1 & 0 & 0 & 0 & 0 \\ 0 & 0 & 0 & -3 & 1 & 1 & 1 \end{pmatrix} & i_0 \\ & j_3 \\ & j_4 \\ & j_1 \end{matrix} \quad (3.6)$$

Then

$$\frac{\mathcal{N}_{\text{local}}}{\mathcal{N}} = \det(1 + BG) = \frac{1}{2\pi} - \frac{5}{2\pi^2} + \frac{4}{\pi^3} \quad (3.7)$$

gives the probability that a random spanning tree meets these conditions.

In the second term in Fig. 2, the arrow from j_1 must point to i_0 , and the arrow from i_0 must point to j_4 , and there must be some chain of arrows that takes us from j_4 to j_1 , forming a closed loop. The sites j_2 and j_3 are disconnected from i_0 , and we also require that there be no other closed loops. Because we have a closed loop of arrows, this term is not a subset of the set of spanning trees. The condition on the graphs is not local, so this term cannot be calculated by the Majumdar-Dhar method.

Priezzhev showed [10] how to adapt the Kirchoff theorem to deal with closed loop diagrams such as these. He showed that if n bond weights in the toppling matrix are set to $-\epsilon$, then

$$\lim_{\epsilon \rightarrow \infty} \frac{\det(\Delta')}{\epsilon^n} \quad (3.8)$$

counts the total number of arrow configurations where each of the n bonds is required to be in a closed loop, and each closed loop contains at least one of the n bonds; in this count, each configuration is weighted by $(-1)^c$, where c is the number of closed loops.

The second graph in Fig. 2 can thus be calculated by giving the bond from i_0 to j_4 weight $-\epsilon$, as represented by the dashed line, and making other appropriate local modifications. The matrix B is then given by

$$B = \begin{matrix} & i_0 & j_4 & j_3 & j_2 \\ \begin{pmatrix} 0 & -\epsilon & 0 & 0 \\ 1 & 0 & -1 & 0 \\ 1 & 0 & 0 & -1 \end{pmatrix} & i_0 \\ & j_3 \\ & j_2 \end{matrix} \quad (3.9)$$

Since we are defining $\mathcal{N}_{\text{loop}}$ to be the number of graphs, and each configuration gets a factor of $(-1)^c$, $\mathcal{N}_{\text{loop}}/\mathcal{N}$ is given by $-\det(1 + BG)$, rather than $\det(1 + BG)$, and is found to be equal to

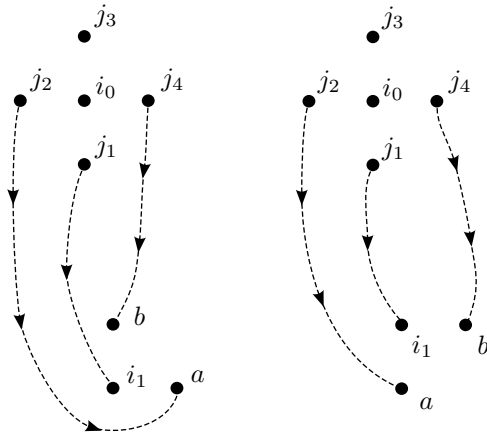
$$\frac{\mathcal{N}_{\text{loop}}}{\mathcal{N}} = -\frac{1}{4\pi^2} + \frac{2(\pi - 2)}{\pi^3} G_{0,0}. \quad (3.10)$$

It contains a term proportional to $G_{0,0}$, the inverse of the discrete Laplacian at coincident sites, which is infinite, see below Eq. (3.15) (for a finite lattice, $G_{0,0}$ diverges as $\log L$, where L is the system size). The divergence of this second term in Fig. 2 reflects the fact that the number of diagrams with loops is much greater than the number of spanning trees. Since X_1 is a finite fraction of the total number of spanning trees, the factors of $G_{0,0}$ must cancel in the second and third terms of Eq. (3.5).

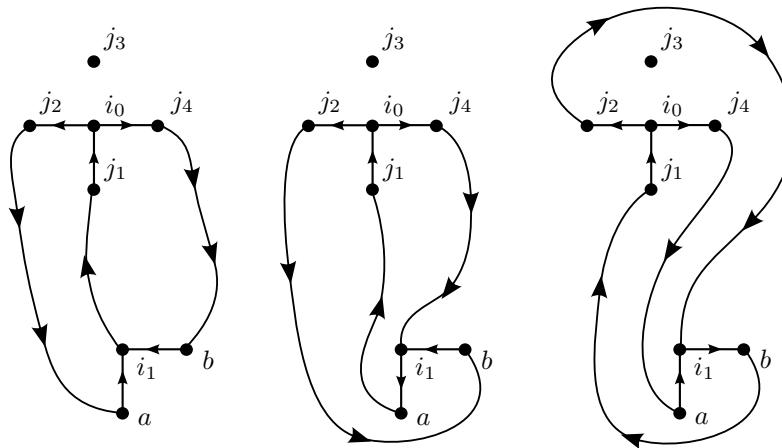
C. θ -graphs

While the first and second terms in Fig. 2 can be calculated by finite matrix determinants, the third term is more complicated. Priezzhev called these θ -graphs. In these graphs we have two arrows from i_0 (instead of the usual case of one arrow), to j_2 and j_4 , and both arrows are parts of two separate closed loops, that go through j_1 to get back to i_0 ; j_3 is disconnected from i_0 . The number \mathcal{N}_θ of θ -graphs cannot be calculated by a single matrix determinant, and the bulk of the work in calculating P_2 lies here. To do this, Priezzhev used an elegant technique, known as the “bridge” trick.

The two paths from i_0 must meet at some point before returning to i_0 —we call that point i_1 . Priezzhev then considered two possible graphs, labelled the L and Γ graphs, each of which has three $-\epsilon$ bonds (“bridges”) between non-adjacent sites, as shown in Fig. 3. Looking at the Γ graph on the right side, we see that there are several possible ways to fulfill the condition that every $-\epsilon$ bond be in a closed loop. One possibility is to make three closed loops by separate paths from a to j_2 , i_1 to j_1 , and b to j_4 . The other possibility is to have one closed path that contains all three of the $-\epsilon$ bonds. This second possibility can occur in two possible ways. First, by paths from a to j_1 ,

FIG. 3: The bridge trick: L and Γ configurations.

i_1 to j_4 , and b to j_2 . And second, by paths from a to j_4 , b to j_1 , and i_1 to j_2 . This gives the three possible θ -graphs shown in Fig. 4, after reversing the direction of some of the paths, which does not affect the overall counting. (Note that the topology forbids cases where the three $-\epsilon$ bonds only produce two closed loops. If such cases existed, they would get a different factor of $(-1)^c$, where c is the number of closed loops, and ruin the bridge trick.)

FIG. 4: Three possible θ -graphs from the Γ configuration of the bridge trick.

When all the graphs produced by the L and Γ bridge configurations are considered, it is found that almost all the θ -graphs are listed. Characterizing the θ -graphs by the three sites adjacent to i_1 that are connected by paths to j_1 , j_2 , and j_4 , it is found that we are lacking all cases where the three sites are $\{i_1 - \hat{x}, i_1 + \hat{y}, i_1 - \hat{y}\}$, and have overcounted (by a factor of 2) all cases where the three sites are $\{i_1 + \hat{x}, i_1 + \hat{y}, i_1 - \hat{y}\}$. However, since the ASM is symmetric under horizontal flips, the overcounting and undercounting exactly cancel.

The bridge diagrams shown in Fig. 3 are calculated with the following B matrix:

$$B = \begin{matrix} & j_3 & i_0 & i_1 & a & b \\ \begin{pmatrix} -1 & 1 & 0 & 0 & 0 \\ 0 & 0 & -\epsilon & 0 & 0 \\ 0 & 0 & 0 & -\epsilon & 0 \\ 0 & 0 & 0 & 0 & -\epsilon \end{pmatrix} & j_3 \\ & j_1 \\ & j_2 \\ & j_4 \end{matrix} \quad (3.11)$$

Since i_1 can be anywhere, we need to sum over all possible locations of i_1 on the plane,

$$\sum_{i_1} [\mathcal{N}_L(i_1) + \mathcal{N}_\Gamma(i_1)]. \quad (3.12)$$

$\mathcal{N}_L(i_1)$ and $\mathcal{N}_\Gamma(i_1)$ are both given by $\det(1 + BG)$, with B as in Eq. (3.11). $\mathcal{N}_L(i_1)$ and $\mathcal{N}_\Gamma(i_1)$ differ only in the locations of a and b with respect to i_1 (see Fig. 3). While B has the same form in each case, the row and column indices associated with i_1 , a and b are different for different terms, which then involve different entries of the matrix G .

However, Eq. (3.12) does not exactly give \mathcal{N}_θ . The bridge trick (i.e. the equivalence of the bridge diagram and the relevant θ -graphs) requires that the sets $\{i_0, j_2, j_4\}$ and $\{i_1, a, b\}$ have no points in common. When i_1 and i_0 are the same, or close, Eq. (3.11) may or may not correspond to the subset of θ -graphs shown in Fig. 3. Priezzhev checked all such cases, and found what we will call “special” cases, where Eq. (3.11) either produces graphs that are not θ -graphs (in which case these terms need to be subtracted from the infinite sum), or misses certain θ -graphs (in which cases new terms need to be added to the infinite sum). When these special terms are accounted for, the total number of θ -graphs is given by

$$\begin{aligned} \mathcal{N}_\theta = \sum_{i_1} [\mathcal{N}_L(i_1) + \mathcal{N}_\Gamma(i_1)] &+ \mathcal{N}_L(j_4) + \mathcal{N}_\Gamma(j_4) + 2\mathcal{N}_T(j_4) - \mathcal{N}_L(j_2) - \mathcal{N}_\Gamma(j_2) \\ &- \mathcal{N}_L(i_0) - \mathcal{N}_\Gamma(i_0) - \mathcal{N}_\Gamma(j_3), \end{aligned} \quad (3.13)$$

where $\mathcal{N}_T(j_4)$ is the graph obtained by adding the three $-\epsilon$ bonds as shown in Fig. 5, and removing the bond between j_3 and i_0 as before.

All of the individual terms in Eq. (3.13) can be calculated by taking finite-dimensional determinants (using Eq. (3.11) for all terms except $\mathcal{N}_T(j_4)$). The final difficulty is in the infinite sum over i_1 . The two matrix determinants in $\mathcal{N}_L(i_1)$ and $\mathcal{N}_\Gamma(i_1)$ differ only in a single column, and can

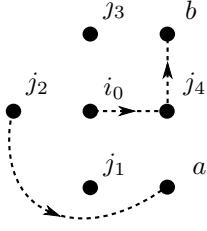


FIG. 5: The T configuration used to compute $\mathcal{N}_T(j_4)$. The sites a and b are nearest neighbours of j_4 .

thus be combined in a single matrix determinant:

$$\sum_{i_1} \left[\frac{\mathcal{N}_L(i_1)}{\mathcal{N}} + \frac{\mathcal{N}_\Gamma(i_1)}{\mathcal{N}} \right] = \sum_{k, \ell \in \mathbb{Z}} \det \begin{pmatrix} G_{1,0} - G_{0,0} & G_{k,\ell} & G_{k+1,\ell} & G_{k,\ell-1} - G_{k,\ell+1} \\ G_{0,0} - G_{1,0} - 1 & G_{k,\ell-1} & G_{k+1,\ell-1} & G_{k,\ell-2} - G_{k,\ell} \\ G_{1,1} - G_{1,0} & G_{k-1,\ell} & G_{k,\ell} & G_{k-1,\ell-1} - G_{k-1,\ell+1} \\ G_{1,1} - G_{1,0} & G_{k+1,\ell} & G_{k+2,\ell} & G_{k+1,\ell-1} - G_{k+1,\ell+1} \end{pmatrix}, \quad (3.14)$$

where $G_{k,\ell}$ stands for the entry $\Delta_{i,j}^{-1}$ with $(k,\ell) = i - j$. A convenient integral representation of it is

$$G_{k,\ell} = \iint_{-\pi}^{\pi} \frac{d\alpha d\beta}{8\pi^2} \frac{e^{i\alpha k + i\beta \ell}}{2 - \cos \alpha - \cos \beta}. \quad (3.15)$$

D. Final results for $h = 2$ on the plane

The Green function $G_{k,\ell}$ can be computed explicitly for small values of k and ℓ , so that the first column of the matrix in Eq. (3.14) contains known numbers. For the other three columns, the representation Eq. (3.15) can be used to write each entry as a two-dimensional integral, over the variables (α_3, β_3) in the second column, (α_2, β_2) in the third column, and (α_1, β_1) in the fourth column. The sum over k and ℓ produces two δ -functions $\delta(\alpha_1 + \alpha_2 + \alpha_3) \delta(\beta_1 + \beta_2 + \beta_3)$, which allow to integrate over α_3, β_3 . So we end up with a four-dimensional integral (two further integrations can be carried out analytically, see Section VII). The end result is the expression obtained by Priezzhev [10] for the height two probability, namely

$$P_2 = \frac{1}{2} - \frac{3}{2\pi} - \frac{2}{\pi^2} + \frac{12}{\pi^3} + \frac{1}{4} I \left(1, \frac{4}{\pi} - 1, 3 \right), \quad (3.16)$$

where

$$I(c_1, c_2, c_3) \equiv \iint_{-\pi}^{\pi} \frac{d\alpha_1 d\beta_1}{4\pi^2} \iint_{-\pi}^{\pi} \frac{d\alpha_2 d\beta_2}{4\pi^2} \frac{i \sin \beta_1 \cdot \det M(c_1, c_2, c_3)}{L(\alpha_1, \beta_1) L(\alpha_2, \beta_2) L(\alpha_1 + \alpha_2, \beta_1 + \beta_2)}, \quad (3.17)$$

with $L(\alpha, \beta) = 2 - \cos \alpha - \cos \beta$, and

$$M(c_1, c_2, c_3) = \begin{pmatrix} c_1 & 1 & e^{i\alpha_2} & 1 \\ c_3 & e^{i(\beta_1+\beta_2)} & e^{i(\alpha_2-\beta_2)} & e^{-i\beta_1} \\ c_2 & e^{i(\alpha_1+\alpha_2)} & 1 & e^{-i\alpha_1} \\ c_2 & e^{-i(\alpha_1+\alpha_2)} & e^{2i\alpha_2} & e^{i\alpha_1} \end{pmatrix}. \quad (3.18)$$

We now make an observation that will be useful for comparison with P_3 later. The function $I(c_1, c_2, c_3)$ does not depend on c_3 , because all the terms in the integrand proportional to c_3 are antisymmetric under $\beta_1 \rightarrow -\beta_1, \beta_2 \rightarrow -\beta_2$. Since the integral is linear in c_1 and c_2 , we can write it as the sum of two separate four-dimensional integrals:

$$I(c_1, c_2) = c_1 J_1 + c_2 J_2. \quad (3.19)$$

J_1 and J_2 still need to be evaluated numerically, so this decomposition does not help us get a closed form expression for P_2 , but we will see in the next section that it does allow us to get a closed form relationship between P_2 and P_3 . Numerical integrations yield $J_1 = -0.26866$ and, quite unexpectedly, $J_2 = 0.5$ with a error smaller than 10^{-12} , leading to the value $P_2 = 0.1739$, as quoted in [10]. Although we could not evaluate it exactly, it is very tempting to conjecture that J_2 is exactly equal to $\frac{1}{2}$. As we will see in the next section, this would imply an exact, closed and simple formula for the 1-site height probabilities P_i on the plane.

IV. HEIGHT THREE ON THE PLANE

While Priezzhev calculated the height two and height three probabilities on the plane, he only gave the details of the height two calculation. In this Section, we give the details of our derivation of the height three probability, both because these details are necessary for the calculation of the height three probability in the UHP, and to derive an exact relationship between P_2 and P_3 .

A. Height Three Decomposition

For the height three probability, we need X_2 , the number of spanning trees where exactly two neighbours of i_0 are predecessors. This can happen in three ways, as shown in Fig. 6. Priezzhev showed that $X_2^{(2)}$ can be written as a linear combination of simple local graphs, as shown in Fig. 7, yielding (there appears to be a misprint in Eq.(32) of [10])

$$\frac{X_2^{(2)}}{\mathcal{N}} = \frac{8}{\pi} - \frac{24}{\pi^2}. \quad (4.1)$$

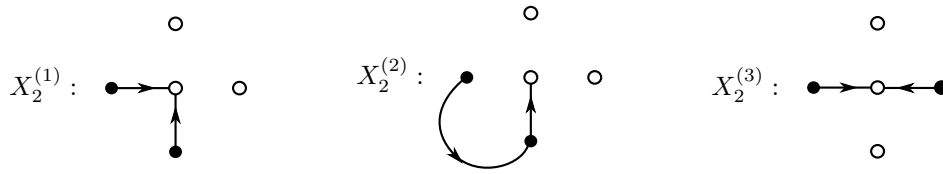


FIG. 6: Definitions of $X_2^{(1)}$, $X_2^{(2)}$, and $X_2^{(3)}$.

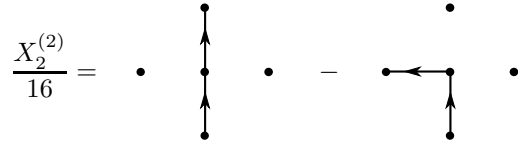


FIG. 7: A simple decomposition of $X_2^{(2)}$.

The calculation of $X_2^{(1)}$ and $X_2^{(3)}$ is more complicated. Just as Priezzhev broke X_1 into local, loop, and more complicated terms (see Fig. 2), by counting arrow configurations, we can break up $X_2^{(1)}$ and $X_2^{(3)}$ into similar terms. We discuss the decomposition of $X_2^{(1)}$ in some detail. The derivation is shown graphically in Figs. 8, 9, and 10.

We begin by explaining the derivation in Fig. 8. For $X_2^{(1)}$, we get the same number of spanning trees whether the arrow from i_0 points to j_3 or j_4 , so without loss of generality, we pick j_4 . Next, recall that the open circle on j_3 indicates that it is not a predecessor of i_0 . We have no simple matrix method for calculating subsets of spanning trees with such a restriction. So we start off with the subset with no such restriction, and then subtract off the different ways that j_3 can be a predecessor of i_0 : j_3 can be a predecessor of i_0 either by a path through j_2 , or by a path through j_1 . This gives the last line in Fig. 8.

The first graph in the last line of Fig. 8 can be calculated by the Majumdar-Dhar method. The last two graphs in this line require further manipulation to be put into a form that can be

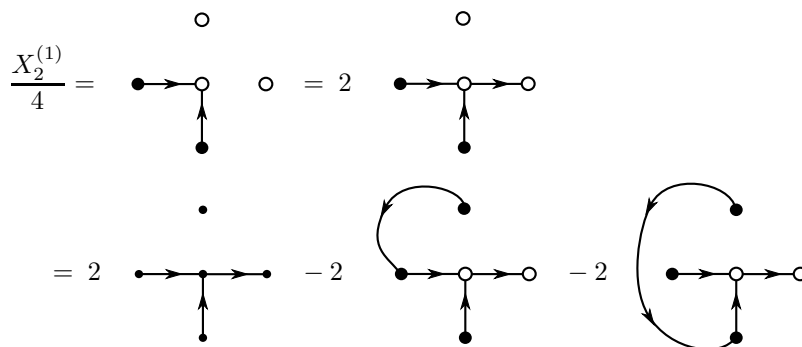
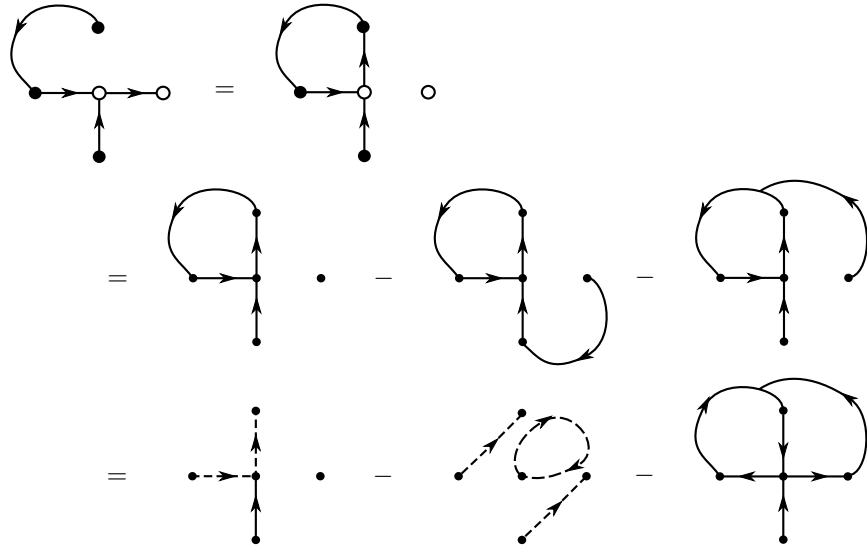


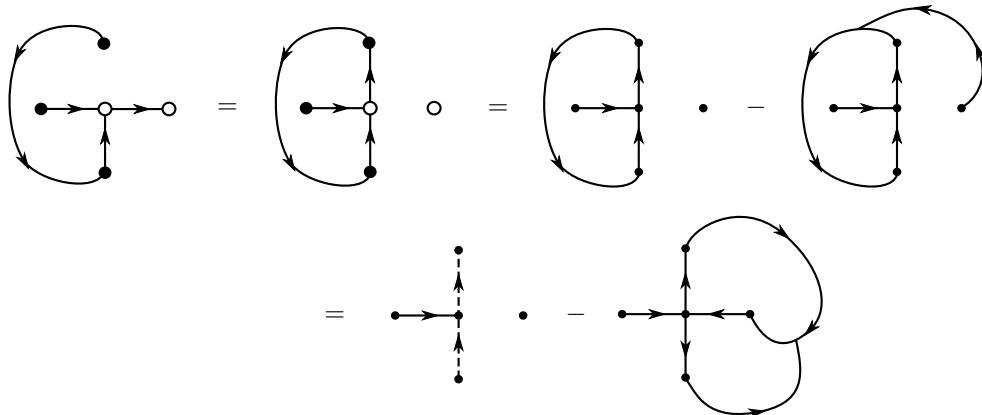
FIG. 8: Decomposition of $X_2^{(1)}$, Part 1.

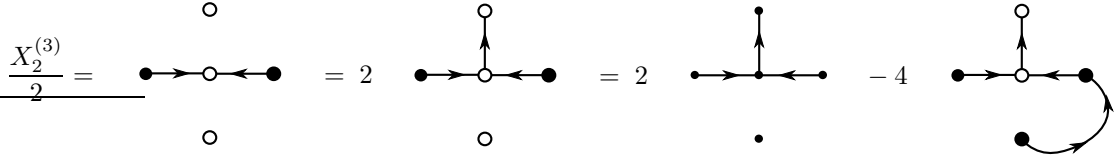
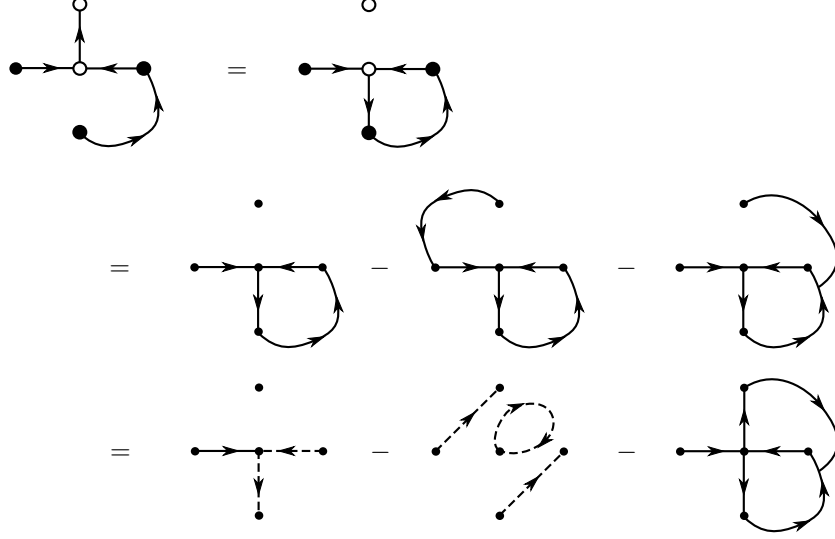
FIG. 9: Decomposition of $X_2^{(1)}$, Part 2.

calculated with matrix determinants. They are calculated in Figs. 9 and 10.

In Fig. 9, we first use the fact that redirecting the $i_0 \rightarrow j_4$ arrow to an $i_0 \rightarrow j_3$ arrow will not affect the total number of arrow configurations. j_4 is not permitted to be a predecessor of i_0 , and as before, we deal with this condition by starting without this condition, and subtracting off the different ways that j_4 can be a predecessor of i_0 . This gives the second line of Fig. 9. The first two graphs in this line can be calculated as matrix determinants, by adding $-\epsilon$ bonds. The last graph in Fig. 9 is what we call a $\tilde{\theta}$ -graph. In the last line of Fig. 9 we no longer draw large filled or large empty circles, because there are no predecessor conditions imposed, other than those that follow naturally from the arrows drawn.

The analysis in Fig. 10 is similar. In the last line of that equation we again use the fact that

FIG. 10: Decomposition of $X_2^{(1)}$, Part 3.

FIG. 11: Decomposition of $X_2^{(3)}$, Part 1.FIG. 12: Decomposition of $X_2^{(3)}$, Part 2.

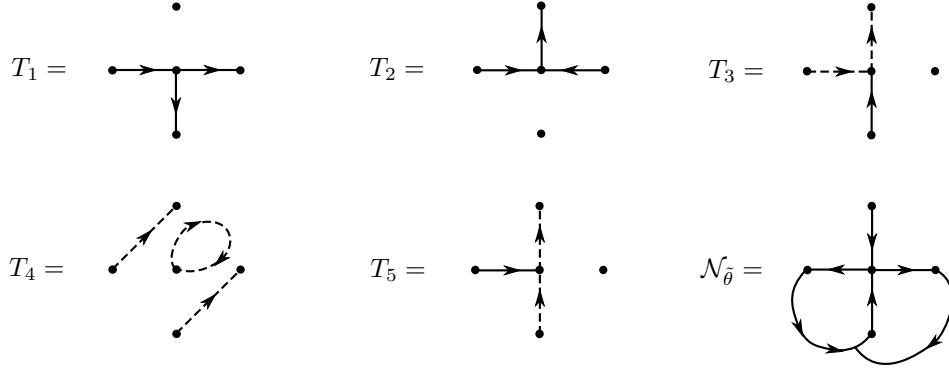
dashed lines must be contained in closed loops, and the fact that directions of paths of arrows can be reversed without changing the total number of graphs.

The graphical decomposition of $X_2^{(3)}$ uses a similar logic, and is shown in Figs. 11 and 12. Defining the graphs as in Fig. 13, we have

$$X_2^{(1)} = 8(T_1 - T_3 + T_4 - T_5) + 16\mathcal{N}_{\tilde{\theta}}, \quad (4.2)$$

$$X_2^{(3)} = 4(T_2 - 2T_3 + 2T_4) + 8\mathcal{N}_{\tilde{\theta}}. \quad (4.3)$$

The $\tilde{\theta}$ -graph is defined similarly to the θ -graph, and is shown in Fig. 13 rotated to its standard form. Just as with the θ -graph, there are two arrows from i_0 , pointing to j_2 and j_4 , which form two closed loops that reach i_1 through j_1 . The only difference from the θ -graph is that now, instead of removing the bond from j_3 to i_0 , we require an arrow from j_3 to i_0 . (The paths from j_4 and j_2 now cannot go through j_3 , since they must still reach i_0 via j_1 .) To represent the $\tilde{\theta}$ -graphs, we use the fact that if a $-\epsilon$ bond is added from a site to itself (i.e. along the diagonal of the B -matrix), it effectively turns that site into a sink, where arrows can terminate, but not begin. So by adding a $-\epsilon$ bond from j_3 to itself, we fulfill the conditions necessary for a $\tilde{\theta}$ graph.

FIG. 13: Definitions of the T_i and $\tilde{\theta}$ graphs.

B. $\tilde{\theta}$ -graphs

Since the $\tilde{\theta}$ -graph differs from the θ -graph only in that a $-\epsilon$ bond has been added from j_3 to itself, the only change from the $h = 2$ infinite sum is that instead of Eq. (3.11), we have

$$B = \begin{pmatrix} j_3 & i_1 & a & b \\ -\epsilon & 0 & 0 & 0 \\ 0 & -\epsilon & 0 & 0 \\ 0 & 0 & -\epsilon & 0 \\ 0 & 0 & 0 & -\epsilon \end{pmatrix} \begin{matrix} j_3 \\ i_0 \\ j_2 \\ j_4 \end{matrix} \quad (4.4)$$

The analysis of the $\tilde{\theta}$ -graphs then proceeds identically to that for the θ -graphs. There are again a number of special cases that arise when i_1 borders or is equal to i_0 . Checking these cases by hand gives correction terms analogous to those in Eq. (3.13):

$$\mathcal{N}_{\tilde{\theta}} = \sum_{i_1} \left[\tilde{\mathcal{N}}_L(i_1) + \tilde{\mathcal{N}}_\Gamma(i_1) \right] + \tilde{\mathcal{N}}_L(j_4) + \tilde{\mathcal{N}}_\Gamma(j_4) + \tilde{\mathcal{N}}_T(j_4) - \tilde{\mathcal{N}}_L(j_2) - \tilde{\mathcal{N}}_\Gamma(j_2) - \tilde{\mathcal{N}}_\Gamma(i_0). \quad (4.5)$$

$\tilde{\mathcal{N}}_L(i_1)$ and $\tilde{\mathcal{N}}_\Gamma(i_1)$ are given by $\det(1 + BG)$, where B is given by Eq. (4.4), and a and b are located as shown in Fig. 3. The \tilde{T} graph is defined similarly to the T graph in Fig. 5, except that instead of forbidding the arrow from j_3 to i_0 , we add a $-\epsilon$ bond from j_3 to itself.

C. Final results on the plane

As in the height two case, all the individual terms in Eq. (4.5) can be calculated as finite-dimensional matrix determinants. The infinite sum is similar to the one in Eq. (3.14). Because only one bond of the B matrix has been changed, only the first column of the matrix in Eq. (3.14)

is changed, as follows:

$$\begin{pmatrix} G_{1,0} - G_{0,0} \\ G_{0,0} - G_{1,0} - 1 \\ G_{1,1} - G_{1,0} \\ G_{1,1} - G_{1,0} \end{pmatrix} \rightarrow - \begin{pmatrix} G_{1,0} \\ G_{0,0} \\ G_{1,1} \\ G_{1,1} \end{pmatrix} \quad (4.6)$$

Note that this column is no longer finite; instead, all its terms diverge as $G_{0,0}$.

Just as with the height two probability, our end result for P_3 is a sum of local and loop graphs, which can be computed exactly, and an infinite sum, which results in a four-dimensional integral. Since only the first column of Eq. (3.14) is changed, the four-dimensional integral still has the form in Eq. (3.17), and we get the same integrals J_1 and J_2 , but with different coefficients. We obtain explicitly

$$\frac{X_2^{(1)}}{\mathcal{N}} = 1 - \frac{6}{\pi} + \frac{24}{\pi^2} - \frac{32}{\pi^3} - \left(J_1 + \frac{4}{\pi} J_2 \right) + G_{0,0} \left(4(J_1 + J_2) - \frac{8}{\pi^2}(\pi - 2) \right), \quad (4.7)$$

$$\frac{X_2^{(3)}}{\mathcal{N}} = -\frac{3}{2} + \frac{7}{\pi^2} - \frac{16}{\pi^3} - \frac{1}{2} \left(J_1 + \frac{4}{\pi} J_2 \right) + G_{0,0} \left(2(J_1 + J_2) - \frac{4}{\pi^2}(\pi - 2) \right). \quad (4.8)$$

Even for an infinite lattice, the ratios $X_2^{(1)}/\mathcal{N}$ and $X_2^{(3)}/\mathcal{N}$ must be finite since they represent fractions of all spanning trees. $G_{0,0}$ being infinite, this immediately requires that the coefficients of $G_{0,0}$ must cancel, giving

$$J_1 + J_2 = \frac{2}{\pi^2}(\pi - 2). \quad (4.9)$$

While we could not evaluate J_1 and J_2 analytically, not even their sum, the numerical values mentioned before confirm Eq. (4.9).

We find P_3 from Eq. (2.3), with $X_2 = X_2^{(1)} + X_2^{(2)} + X_2^{(3)}$, and then rewrite both P_2 and P_3 with Eq. (4.9), reproducing the values found in [10], namely

$$P_2 = \frac{1}{2} - \frac{1}{\pi} - \frac{3}{\pi^2} + \frac{12}{\pi^3} - \frac{\pi - 2}{2\pi} J_2 \simeq 0.1739, \quad (4.10)$$

$$P_3 = \frac{1}{4} + \frac{2}{\pi} - \frac{12}{\pi^3} - \frac{8 - \pi}{4\pi} J_2 \simeq 0.3063. \quad (4.11)$$

These two equations give us an exact relationship between P_2 and P_3 :

$$(\pi - 8)P_2 + 2(\pi - 2)P_3 = \pi - 2 - \frac{3}{\pi} + \frac{12}{\pi^2} - \frac{48}{\pi^3}. \quad (4.12)$$

To our knowledge, this exact relation is new.

Using the value of $P_1 = \frac{2(\pi-2)}{\pi^3}$, we can rewrite the previous relation as

$$\frac{48 - 12\pi + 5\pi^2 - \pi^3}{2(\pi - 2)} P_1 + (\pi - 8) P_2 + 2(\pi - 2) P_3 = \frac{(\pi - 2)(\pi - 1)}{\pi}. \quad (4.13)$$

The significance of this new relation will be made clear in Section VIII.

Coming back to the conjecture we made at the end of the previous section, namely that $J_2 = \frac{1}{2}$ exactly (and checked to 12 decimal places), we see that, together with (4.10) and (4.11), it yields a very simple and exact formula for P_2 and P_3 , similar to the formula for P_1 :

$$P_2 = \frac{1}{4} - \frac{1}{2\pi} - \frac{3}{\pi^2} + \frac{12}{\pi^3}, \quad P_3 = \frac{3}{8} + \frac{1}{\pi} - \frac{12}{\pi^3}. \quad (4.14)$$

These formulas solely rely on J_2 being exactly equal to $\frac{1}{2}$. An integral representation for J_2 has been given at the end of Section III. By carrying out two of the four integrations, we can rewrite it in a simpler form, as a two-fold integral,

$$J_2 = \frac{4}{\pi^2} - \frac{14}{\pi} - 8 - \frac{4\sqrt{2}}{\pi^2} \int_0^\pi \frac{d\beta_1}{\sqrt{3 - \cos \beta_1}} \int_{-\pi}^\pi \frac{d\beta_2}{1 - t_1 t_2 t_3} \sin \frac{\beta_1 - \beta_2}{2} \left[\cos \frac{\beta_1 - \beta_2}{2} - 2 \cos \frac{\beta_1 + \beta_2}{2} \right] \\ \times \left[(3 - \cos \beta_1 + \cos \beta_2) \cos \frac{\beta_1}{2} - 2 \sin \beta_2 \sin \frac{\beta_1}{2} \right], \quad (4.15)$$

where $t_i = y_i - \sqrt{y_i^2 - 1}$, $y_i = 2 - \cos \beta_i$ and $\beta_3 = -(\beta_1 + \beta_2)$. This integral expression has been used for the numerical evaluation of J_2 , yielding $J_2 = 0.5 + o(10^{-12})$.

V. HEIGHTS TWO AND THREE ON THE UPPER HALF-PLANE

The calculations of the height two and three probabilities on the UHP use the same formalism as the infinite plane calculations. The relation between the 1-site height probabilities in the ASM, and the probabilities of numbers of predecessors in spanning trees, stated in Eq. (2.3), still holds in the presence of a boundary. The corresponding equation for the height 1, Eq. (3.1), has been used by Brankov *et al.* to obtain the 1-site height one probabilities on the UHP in the presence of an open or a closed boundary [7].

On the UHP, we will use integer coordinates (m, n) , where $n \in \mathbb{Z}$ runs along the horizontal axis, $m \in \mathbb{Z}_+$ along the vertical axis, and with the boundary located at $m = 1$. We want to compute the 1-site height probabilities $P_a(m)$ for having a height a at the site $(0, m)$, and when the boundary is either fully open or fully closed. By horizontal translation invariance, the coordinate n plays no role.

When calculating X_1 on the plane, we obtained a factor of 12 in Fig. 2 because of the symmetry between the four possible predecessors of i_0 , and between the three possible directions of the arrow from i_0 . In the UHP, we still have the latter factor of three, but the four choices of predecessors are no longer symmetric in the presence of a boundary. We thus need to break X_1 up into the A ,

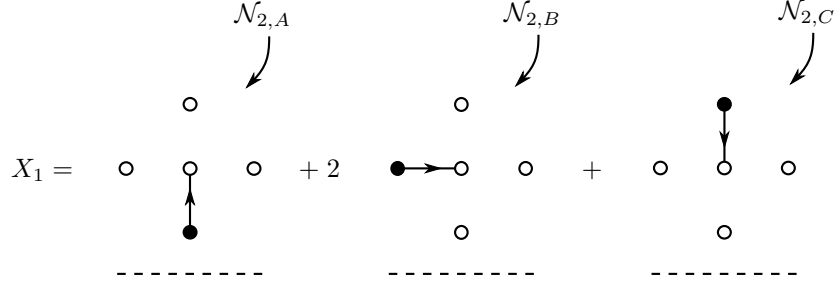


FIG. 14: Inequivalent rotations of X_1 with a boundary to the south.

B , and C configurations in Fig. 14, where the dashed line indicates the boundary. (The cases with j_2 and j_4 as predecessors are still symmetric.)

Just as in the bulk, each of these configurations can be broken up into local, loop, and θ -diagrams (see Fig. 2). The θ -graph can then be written as an infinite sum, and some special correction graphs where i_1 is close to i_0 .

The local, loop, and special correction graphs can all again be calculated as matrix determinants. In these terms, the only effect of the boundary is to modify the lattice Green function. The lattice Green functions in the presence of open or closed boundaries can be found in terms of that on the plane using the image method:

$$G_{m_1, m_2, n_1 - n_2}^{\text{open}} \equiv G_{(n_1, m_1), (n_2, m_2)}^{\text{open}} = G_{n_1 - n_2, m_1 - m_2} - G_{n_1 - n_2, m_1 + m_2}, \quad (5.1)$$

$$G_{m_1, m_2, n_1 - n_2}^{\text{cl}} \equiv G_{(n_1, m_1), (n_2, m_2)}^{\text{cl}} = G_{n_1 - n_2, m_1 - m_2} + G_{n_1 - n_2, m_1 + m_2 - 1}. \quad (5.2)$$

For the local, loop, and special correction graphs, we only need the lattice Green function between two sites near $(0, m)$, and thus simply expand out the above Green functions for $m_1 \approx m_2 \approx m \gg 1$ and $n_1 \approx n_2$. The relevant expansion in inverse powers of m reads ($k, n \ll m$)

$$G_{k, 2m+n} = G_{0,0} - \frac{1}{2\pi} \log(2m) - \frac{n}{4\pi m} - \frac{1}{\pi} \left(\frac{\gamma}{2} + \frac{3}{4} \log 2 \right) + \frac{1 + 6(n^2 - k^2)}{96\pi m^2} + \mathcal{O}\left(\frac{1}{m^3}\right), \quad (5.3)$$

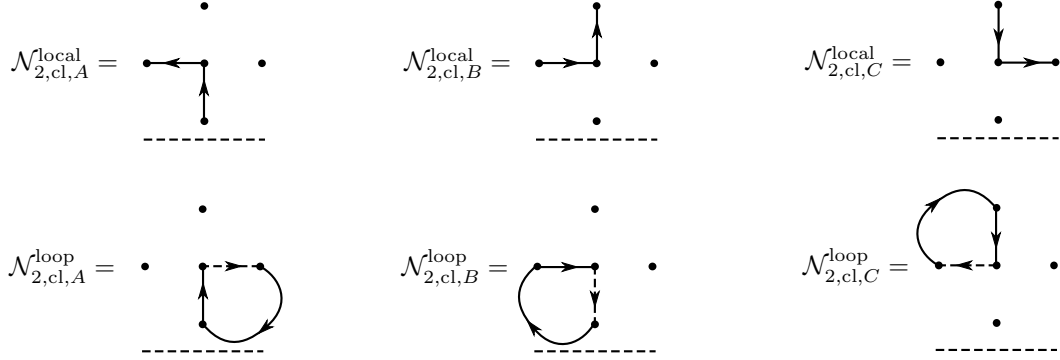
where $\gamma = 0.57721 \dots$ is the Euler-Mascheroni constant.

The local graphs have the same values as on the plane, up to terms of $\mathcal{O}(m^{-1})$. For example, $\mathcal{N}_{\text{local}}$ in Fig. 2 becomes three terms corresponding to the three orientations in Fig. 14, also shown in Fig. 15. For the closed boundary case we have

$$\frac{\mathcal{N}_{2, \text{cl}, A}^{\text{local}}}{\mathcal{N}} = \frac{\mathcal{N}_{2, \text{local}}}{\mathcal{N}} + \frac{\pi - 2}{4\pi^3 m} - \frac{\pi^2 - 10\pi + 18}{16\pi^3 m^2} + \mathcal{O}\left(\frac{1}{m^3}\right), \quad (5.4)$$

$$\frac{\mathcal{N}_{2, \text{cl}, B}^{\text{local}}}{\mathcal{N}} = \frac{\mathcal{N}_{2, \text{local}}}{\mathcal{N}} + \frac{\pi - 2}{4\pi^3 m} - \frac{\pi^2 - 10\pi + 22}{16\pi^3 m^2} + \mathcal{O}\left(\frac{1}{m^3}\right), \quad (5.5)$$

$$\frac{\mathcal{N}_{2, \text{cl}, C}^{\text{local}}}{\mathcal{N}} = \frac{\mathcal{N}_{2, \text{local}}}{\mathcal{N}} - \frac{\pi - 2}{4\pi^3 m} - \frac{\pi^2 - 6\pi + 10}{16\pi^3 m^2} + \mathcal{O}\left(\frac{1}{m^3}\right). \quad (5.6)$$

FIG. 15: Rotations of graphs used to calculate X_1 on the UHP.

where $\mathcal{N}_{2,\text{local}}$ refers to the plane value in Eq. (3.7).

The loop graphs are also matrix determinants with exactly the same B matrices as on the plane. Recall that on the plane, loop graphs had terms proportional to $G_{0,0}$, the constant diverging part of the Green function. When there are boundaries, we define

$$g(m) \equiv -\frac{1}{2\pi} \left[\log m + \gamma + \frac{5}{2} \ln 2 \right] + 2G_{0,0} = G_{0,0} + G_{2m,0} + \mathcal{O}\left(\frac{1}{m^2}\right), \quad (5.7)$$

$$\tilde{g}(m) \equiv -\frac{1}{2\pi} \left[\log m + \gamma + \frac{5}{2} \ln 2 \right] = G_{0,0} - G_{2m,0} + \mathcal{O}\left(\frac{1}{m^2}\right), \quad (5.8)$$

to be the dimension zero terms of the Green functions in the closed and open cases respectively.

One then finds that the loop graphs in the closed case are given by

$$\begin{aligned} \frac{\mathcal{N}_{2,\text{closed},A}^{\text{loop}}}{\mathcal{N}} = \frac{\mathcal{N}_{2,\text{closed},B}^{\text{loop}}}{\mathcal{N}} &= -\frac{1}{4\pi^2} + \frac{2(\pi-2)}{\pi^3} g(m) + \frac{1}{\pi^2 m} \left(\frac{1}{4} - \frac{1}{\pi^2} \right) \\ &+ \frac{1}{\pi^2 m^2} \left(\frac{3}{16} + \frac{1}{48\pi} - \frac{13}{21\pi^2} - \frac{\pi-2}{2\pi} g(m) \right) + \mathcal{O}\left(\frac{1}{m^3}\right), \end{aligned} \quad (5.9)$$

$$\begin{aligned} \frac{\mathcal{N}_{2,\text{closed},C}^{\text{loop}}}{\mathcal{N}} &= -\frac{1}{4\pi^2} + \frac{2(\pi-2)}{\pi^3} g(m) - \frac{1}{\pi^2 m} \left(\frac{1}{4} - \frac{1}{\pi} + \frac{1}{\pi^2} \right) \\ &- \frac{1}{\pi^2 m^2} \left(\frac{1}{16} - \frac{25}{48\pi} + \frac{13}{21\pi^2} + \frac{\pi-2}{2\pi} g(m) \right) + \mathcal{O}\left(\frac{1}{m^3}\right). \end{aligned} \quad (5.10)$$

Once the local, loop, and special correction graphs have all been computed as series in $1/m$, all that remains to evaluate is the infinite sum contribution to $\mathcal{N}(\theta)$, which is the most difficult part to analyze. The infinite sum contribution can be set up similarly to the bulk case, with two differences. First, the boundary Green functions must be used; second, the summation over i_1 must cover the UHP, rather than the whole plane. For example, for the A -orientation of \mathcal{N}_2 in the closed case, we obtain the sum ((k, ℓ) are the coordinates of i_1)

$$I_A^{h=2,\text{cl}} = \sum_{k=-\infty}^{\infty} \sum_{\ell=1-m}^{\infty} \left[\frac{\mathcal{N}_L(i_1)}{\mathcal{N}} + \frac{\mathcal{N}_\Gamma(i_1)}{\mathcal{N}} \right], \quad (5.11)$$

with

$$\frac{\mathcal{N}_L}{\mathcal{N}} = \begin{vmatrix} G_{m+1,m+1,0}^{\text{cl}} - G_{m+1,m,0}^{\text{cl}} - 1 & G_{m+1,m,0}^{\text{cl}} - G_{m,m,0}^{\text{cl}} & G_{m+1,m,1}^{\text{cl}} - G_{m,m,1}^{\text{cl}} & G_{m+1,m,1}^{\text{cl}} - G_{m,m,1}^{\text{cl}} \\ G_{m+\ell,m+1,k}^{\text{cl}} & G_{m+\ell,m,k}^{\text{cl}} & G_{m+1,m,k+1}^{\text{cl}} & G_{m+\ell,m,k-1}^{\text{cl}} \\ G_{m+\ell,m+1,k+1}^{\text{cl}} & G_{m+\ell,m,k+1}^{\text{cl}} & G_{m+\ell,m,k+2}^{\text{cl}} & G_{m+\ell,m,k}^{\text{cl}} \\ G_{m+\ell+1,m+1,k}^{\text{cl}} & G_{m+\ell+1,m,k}^{\text{cl}} & G_{m+\ell+1,m,k+1}^{\text{cl}} & G_{m+\ell+1,m,k-1}^{\text{cl}} \end{vmatrix}, \quad (5.12)$$

and

$$\frac{\mathcal{N}_\Gamma}{\mathcal{N}} = \begin{vmatrix} G_{m+1,m+1,0}^{\text{cl}} - G_{m+1,m,0}^{\text{cl}} - 1 & G_{m+1,m,0}^{\text{cl}} - G_{m,m,0}^{\text{cl}} & G_{m+1,m,1}^{\text{cl}} - G_{m,m,1}^{\text{cl}} & G_{m+1,m,1}^{\text{cl}} - G_{m,m,1}^{\text{cl}} \\ G_{m+\ell,m+1,k}^{\text{cl}} & G_{m+\ell,m,k}^{\text{cl}} & G_{m+1,m,k+1}^{\text{cl}} & G_{m+\ell,m,k-1}^{\text{cl}} \\ G_{m+\ell,m+1,k+1}^{\text{cl}} & G_{m+\ell,m,k+1}^{\text{cl}} & G_{m+\ell,m,k+2}^{\text{cl}} & G_{m+\ell,m,k}^{\text{cl}} \\ -G_{m+\ell-1,m+1,k}^{\text{cl}} & -G_{m+\ell-1,m,k}^{\text{cl}} & -G_{m+\ell-1,m,k+1}^{\text{cl}} & -G_{m+\ell-1,m,k-1}^{\text{cl}} \end{vmatrix}. \quad (5.13)$$

The end result for the θ -graph contribution to the A -orientation of \mathcal{N}_2 in the closed case is (including the special correction graphs)

$$\begin{aligned} \frac{\mathcal{N}_{2,\text{closed},A}^\theta}{\mathcal{N}} &= -\frac{1}{8} + \frac{7}{8\pi} - \frac{5}{4\pi^2} - \frac{2(\pi-2)}{\pi^3}g(m) + \frac{1}{m} \left(\frac{1}{\pi^4} - \frac{3}{2\pi^3} + \frac{3}{16\pi} \right) \\ &+ \frac{1}{m^2} \left(\frac{13}{24\pi^4} - \frac{43}{48\pi^3} - \frac{3}{32\pi^2} + \frac{13}{64\pi} - \frac{(\pi-1)(\pi-2)}{2\pi^3}g(m) \right) + I_A^{h=2,\text{cl}}. \end{aligned} \quad (5.14)$$

The overall result for the A -orientation is then

$$\begin{aligned} \frac{\mathcal{N}_{2,\text{closed},A}}{\mathcal{N}} &= \frac{\mathcal{N}_{2,\text{closed},A}^{\text{local}}}{\mathcal{N}} + \frac{\mathcal{N}_{2,\text{closed},A}^{\text{loop}}}{\mathcal{N}} - \frac{\mathcal{N}_{2,\text{closed},A}^\theta}{\mathcal{N}} = \frac{1}{8} - \frac{3}{8\pi} - \frac{1}{\pi^2} + \frac{4}{\pi^3} + \frac{1}{m} \left(\frac{1}{\pi^3} - \frac{3}{16\pi} \right) \\ &+ \frac{1}{m^2} \left(-\frac{1}{4\pi^3} + \frac{17}{32\pi^2} - \frac{17}{64\pi} + \frac{\pi-2}{2\pi^2}g(m) \right) - I_A^{h=2,\text{cl}}. \end{aligned} \quad (5.15)$$

Terms $I_B^{h=2,\text{cl}}$ and $I_C^{h=2,\text{cl}}$ are defined similarly to $I_A^{h=2,\text{cl}}$, but with the sites in the Green functions rotated appropriately. We then get the probability that a site a distance m from the boundary has height two:

$$P_2^{\text{cl}}(m) = P_1^{\text{cl}}(m) + \frac{\mathcal{N}_{2,\text{closed},A}}{\mathcal{N}} + 2\frac{\mathcal{N}_{2,\text{closed},B}}{\mathcal{N}} + \frac{\mathcal{N}_{2,\text{closed},C}}{\mathcal{N}}. \quad (5.16)$$

Putting everything together, $P_2^{\text{cl}}(m)$ can be written as the sum of a power series in $1/m$ and three infinite sums of matrix determinants. It appears in the next section, along with corresponding expressions for other heights and boundary conditions.

The analysis of $P_3(m)$ in the UHP is similar to that of $P_2(m)$. The local and loop contributions, and the correction terms for the $\tilde{\theta}$ -graph, can again be calculated as matrix determinants, and expanded in $1/m$. Just as on the plane, the key change is that for the $\tilde{\theta}$ -graphs, we have an $-\epsilon$ bond from j_3 to itself, which changes the first row of the matrix determinants in Eqs. (5.12) and (5.13).

VI. GRAPH THEORETICAL RESULTS

We collect in this section the results obtained by putting together the various pieces corresponding to the local, loop and $\theta, \tilde{\theta}$ -graphs contributions to the 1-site probabilities $P_2(m)$ and $P_3(m)$, when the reference site lies at a distance m from the boundary. For each probability, we consider a closed and an open boundary. As in the previous section, I_B refers to the b -orientation, while $I_{AC} = I_A + I_C$ is the sum of the other two orientations.

When the boundary is closed, the probabilities are given by the following expressions,

$$\begin{aligned} P_2^{\text{cl}}(m) &= \frac{\pi^3 - 3\pi^2 - 4\pi + 24}{2\pi^3} + \frac{3\pi^2 - 6\pi - 8}{8\pi^3 m} - \frac{4\pi^2 - 9\pi + 20 - 16\pi(\pi - 2)g(m)}{8\pi^3 m^2} \\ &\quad - I_{AC}^{h=2,\text{cl}} - 2I_B^{h=2,\text{cl}} + \dots \end{aligned} \quad (6.1)$$

$$\begin{aligned} P_3^{\text{cl}}(m) &= P_2^{\text{cl}}(m) - \frac{\pi^3 - 18\pi^2 + 96 + 24\pi(\pi - 2)g(m)}{4\pi^3} + \frac{9(\pi - 4)}{16\pi^2 m} \\ &\quad + \frac{47\pi^2 - 128\pi + 52 + 24\pi(20 - 7\pi)g(m)}{32\pi^3 m^2} + 3I_{AC}^{h=3,\text{cl}} + 6I_B^{h=3,\text{cl}} + \dots \end{aligned} \quad (6.2)$$

with $g(m) = 2G_{0,0} - \frac{1}{2\pi}[\log m + \gamma + \frac{5}{2}\log 2] = G_{2m,0} + G_{0,0} + \mathcal{O}(m^{-2})$.

When the boundary is open, the expressions are slightly different and read

$$\begin{aligned} P_2^{\text{open}}(m) &= \frac{\pi^3 - 3\pi^2 - 4\pi + 24}{2\pi^3} - \frac{3\pi^2 - 6\pi - 8}{8\pi^3 m} + \frac{11\pi^2 - 40\pi + 64 + 32\pi(\pi - 2)\tilde{g}(m)}{16\pi^3 m^2} \\ &\quad - I_{AC}^{h=2,\text{op}} - 2I_B^{h=2,\text{op}} + \dots \end{aligned} \quad (6.3)$$

$$\begin{aligned} P_3^{\text{open}}(m) &= P_2^{\text{open}}(m) - \frac{\pi^3 - 18\pi^2 + 96 + 24\pi(\pi - 2)\tilde{g}(m)}{4\pi^3} - \frac{3(3\pi^2 - 4\pi - 16)}{16\pi^3 m} \\ &\quad - \frac{19\pi^2 - 94\pi + 158 - 12\pi(20 - 7\pi)\tilde{g}(m)}{16\pi^3 m^2} + 3I_{AC}^{h=3,\text{op}} + 6I_B^{h=3,\text{op}} + \dots \end{aligned} \quad (6.4)$$

with $\tilde{g}(m) = -\frac{1}{2\pi}[\log m + \gamma + \frac{5}{2}\log 2] = G_{2m,0} - G_{0,0} + \mathcal{O}(m^{-2})$.

In the previous four expressions, the explicit terms represent the local and loop contributions, as well as the special correction graphs encountered in the θ and $\tilde{\theta}$ graphs. All expansions are made to order 2 in m^{-1} , the ellipses standing for higher order terms. Finally, the remaining I_B and I_{AC} pieces correspond to the infinite sum contributions of the θ and $\tilde{\theta}$ graphs, which we now specify. As we have seen above, these terms include a summation over the discrete UHP, and also multiple integrals from the integral representation of the Green matrix entries. They are functions of the single variable m .

The functions I_{AC} in the various cases are equal to

$$I_{AC}(m) = \sum_{k \in \mathbb{Z}} \sum_{\ell=1-m}^{\infty} \iint_{-\pi}^{\pi} \frac{d\alpha_1 d\beta_1}{8\pi^2} \frac{e^{-i\ell\alpha_1} \pm e^{i(2m+\ell-1)\alpha_1}}{2 - \cos \alpha_1 - \cos \beta_1} \iint_{-\pi}^{\pi} \frac{d\alpha_2 d\beta_2}{8\pi^2} \frac{e^{-i\ell\alpha_2} \pm e^{i(2m+\ell-1)\alpha_2}}{2 - \cos \alpha_2 - \cos \beta_2}$$

$$\times \iint_{-\pi}^{\pi} \frac{d\alpha_3 d\beta_3}{8\pi^2} (-2i \sin \alpha_3) \frac{e^{-i\ell\alpha_3} \mp e^{i(2m+\ell-1)\alpha_3}}{2 - \cos \alpha_3 - \cos \beta_3} e^{ik(\beta_1+\beta_2+\beta_3)} e^{i\beta_2} [\det M_A - \det M_C], \quad (6.5)$$

where the matrices M_A and M_C take the form

$$M_A = \begin{pmatrix} c+e & e^{i\alpha_1} & e^{i\alpha_2} & e^{i\alpha_3} \\ \frac{a+c}{2} & 1 & 1 & 1 \\ \frac{b+c}{2} & e^{i\beta_1} & e^{i\beta_2} & e^{i\beta_3} \\ \frac{b+c}{2} & e^{-i\beta_1} & e^{-i\beta_2} & e^{-i\beta_3} \end{pmatrix}, \quad M_C = \begin{pmatrix} -d+e & e^{-i\alpha_1} & e^{-i\alpha_2} & e^{-i\alpha_3} \\ \frac{a-c}{2} & 1 & 1 & 1 \\ \frac{b-c}{2} & e^{i\beta_1} & e^{i\beta_2} & e^{i\beta_3} \\ \frac{b-c}{2} & e^{-i\beta_1} & e^{-i\beta_2} & e^{-i\beta_3} \end{pmatrix}. \quad (6.6)$$

In the integrand, the upper signs are chosen for a closed boundary, and the lower ones for an open boundary, independently of the height value ($h = 2$ or $h = 3$) one considers. The dependence on h is entirely contained in the values of the parameters a, b, c, d and e , which also depend on the type of boundary condition:

$$\text{height 2, closed : } \begin{cases} a = -\frac{1}{2} + \frac{1}{8\pi m^2}, & c = -\frac{2m+1}{4\pi m^2}, \\ b = \frac{1}{2} - \frac{2}{\pi} + \frac{1}{8\pi m^2}, & d = 0, \quad e = -\frac{3}{4} + \frac{1}{4\pi m} + \frac{5}{16\pi m^2}, \end{cases} \quad (6.7)$$

$$\text{height 2, open : } \begin{cases} a = -\frac{1}{2} - \frac{1}{8\pi m^2}, & c = \frac{1}{2\pi m}, \\ b = \frac{1}{2} - \frac{2}{\pi} - \frac{1}{8\pi m^2}, & d = 0, \quad e = -\frac{3}{4} - \frac{1}{4\pi m} - \frac{3}{16\pi m^2}, \end{cases} \quad (6.8)$$

$$\text{height 3, closed : } \begin{cases} a = 2g(m) - \frac{1}{2} + \frac{1}{2\pi m} + \frac{13}{48\pi m^2}, & c = d = -\frac{2m+1}{4\pi m^2}, \\ b = 2g(m) - \frac{2}{\pi} + \frac{1}{2\pi m} + \frac{7}{48\pi m^2}, & e = g(m) + \frac{1}{4\pi m} + \frac{31}{96\pi m^2}, \end{cases} \quad (6.9)$$

$$\text{height 3, open : } \begin{cases} a = -2\tilde{g}(m) - \frac{1}{2} - \frac{7}{48\pi m^2}, & c = d = \frac{1}{2\pi m}, \\ b = -2\tilde{g}(m) - \frac{2}{\pi} - \frac{1}{48\pi m^2}, & e = -\tilde{g}(m) - \frac{25}{96\pi m^2}. \end{cases} \quad (6.10)$$

In a similar way, the other functions I_B can be written

$$\begin{aligned} I_B(m) &= \sum_{k \in \mathbb{Z}} \sum_{\ell=1-m}^{\infty} \iint_{-\pi}^{\pi} \frac{d\alpha_1 d\beta_1}{8\pi^2} \frac{e^{-i\ell\alpha_1} \pm e^{i(2m+\ell-1)\alpha_1}}{2 - \cos \alpha_1 - \cos \beta_1} \iint_{-\pi}^{\pi} \frac{d\alpha_2 d\beta_2}{8\pi^2} \frac{e^{-i\ell\alpha_2} \pm e^{i(2m+\ell-1)\alpha_2}}{2 - \cos \alpha_2 - \cos \beta_2} \\ &\times \iint_{-\pi}^{\pi} \frac{d\alpha_3 d\beta_3}{8\pi^2} \frac{[e^{i(1-\ell)\alpha_3} \pm e^{i(2m+\ell-2)\alpha_3}]e^{-i\beta_2} + [e^{-i(\ell+1)\alpha_3} \pm e^{i(2m+\ell)\alpha_3}]e^{i\beta_2}}{2 - \cos \alpha_3 - \cos \beta_3} \\ &\times e^{ik(\beta_1+\beta_2+\beta_3)} \det M_B, \end{aligned} \quad (6.11)$$

where the matrix M_B has the form

$$M_B = \begin{pmatrix} a' & e^{-i\beta_1} & e^{-i\beta_2} & e^{-i\beta_3} \\ b' & 1 & 1 & 1 \\ c' - d' & e^{i\alpha_1} & e^{i\alpha_2} & e^{i\alpha_3} \\ c' + d' & e^{-i\alpha_1} & e^{-i\alpha_2} & e^{-i\alpha_3} \end{pmatrix}. \quad (6.12)$$

The choice of the signs is the same as for I_{AC} , and again the actual values of the parameters a', b', c' and d' depend on which height variable and which boundary condition one considers,

$$\text{height 2, closed : } \begin{cases} a' = -\frac{3}{4} + \frac{1}{16\pi m^2}, & c' = \frac{1}{4} - \frac{1}{\pi} - \frac{1}{16\pi m^2}, \\ b' = -\frac{1}{4} - \frac{1}{16\pi m^2}, & d' = 0, \end{cases} \quad (6.13)$$

$$\text{height 2, open : } \begin{cases} a' = -\frac{3}{4} - \frac{1}{16\pi m^2}, & c' = \frac{1}{4} - \frac{1}{\pi} + \frac{1}{16\pi m^2}, \\ b' = -\frac{1}{4} + \frac{1}{16\pi m^2}, & d' = 0, \end{cases} \quad (6.14)$$

$$\text{height 3, closed : } \begin{cases} a' = g(m) + \frac{1}{4\pi m} + \frac{7}{96\pi m^2}, & c' = g(m) - \frac{1}{\pi} + \frac{1}{4\pi m} + \frac{7}{96\pi m^2}, \\ b' = g(m) - \frac{1}{4} + \frac{1}{4\pi m} + \frac{1}{96\pi m^2}, & d' = \frac{2m+1}{8\pi m^2}, \end{cases} \quad (6.15)$$

$$\text{height 3, open : } \begin{cases} a' = -\tilde{g}(m) - \frac{1}{96\pi m^2}, & c' = -\tilde{g}(m) - \frac{1}{\pi} - \frac{1}{96\pi m^2}, \\ b' = -\tilde{g}(m) - \frac{1}{4} + \frac{5}{96\pi m^2}, & d' = -\frac{1}{4\pi m}. \end{cases} \quad (6.16)$$

In order to make the expressions of $P_2(m)$ and $P_3(m)$ completely explicit, the remaining task is to compute the asymptotic value of the functions I_{AC} and I_B , for the different heights and boundary conditions. As we will see, these functions have an expansion in inverse powers of m , times logarithmic corrections, which we need to compute to order m^{-2} .

VII. ASYMPTOTIC ANALYSIS

We will not give all the details of the calculation of I_{AC} and I_B for the open and closed boundaries, as the analysis is technical and rather long. However, as an illustration of how this analysis can actually be carried out, we give here some details of the analysis of I_{AC} for the closed boundary. The reader who is not interested in these technical details may skip this section and go straight to the next one, where the final results for the probabilities $P_2(m)$ and $P_3(m)$ are given.

The analysis proceeds by a long sequence of otherwise elementary steps. As a very first step, the similarity of M_A and M_C allows us to write the difference of their determinants (appearing in $I_{AC}^{cl}(m)$) in a simpler form:

$$\det M_A - \det M_C = \begin{vmatrix} c+d & \cos \alpha_1 & \cos \alpha_2 & \cos \alpha_3 \\ c & 1 & 1 & 1 \\ c & e^{i\beta_1} & e^{i\beta_2} & e^{i\beta_3} \\ c & e^{-i\beta_1} & e^{-i\beta_2} & e^{-i\beta_3} \end{vmatrix} + \begin{vmatrix} 0 & i \sin \alpha_1 & i \sin \alpha_2 & i \sin \alpha_3 \\ a & 1 & 1 & 1 \\ b & e^{i\beta_1} & e^{i\beta_2} & e^{i\beta_3} \\ b & e^{-i\beta_1} & e^{-i\beta_2} & e^{-i\beta_3} \end{vmatrix}, \quad (7.1)$$

which no longer depends on e . We leave the parameters a, b, c and d free to cover the two cases $h = 2$ and $h = 3$. We denote by U_1 and U_2 the two new matrices in the previous equation, and accordingly we decompose I_{AC} into two pieces, $I_{AC}^{cl}(m) = I_1^{cl}(m) + I_2^{cl}(m)$. They can be handled in the same way, so we focus on the contribution of U_2 , that of U_1 being simpler.

In (6.5), the summation over k and a number of integrations can be performed: the summation over k produces a delta function $2\pi\delta(\beta_1 + \beta_2 + \beta_3)$, which then makes trivial the integration over β_3 ; the contour integrations over the three variables $\alpha_1, \alpha_2, \alpha_3$ may also be carried out. This eventually leaves an expression which involves one semi-infinite summation over ℓ , and two integrations over β_1, β_2 . Before giving the result of these easy steps, we introduce the following notation. We set

$$y(\beta) = 2 - \cos \beta, \quad t(\beta) = y - \sqrt{y^2 - 1}, \quad u(\beta) = t^{-1} = y + \sqrt{y^2 - 1}, \quad (7.2)$$

and the same functions with indices y_j, t_j, u_j if the argument is β_j . They are even periodic functions of β_j , with t_j (resp. u_j) being the root of $z^2 - 2y_j z + 1 = 0$ inside (resp. outside) the unit circle, for $y > 1$. The range of values of $y(\beta)$ is the interval $[1, 3]$, but more importantly for what follows, $t(\beta)$ is strictly positive, smaller than 1, and takes the value 1 at $\beta = 0$ only (or a multiple of 2π). The functions $t(\beta)$ and $u(\beta)$ are continuous but have discontinuous derivatives at $\beta = 0$.

By expanding the determinant of U_2 on the first row, we obtain

$$\det U_2 = -i \sin \alpha_1 D(\beta_2, \beta_3) + i \sin \alpha_2 D(\beta_1, \beta_3) - i \sin \alpha_3 D(\beta_1, \beta_2), \quad (7.3)$$

where the function $D(x, y)$ is a 3-by-3 subdeterminant, given by

$$D(x, y) = 4i \left[a \cos \frac{x-y}{2} - b \cos \frac{x+y}{2} \right] \sin \frac{x-y}{2}. \quad (7.4)$$

By using the following formulas, in which $n \in \mathbb{Z}$,

$$\int_{-\pi}^{\pi} \frac{d\alpha}{2\pi} \frac{e^{in\alpha}}{y - \cos \alpha} = \frac{t^{|n|}}{\sqrt{y^2 - 1}}, \quad \int_{-\pi}^{\pi} \frac{d\alpha}{2\pi} \frac{e^{in\alpha} \sin \alpha}{y - \cos \alpha} = i \operatorname{sgn}(n) t^{|n|}, \quad (\operatorname{sgn}(0) = 0) \quad (7.5)$$

$$\int_{-\pi}^{\pi} \frac{d\alpha}{2\pi} \frac{e^{in\alpha} \sin^2 \alpha}{y - \cos \alpha} = \left[-\sqrt{y^2 - 1} + \frac{u}{2} \delta_{n^2, 1} + y \delta_{n, 0} \right] t^{|n|}, \quad (7.6)$$

the summation over k and the integration over $\alpha_1, \alpha_2, \alpha_3$ and β_3 yield

$$\begin{aligned}
I_2^{\text{cl}}(m) &= \frac{1}{16\pi^2} \iint_{-\pi}^{\pi} d\beta_1 d\beta_2 \frac{1}{\sqrt{y_2^2 - 1}} (e^{i\beta_2} - e^{i\beta_1}) D(\beta_2, \beta_3) \\
&\quad \sum_{\ell=1-m}^{\infty} [-\text{sgn}(\ell)t_1^{|\ell|} + t_1^{2m+\ell-1}] [t_2^{|\ell|} + t_2^{2m+\ell-1}] [\text{sgn}(\ell)t_3^{|\ell|} + t_3^{2m+\ell-1}] \\
&+ \frac{1}{16\pi^2} \iint_{-\pi}^{\pi} d\beta_1 d\beta_2 \frac{\sqrt{y_3^2 - 1}}{\sqrt{(y_1^2 - 1)(y_2^2 - 1)}} e^{i\beta_2} D(\beta_1, \beta_2) \\
&\quad \sum_{\ell=1-m}^{\infty} [t_1^{|\ell|} + t_1^{2m+\ell-1}] [t_2^{|\ell|} + t_2^{2m+\ell-1}] [t_3^{|\ell|} - t_3^{2m+\ell-1}] \\
&- \frac{1}{16\pi^2} \iint_{-\pi}^{\pi} d\beta_1 d\beta_2 \frac{1}{\sqrt{(y_1^2 - 1)(y_2^2 - 1)}} e^{i\beta_2} D(\beta_1, \beta_2) \left\{ y_3 (1 + t_1^{2m-1}) (1 + t_2^{2m-1}) \right. \\
&\quad \left. + \frac{1}{2}(t_1 + t_1^{2m})(t_2 + t_2^{2m}) + \frac{1}{2}(t_1 + t_1^{2m-2})(t_2 + t_2^{2m-2}) \right\}, \tag{7.7}
\end{aligned}$$

where we have kept β_3 as a shorthand notation for $-\beta_1 - \beta_2$.

In the third double integral, which has no summation over ℓ , the two variables can be decoupled, and the two simple integrals can be carried out by using

$$\int_{-\pi}^{\pi} d\beta \frac{t^n e^{ik\beta}}{\sqrt{y^2 - 1}} = 4\pi G_{n,k}. \tag{7.8}$$

The result of the integrals is then expanded for large m by using the following asymptotic expansion of the Green matrix ($k, \ell \ll x$)

$$G_{x+\ell,k} = G_{x,0} - \frac{\ell}{2\pi x} + \frac{\ell^2 - k^2}{4\pi x^2} + \dots \tag{7.9}$$

The calculations are straightforward, and one finds that the third double integral in (7.7) equals

$$\begin{aligned}
&(a - b) \left(\frac{1}{2} - \frac{4}{\pi} - \frac{1}{2\pi m^2} \right) [G_{0,0} + G_{2m,0}] + a \left(\frac{1}{2} - \frac{3}{2\pi} + \frac{2}{\pi^2} \right) + b \left(\frac{1}{8} - \frac{2}{\pi^2} \right) \\
&\quad + \frac{a - b}{2\pi m} \left(\frac{1}{4} - \frac{2}{\pi} \right) + \frac{1}{16\pi m^2} \left\{ a \left(\frac{9}{2} - \frac{4}{\pi} \right) + b \left(-3 + \frac{8}{\pi} \right) \right\} + \dots \tag{7.10}
\end{aligned}$$

The summations in the remaining two double integrals are similar: for $\ell > 0$, they are equal up to a sign and the permutation $\beta_1 \leftrightarrow \beta_3$; for $\ell < 0$, they are equal up to a sign. Separating the three parts $\ell > 0$, $\ell = 0$ and $\ell < 0$, which we call respectively Y_1 , Y_2 and Y_3 , we can rewrite the first two integrals in (7.7) as

$$+ \frac{1}{16\pi^2} \iint_{-\pi}^{\pi} d\beta_1 d\beta_2 \frac{D(\beta_1, \beta_2)}{\sqrt{(y_1^2 - 1)(y_2^2 - 1)}} \left[\sqrt{y_3^2 - 1} e^{i\beta_2} - \sqrt{y_1^2 - 1} (e^{i\beta_2} - e^{i\beta_3}) \right]$$

$$\begin{aligned}
& \sum_{\ell=0}^{\infty} (t_1^\ell + t_1^{2m+\ell-1}) (t_2^\ell + t_2^{2m+\ell-1}) (t_3^\ell - t_3^{2m+\ell-1}) \\
& - \frac{1}{16\pi^2} \iint_{-\pi}^{\pi} d\beta_1 d\beta_2 \frac{D(\beta_2, \beta_3)}{\sqrt{y_2^2 - 1}} (e^{i\beta_2} - e^{i\beta_1}) (1 + t_2^{2m-1})(1 - t_1^{2m-1} + t_3^{2m-1}) \\
& + \frac{1}{16\pi^2} \iint_{-\pi}^{\pi} d\beta_1 d\beta_2 \frac{e^{i\beta_2} D(\beta_1, \beta_2) \sqrt{y_3^2 - 1} + (e^{i\beta_2} - e^{i\beta_1}) D(\beta_2, \beta_3) \sqrt{y_1^2 - 1}}{\sqrt{(y_1^2 - 1)(y_2^2 - 1)}} \\
& \sum_{\ell=1-m}^{-1} (t_1^{-\ell} + t_1^{2m+\ell-1}) (t_2^{-\ell} + t_2^{2m+\ell-1}) (t_3^{-\ell} - t_3^{2m+\ell-1}). \tag{7.11}
\end{aligned}$$

Y_2 , the second integral in the previous expression, contains no summation, and is the simplest one to evaluate. If one expands the integrand, each term gives rise to a double integral which can be decoupled, computed exactly, and finally expanded by the procedure explained above. Y_1 and Y_3 are more complicated. We will give the details for Y_1 only, as it contains all the necessary ingredients to compute not only Y_3 but also I_1^{cl} , and in fact all the integrals I_{AC} and I_B needed to compute the 1-site probabilities on the UHP.

The summation in Y_1 is straightforward, and yields

$$\begin{aligned}
Y_1 = \frac{1}{16\pi^2} \iint_{-\pi}^{\pi} d\beta_1 d\beta_2 \frac{D(\beta_1, \beta_2)}{\sqrt{(y_1^2 - 1)(y_2^2 - 1)}} \left[\sqrt{y_3^2 - 1} e^{i\beta_2} - \sqrt{y_1^2 - 1} (e^{i\beta_2} - e^{i\beta_3}) \right] \\
\frac{1}{1 - t_1 t_2 t_3} (1 + t_1^{2m-1}) (1 + t_2^{2m-1}) (1 - t_3^{2m-1}). \tag{7.12}
\end{aligned}$$

Because $D(\beta_1, \beta_2)$ is odd under $\beta_1, \beta_2 \rightarrow -\beta_1, -\beta_2$, the exponentials can be replaced by their imaginary parts,

$$\begin{aligned}
Y_1 = -\frac{1}{2\pi^2} \iint_{-\pi}^{\pi} d\beta_1 d\beta_2 \frac{Q_1(\beta_1, \beta_2)}{\sqrt{(y_1^2 - 1)(y_2^2 - 1)}} \frac{1}{1 - t_1 t_2 t_3} \times \\
[1 + t_1^{2m-1} + t_2^{2m-1} - t_3^{2m-1} + (t_1 t_2)^{2m-1} - (t_1 t_3)^{2m-1} - (t_2 t_3)^{2m-1} - (t_1 t_2 t_3)^{2m-1}], \tag{7.13}
\end{aligned}$$

where the function Q_1 is defined as

$$Q_1(\beta_1, \beta_2) = -\frac{i}{8} D(\beta_1, \beta_2) \left[\sqrt{y_3^2 - 1} \sin \beta_2 - \sqrt{y_1^2 - 1} (\sin \beta_2 - \sin \beta_3) \right]. \tag{7.14}$$

In this expression for Y_1 , we distinguish three pieces according to the number of t_j to a large power that they contain, namely 1, then $t_1^{2m-1} + t_2^{2m-1} - t_3^{2m-1}$, and finally $(t_1 t_2)^{2m-1} - (t_1 t_3)^{2m-1} - (t_2 t_3)^{2m-1} - (t_1 t_2 t_3)^{2m-1}$.

A. First piece in Y_1 : no large power of t_j

This first term is singular: $1/\sqrt{(y_1^2 - 1)(y_2^2 - 1)}$ has a single pole on the lines $\beta_1 = 0$ and $\beta_2 = 0$, where $Q_1(\beta_1, \beta_2)$ does not vanish (moreover $(1 - t_1 t_2 t_3)^{-1}$ is singular at the origin $\beta_1 = \beta_2 = 0$,

though that singularity alone is integrable). In order to isolate the singular part, we write this first piece as

$$\begin{aligned} & -\frac{1}{2\pi^2} \iint_{-\pi}^{\pi} \frac{d\beta_1 d\beta_2}{\sqrt{(y_1^2-1)(y_2^2-1)}} \left[\frac{Q_1(\beta_1, \beta_2)}{1-t_1 t_2 t_3} - \frac{Q_1(0, \beta_2)}{1-t_2^2} - \frac{Q_1(\beta_1, 0)}{1-t_1^2} \right] \\ & -\frac{1}{2\pi^2} \iint_{-\pi}^{\pi} \frac{d\beta_1 d\beta_2}{\sqrt{(y_1^2-1)(y_2^2-1)}} \left[\frac{Q_1(0, \beta_2)}{1-t_2^2} + \frac{Q_1(\beta_1, 0)}{1-t_1^2} \right]. \end{aligned} \quad (7.15)$$

The second integral contains the singularity, proportional to $G_{0,0}$. Using $Q_1(\beta, 0) = Q_1(0, \beta) = -\frac{a-b}{4} \sqrt{y^2-1} \sin^2 \beta$, it is equal to

$$\frac{1}{2\pi^2} \frac{a-b}{2} \int_{-\pi}^{\pi} \frac{d\beta_1}{\sqrt{y_1^2-1}} \int_{-\pi}^{\pi} d\beta_2 \frac{\sin^2 \beta_2}{1-t_2^2} = \frac{a-b}{\pi} \left(2 + \frac{\pi}{2}\right) G_{0,0}. \quad (7.16)$$

The first integral is convergent by construction, and separating into parts proportional to a and b , can be written as $-\frac{a}{4\pi^2} T_1 + \frac{b}{4\pi^2} T_2$, where T_1, T_2 are numerical integrals:

$$\begin{aligned} T_1 = \int_0^{\pi} \frac{d\beta_1}{\sqrt{y_1^2-1}} \int_{-\pi}^{\pi} \frac{d\beta_2}{\sqrt{y_2^2-1}} \left\{ \frac{\sin(\beta_1 - \beta_2)}{1-t_1 t_2 t_3} \left[\sqrt{y_3^2-1} \sin \beta_2 - \sqrt{y_1^2-1} (\sin \beta_2 - \sin \beta_3) \right] \right. \\ \left. + \frac{\sqrt{y_1^2-1} \sin^2 \beta_1}{1-t_1^2} + \frac{\sqrt{y_2^2-1} \sin^2 \beta_2}{1-t_2^2} \right\}, \end{aligned} \quad (7.17)$$

$$\begin{aligned} T_2 = \int_0^{\pi} \frac{d\beta_1}{\sqrt{y_1^2-1}} \int_{-\pi}^{\pi} \frac{d\beta_2}{\sqrt{y_2^2-1}} \left\{ \frac{\sin \beta_1 - \sin \beta_2}{1-t_1 t_2 t_3} \left[\sqrt{y_3^2-1} \sin \beta_2 - \sqrt{y_1^2-1} (\sin \beta_2 - \sin \beta_3) \right] \right. \\ \left. + \frac{\sqrt{y_1^2-1} \sin^2 \beta_1}{1-t_1^2} + \frac{\sqrt{y_2^2-1} \sin^2 \beta_2}{1-t_2^2} \right\}. \end{aligned} \quad (7.18)$$

These integrals cannot be factorized, and therefore not easy to evaluate analytically, but a numerical integration yields the values

$$T_1 = 16.0897, \quad T_2 = 17.4056. \quad (7.19)$$

The contribution of the first term is thus

$$\text{first term of } Y_1 = (a-b) \frac{\pi+4}{2\pi} G_{0,0} - \frac{a}{4\pi^2} T_1 + \frac{b}{4\pi^2} T_2. \quad (7.20)$$

B. Second piece in Y_1 : one large power of a t_j

The second piece contains the three terms in Y_1 that involve only one t_j to a large power, see (7.13). Making appropriate permutations of the variables and using the reflection symmetry $Q_1(-\beta_1, -\beta_2) = Q_1(\beta_1, \beta_2)$, it may be written as

$$-\frac{1}{2\pi^2} \iint_{-\pi}^{\pi} \frac{d\beta_1 d\beta_2}{\sqrt{y_2^2-1}} \frac{t_1^{2m-1}}{1-t_1 t_2 t_3} \left\{ 2 \frac{Q_1^{\text{sym}}(\beta_1, \beta_2)}{\sqrt{y_1^2-1}} - \frac{Q_1^{\text{sym}}(\beta_2, \beta_3)}{\sqrt{y_1^3-1}} \right\} \equiv -\frac{1}{2\pi^2} \int_0^{\pi} d\beta_1 t_1^{2m-1} f(\beta_1), \quad (7.21)$$

where $Q_1^{\text{sym}}(x, y) = \frac{1}{2}[Q_1(x, y) + Q_1(y, x)]$ is the symmetrized function.

The function $t_1 = t(\beta_1)$ equals 1 at $\beta_1 = 0$ and decreases monotonically as β_1 increases towards π . Therefore for m large, t_1^m is exponentially decreasing, so that the dependence in m of the integral is controlled by the way the function f behaves near $\beta_1 = 0$.

To see this more precisely, let us first establish the following bound, which will prove extremely useful later,

$$\left| t(\beta)^m - e^{-m|\beta|} \left(1 + \frac{m|\beta|^3}{12} - \frac{m|\beta|^5}{96} \right) \right| \leq \frac{162 e^{-6}}{m^4} + \mathcal{O}(m^{-6}). \quad (7.22)$$

To prove it, one may notice that the function on the l.h.s. (i.e. the difference) vanishes at $\beta = 0$, and has a unique maximum which moves towards the origin and decreases in height as m increases. The location of the maximum, β^* , can be solved iteratively as a series in $\frac{1}{m}$, yielding $\beta^* = \frac{6}{m} + \frac{237}{70m^3} + \frac{2607}{196m^5} + \dots$. One then simply bounds the l.h.s. by its value at β^* . The function $e^{-m\beta} \left(1 + \frac{m\beta^3}{12} - \frac{m\beta^5}{96} \right)$ was chosen so that its Taylor expansion around zero matched that of $t(\beta)^m$ to order 5.

Assume that the power expansion of $f(\beta_1)$ contains a term of dimension $k \geq -1$, namely a term β_1^k , times possible powers of $\log \beta_1$. Then at the order m^{-2} , and for $k > -1$,

$$\int_0^\pi d\beta_1 t_1^m \beta_1^k \simeq \int_0^\infty d\beta_1 e^{-m\beta_1} \left(1 + \frac{m\beta_1^3}{12} - \frac{m\beta_1^5}{96} \right) \beta_1^k \simeq \int_0^\infty d\beta_1 e^{-m\beta_1} \beta_1^k = \mathcal{O}(m^{-1-k}). \quad (7.23)$$

We see that we may simply replace t_1^m by $e^{-m\beta_1}$, and that the terms in the expansion of f of degree 2 or higher in β_1 do not contribute at order m^{-2} . A simple dimensional analysis shows that powers of $\log \beta_1$ simply bring powers of m in the result of the integral.

When $k = -1$, the previous result essentially goes through (up to a divergent constant term and a logarithmic term). Since $\sqrt{y_1^2 - 1} = \beta_1 + \dots$ near the positive origin, one has

$$\int_0^\pi d\beta_1 \frac{t_1^{2m}}{\beta_1} = \int_0^\pi d\beta_1 \frac{t_1^{2m}}{\sqrt{y_1^2 - 1}} + \mathcal{O}(m^{-1}) = 2\pi G_{2m,0} + \mathcal{O}(m^{-1}). \quad (7.24)$$

Coming back to (7.21), the function $f(\beta_1)$ is itself given by an integral

$$f(\beta_1) = 2 \int_{-\pi}^\pi \frac{d\beta_2}{\sqrt{y_2^2 - 1}} \frac{1}{1 - t_1 t_2 t_3} \left\{ 2 \frac{Q_1^{\text{sym}}(\beta_1, \beta_2)}{\sqrt{y_1^2 - 1}} - \frac{Q_1^{\text{sym}}(\beta_2, \beta_3)}{\sqrt{y_1^3 - 1}} \right\} \equiv \int_{-\pi}^\pi d\beta_2 \frac{G_1(\beta_1, \beta_2)}{1 - t_1 t_2 t_3}. \quad (7.25)$$

To evaluate the dimension of $f(\beta_1)$ near $\beta_1 = 0$, one can make a Laurent expansion in β_1 inside the integral, that is, of the integrand $G_1(\beta_1, \beta_2)/(1 - t_1 t_2 t_3)$. One easily checks that it starts with a dimension -1 term near $\beta_1 = 0$, and so does the expansion of $f(\beta_1)$. It implies that the integral (7.21) will contribute to order m^0 (a divergent term), and to orders m^{-1} and m^{-2} .

Although this procedure of making the Laurent expansion go through the integral—we call it the ETI procedure, Expand Then Integrate—gives the right dimension of f , it is not valid in general when the actual series expansion is required. In particular, it can lead to wrong results when the expansion in powers of β_1 of the integrand has coefficients which are non-integrable functions of β_2 , thereby producing potentially spurious divergences which the original integral does not have. These spurious divergences are the signal that the integral defining the function f in fact does not have a Laurent expansion. In our case, this phenomenon will manifest itself by the presence of logarithms.

We decompose the integration domain of β_2 into three pieces, $[0, \pi]$, $[-\beta_1, 0]$ and $[-\pi, -\beta_1]$, and first consider the region $[0, \pi]$. The expansion of G_1 in β_1 is well-defined, with regular coefficients,

$$G_1(\beta_1, \beta_2) = \frac{c_{-1}(\beta_2)}{\beta_1} + c_0(\beta_2) + c_1(\beta_2)\beta_1 + \dots \quad (7.26)$$

Since $1 - t_1 t_2 t_3$ does not vanish (for $\beta_1 > 0$), the previous expansion may be inserted in the integral over β_2 , leading to a sum of terms of the form $\int d\beta_2 c(\beta_2)/(1 - t_1 t_2 t_3)$, where $c(\beta_2)$ is one of the coefficients in the expansion of G_1 . These in turn can be written

$$\begin{aligned} \int_0^\pi d\beta_2 \frac{c(\beta_2)}{1 - t_1 t_2 t_3} &= \int_0^\pi d\beta_2 \left\{ \frac{c(\beta_2)}{1 - t_1 t_2 t_3} - \frac{c(0) - \beta_1 c'(0) + \beta_1^2 [c(0)/8 + c''(0)/2]}{2\sqrt{y_3^2 - 1}} \right\} \\ &+ \int_0^\pi d\beta_2 \frac{c(0) - \beta_1 c'(0) + \beta_1^2 [c(0)/8 + c''(0)/2]}{2\sqrt{y_3^2 - 1}}. \end{aligned} \quad (7.27)$$

The virtue of this decomposition is that the first integral, with its subtraction term, has a β_1 expansion with coefficients which are integrable functions of β_2 (up to order 2 in β_1), for which the ETI procedure may be used. Thus

$$\begin{aligned} \int_0^\pi d\beta_2 \frac{c(\beta_2)}{1 - t_1 t_2 t_3} &= \int_0^\pi d\beta_2 \frac{c(\beta_2)}{1 - t_1 t_2 t_3} \Big|_{\text{ETI}} \\ &+ \frac{1}{2} \left(c(0) - \beta_1 c'(0) + \beta_1^2 \left[\frac{c(0)}{8} + \frac{c''(0)}{2} \right] + \dots \right) \int_0^\pi d\beta_2 \left\{ \frac{1}{\sqrt{y_3^2 - 1}} - \frac{1}{\sqrt{y_3^2 - 1}} \Big|_{\text{ETI}} \right\}. \end{aligned} \quad (7.28)$$

From the explicit expansion of the coefficients near the positive origin, $\beta_2 \sim 0^+$,

$$c_{-1}(\beta_2) = -(a - b)\beta_2^2 + \dots, \quad c_0(\beta_2) = \frac{a - b}{4}\beta_2^3 + \dots, \quad c_1(\beta_2) = \frac{3(a - b)}{2} + \dots, \quad (7.29)$$

we obtain

$$\int_0^\pi d\beta_2 \frac{G_1(\beta_1, \beta_2)}{1 - t_1 t_2 t_3} = \int_0^\pi d\beta_2 \frac{G_1(\beta_1, \beta_2)}{1 - t_1 t_2 t_3} \Big|_{\text{ETI}} + \frac{a - b}{4}\beta_1 \int_0^\pi d\beta_2 \left\{ \frac{1}{\sqrt{y_3^2 - 1}} - \frac{1}{\sqrt{y_3^2 - 1}} \Big|_{\text{ETI}} \right\} + \dots \quad (7.30)$$

The last two integrals can be computed explicitly to order 0 in β_1 ,

$$\begin{aligned} \int_0^\pi \frac{d\beta_2}{\sqrt{y_3^2 - 1}} &= \int_{\beta_1}^{\pi+\beta_1} \frac{d\beta_2}{\sqrt{y_2^2 - 1}} \simeq \int_{\beta_1}^\pi \frac{d\beta_2}{\sqrt{y_2^2 - 1}} = \operatorname{arcth} \frac{\sqrt{2} \cos \frac{\beta_1}{2}}{\sqrt{3 + \cos(\pi - \beta_1)}} \\ &= -\log \beta_1 + \frac{3}{2} \log 2 + \dots \end{aligned} \quad (7.31)$$

whereas the other one yields $2\pi G_{0,0}$ to order 0. We find

$$\int_0^\pi d\beta_2 \frac{G_1(\beta_1, \beta_2)}{1 - t_1 t_2 t_3} = \int_0^\pi d\beta_2 \frac{G_1(\beta_1, \beta_2)}{1 - t_1 t_2 t_3} \Big|_{\text{ETI}} - \frac{a-b}{4} \beta_1 [2\pi G_{0,0} + \log \beta_1 - \frac{3}{2} \log 2] + \dots \quad (7.32)$$

The region $\beta_2 \in [-\beta_1, 0]$ is left invariant under the change of variable $\beta_2 \rightarrow -\beta_1 - \beta_2 = \beta_3$.

Thus the integrand may be symmetrized in $\beta_2 \leftrightarrow \beta_3$,

$$\int_{-\beta_1}^0 d\beta_2 \frac{G_1(\beta_1, \beta_2)}{1 - t_1 t_2 t_3} = \frac{1}{2} \int_{-\beta_1}^0 d\beta_2 \frac{G_1(\beta_1, \beta_2) + G_1(\beta_1, \beta_3)}{1 - t_1 t_2 t_3}. \quad (7.33)$$

The two variables β_1 and β_2 being small, a double series expansion can be used which shows that the integrand has dimension 4 (in the two variables). Therefore the integral over β_2 brings a contribution at order β_1^5 and higher, and can be neglected.

The third and last portion $[-\pi, -\beta_1]$ is sent onto $[0, \pi - \beta_1]$ by the change of variable $\beta_2 \rightarrow \beta_3$, which is then further extended to $[0, \pi]$, since the integrand is of order β_1 around $\beta_2 = \pi$:

$$\int_{-\pi}^{-\beta_1} d\beta_2 \frac{G_1(\beta_1, \beta_2)}{1 - t_1 t_2 t_3} = \int_0^{\pi-\beta_1} d\beta_2 \frac{\tilde{G}_1(\beta_1, \beta_2)}{1 - t_1 t_2 t_3} \simeq \int_0^\pi d\beta_2 \frac{\tilde{G}_1(\beta_1, \beta_2)}{1 - t_1 t_2 t_3}, \quad (7.34)$$

where $\tilde{G}_1(\beta_1, \beta_2) = G_1(\beta_1, \beta_3)$.

Repeating the same calculation as with G_1 , we obtain

$$\int_{-\pi}^{-\beta_1} d\beta_2 \frac{G_1(\beta_1, \beta_2)}{1 - t_1 t_2 t_3} = \int_0^\pi d\beta_2 \frac{\tilde{G}_1(\beta_1, \beta_2)}{1 - t_1 t_2 t_3} \Big|_{\text{ETI}} - \frac{7(a-b)}{4} \beta_1 [2\pi G_{0,0} + \log \beta_1 - \frac{3}{2} \log 2] + \dots \quad (7.35)$$

All together, we find that the function f is given by

$$f(\beta_1) = \int_0^\pi d\beta_2 \frac{G_1 + \tilde{G}_1}{1 - t_1 t_2 t_3} \Big|_{\text{ETI}} - 2(a-b)\beta_1 [2\pi G_{0,0} + \log \beta_1 - \frac{3}{2} \log 2] + \dots \quad (7.36)$$

The remaining integral must be computed by expanding the integrand in powers of β_1 , and then integrating term by term. Given the expansion

$$\frac{G_1}{1 - t_1 t_2 t_3} = \frac{d_{-1}(\beta_2)}{\beta_1} + d_0(\beta_2) + \beta_1 d_1(\beta_2) + \dots, \quad (7.37)$$

we find

$$\begin{aligned} \frac{G_1 + \tilde{G}_1}{1 - t_1 t_2 t_3} &= \frac{d_{-1}(\beta_2) + d_{-1}(-\beta_2)}{\beta_1} + [d_0(\beta_2) + d_0(-\beta_2) - d'_{-1}(-\beta_2)] \\ &+ \beta_1 [d_1(\beta_2) + d_1(-\beta_2) - d'_0(-\beta_2) + \frac{1}{2} d''_{-1}(-\beta_2)] + \dots \end{aligned} \quad (7.38)$$

The symmetrized coefficients read

$$d_{-1}(\beta_2) + d_{-1}(-\beta_2) = -(a-b) \sin^2 \beta_2 \frac{2 - \cos \beta_2 - \sqrt{y_2^2 - 1}}{\sqrt{y_2^2 - 1}}, \quad (7.39)$$

$$d_0(\beta_2) + d_0(-\beta_2) = \frac{\cos^2 \frac{\beta_2}{2}}{(3 - \cos \beta_2) \sqrt{y_2^2 - 1}} \left[P_3(\cos \beta_2) + P_2(\cos \beta_2) \sqrt{y_2^2 - 1} \right], \quad (7.40)$$

$$d_1(\beta_2) + d_1(-\beta_2) = \frac{1}{(3 - \cos \beta_2)(y_2^2 - 1)} \left[P_5(\cos \beta_2) + P_4(\cos \beta_2) \sqrt{y_2^2 - 1} \right], \quad (7.41)$$

where P_2, P_3, P_4 and P_5 are some polynomials of degree 2 up to 5.

The integrals of these coefficients over $[0, \pi]$ can be done exactly. The first two are integrable, but the third one produces a divergent term due to the non-zero value of $P_4(1) = 4(a-b)$. One finds

$$\int_0^\pi [d_{-1}(\beta_2) + d_{-1}(-\beta_2)] = -(a-b) \frac{\pi + 4}{2}, \quad (7.42)$$

$$\int_0^\pi [d_0(\beta_2) + d_0(-\beta_2)] = 4a + a \frac{(5\sqrt{2} - 8)\pi}{2} - b \frac{(\sqrt{2} - 1)\pi}{2}, \quad (7.43)$$

$$\int_0^\pi [d_1(\beta_2) + d_1(-\beta_2)] = 8\pi(a-b)G_{0,0} + \frac{7b-a}{3} + a \frac{(39\sqrt{2} - 29)\pi}{24} - b \frac{(15\sqrt{2} + 13)\pi}{24}. \quad (7.44)$$

The integral of the derivative terms in the expansion (7.38) poses no problem and simply yields $\frac{a-b}{4}\beta_1$. Collecting the various results, the function $f(\beta_1)$ is found to be equal to

$$\begin{aligned} f(\beta_1) = & -\frac{(a-b)\pi + 4}{\beta_1} \frac{\pi + 4}{2} + 4a + a \frac{(5\sqrt{2} - 8)\pi}{2} - b \frac{(\sqrt{2} - 1)\pi}{2} + \beta_1 \left\{ 2(a-b) [2\pi G_{0,0} \right. \\ & \left. - \log \beta_1 + \frac{3}{2} \log 2] + \frac{7b-a}{3} + a \frac{(39\sqrt{2} - 29)\pi}{24} - b \frac{(15\sqrt{2} + 13)\pi}{24} \right\} + \dots \end{aligned} \quad (7.45)$$

It remains to multiply this function by t_1^{2m-1} and to integrate over β_1 . The integrals are carried out by using the following formulas:

$$\int_0^\pi d\beta_1 \frac{t_1^{2m-1}}{\beta_1} = 2\pi G_{2m,0} + \frac{1}{2m} + \frac{7}{48m^2} + \dots \quad (7.46)$$

$$\int_0^\pi d\beta_1 t_1^{2m-1} = \frac{1}{2m} + \frac{1}{4m^2} + \dots \quad \int_0^\pi d\beta_1 t_1^{2m-1} \beta_1 = \frac{1}{4m^2} + \dots \quad (7.47)$$

$$\int_0^\pi d\beta_1 t_1^{2m-1} \beta_1 \log \beta_1 = \frac{1}{4m^2} [1 - \gamma - \log 2m] + \dots \quad (7.48)$$

We eventually find

$$\begin{aligned} \text{second piece of } Y_1 = & -\frac{1}{2\pi^2} \int_0^\pi d\beta_1 t_1^{2m-2} f(\beta_1) \\ = & (a-b) \frac{\pi + 4}{2\pi} G_{2m,0} - \frac{1}{4\pi^2 m} \left\{ 2(a+b) + \frac{(5a-b)\pi}{\sqrt{2}} + \frac{(2b-9a)\pi}{2} \right\} \\ & - \frac{a-b}{2\pi m^2} [2G_{0,0} - G_{2m,0}] - \frac{1}{16\pi^2 m^2} \left\{ a + 11b + \frac{(33a-9b)\pi}{2\sqrt{2}} - \frac{(22a-b)\pi}{2} \right\} + \dots \end{aligned} \quad (7.49)$$

C. Third piece in Y_1 : two and three large powers of t_j

From (7.13), the last piece reads

$$-\frac{1}{2\pi^2} \iint_{-\pi}^{\pi} d\beta_1 d\beta_2 \frac{Q_1^{\text{sym}}(\beta_1, \beta_2)}{\sqrt{(y_1^2 - 1)(y_2^2 - 1)}(1 - t_1 t_2 t_3)} [(t_1 t_2)^{2m-1} - 2(t_1 t_3)^{2m-1} - (t_1 t_2 t_3)^{2m-1}]. \quad (7.50)$$

It is simpler to evaluate than the previous one because it contains at least two t_j to a large power. This implies that the value of the integral is determined by the behaviour of the rest of the integrand around the origin, so that a double series expansion around $\beta_1 = \beta_2 = 0$ can be used. The same dimensional analysis as before shows that the expansion of $Q_1^{\text{sym}}(\beta_1, \beta_2)/\sqrt{(y_1^2 - 1)(y_2^2 - 1)}(1 - t_1 t_2 t_3)$ may be stopped to terms of global dimension 0 (in the two variables).

Special attention must be paid to the double expansions. Each of the three functions $\sqrt{y_j^2 - 1}$ has discontinuous derivatives on the line $\beta_j = 0$. As the integrand involves them all, it has itself discontinuities when one of the lines $\beta_1 = 0$, $\beta_2 = 0$ and $\beta_1 + \beta_2 = 0$ is crossed. As a consequence, the partial derivatives no longer commute, and a series expansion must be computed separately in each of the six regions obtained when the domain $[-\pi, \pi]^2$ is cut by the three lines.

Since the integrand is even under $\beta_1, \beta_2 \rightarrow -\beta_1, -\beta_2$, the integration can be restricted to half the square $\beta_2 \geq 0$. This leaves three separate regions which we denote by (A), (B) and (C):

$$(A) = [0, \pi]^2, \quad (B) = \{\beta_1 \leq 0, \beta_2 \geq 0, \beta_3 \leq 0\}, \quad (C) = \{\beta_1 \leq 0, \beta_2 \geq 0, \beta_3 \geq 0\}. \quad (7.51)$$

In (A), the expansion is carried out for positive values of the two variables, in any order we want. In (B) and (C), the expansion is made for negative values of β_1 , but the order matters: the expansion in β_1 is made first in (B), last in (C).

One may easily check that both the numerator $Q_1^{\text{sym}}(\beta_1, \beta_2)$ and the denominator $\sqrt{(y_1^2 - 1)(y_2^2 - 1)}(1 - t_1 t_2 t_3)$ have dimension 3 around the origin, in the three regions (A), (B) and (C). Thus the ratio has dimension zero, so that the above integral has a single contribution, at order m^{-2} . The explicit expansions read

$$Q_1^{\text{sym}}(\beta_1, \beta_2) = \begin{cases} -\frac{1}{4}(a-b)(\beta_1 + \beta_2)(\beta_1 - \beta_2)^2 + \dots & \text{in region (A),} \\ \frac{1}{4}(a-b)\beta_2(\beta_1 - \beta_2)(2\beta_1 + \beta_2) + \dots & \text{in region (B),} \\ \frac{1}{4}(a-b)\beta_1(\beta_1 - \beta_2)(\beta_1 + 2\beta_2) + \dots & \text{in region (C),} \end{cases} \quad (7.52)$$

and

$$\sqrt{(y_1^2 - 1)(y_2^2 - 1)}(1 - t_1 t_2 t_3) = \begin{cases} 2\beta_1 \beta_2 (\beta_1 + \beta_2) + \dots & \text{in region (A),} \\ -2\beta_1 \beta_2^2 + \dots & \text{in region (B),} \\ 2\beta_1^2 \beta_2 + \dots & \text{in region (C).} \end{cases} \quad (7.53)$$

The integrals can now be computed in the three regions (the formula (7.24) is useful). The integration over (A) yields (the exponents $2m - 1$ of the t_j variables have been replaced by $2m$ since this makes no difference at order m^{-2})

$$\begin{aligned} & \frac{a-b}{16\pi^2} \iint_{(A)} d\beta_1 d\beta_2 \frac{(\beta_1 - \beta_2)^2}{\beta_1 \beta_2} [e^{-2m(\beta_1 + \beta_2)} - 2e^{-2m(2\beta_1 + \beta_2)} - e^{-4m(\beta_1 + \beta_2)}] \\ &= \frac{a-b}{64\pi^2 m^2} \left[-2\pi G_{2m,0} + \frac{1}{2} + \frac{5}{2} \log 2 \right] + \dots \end{aligned} \quad (7.54)$$

The other two are similar,

$$\begin{aligned} & \frac{a-b}{16\pi^2} \iint_{(B)} d\beta_1 d\beta_2 \frac{(\beta_1 - \beta_2)(2\beta_1 + \beta_2)}{\beta_1 \beta_2} [e^{2m(\beta_1 - \beta_2)} - 2e^{-2m\beta_2} - e^{-4m\beta_2}] \\ &= \frac{a-b}{64\pi^2 m^2} \left[-\frac{5\pi}{2} G_{2m,0} + \frac{13}{4} - \frac{11}{4} \log 2 \right] + \dots \end{aligned} \quad (7.55)$$

$$\begin{aligned} & -\frac{a-b}{16\pi^2} \iint_{(C)} d\beta_1 d\beta_2 \frac{(\beta_1 - \beta_2)(\beta_1 + 2\beta_2)}{\beta_1 \beta_2} [e^{2m(\beta_1 - \beta_2)} - 2e^{2m(2\beta_1 + \beta_2)} - e^{4m\beta_1}] \\ &= \frac{a-b}{64\pi^2 m^2} \left[\frac{\pi}{2} G_{2m,0} + \frac{21}{4} - \frac{27}{4} \log 2 \right] + \dots \end{aligned} \quad (7.56)$$

Adding these three contributions, each taken twice to cover the full domain $[-\pi, \pi]^2$, one eventually arrives at

$$\text{third piece of } Y_1 = \frac{a-b}{8\pi^2 m^2} \left[\frac{9}{4} - \frac{7}{4} \log 2 - \pi G_{2m,0} \right] + \dots \quad (7.57)$$

D. Final results

Adding the three contributions (7.20), (7.49) and (7.57) yields our final result for the quantity Y_1 defined in (7.13),

$$\begin{aligned} Y_1 &= (a-b) \frac{\pi+4}{2\pi} [G_{0,0} + G_{2m,0}] - \frac{a}{4\pi^2} T_1 + \frac{b}{4\pi^2} T_2 \\ &- \frac{1}{4\pi^2 m} \left\{ 2(a+b) + \frac{(5a-b)\pi}{\sqrt{2}} + \frac{(2b-9a)\pi}{2} \right\} - \frac{a-b}{8\pi m^2} [8G_{0,0} - 3G_{2m,0}] \\ &+ \frac{1}{32\pi^2 m^2} \left\{ 7a - 31b - \frac{(33a-9b)\pi}{\sqrt{2}} + (22a-b)\pi - 7(a-b) \log 2 \right\} + \dots \end{aligned} \quad (7.58)$$

As mentioned earlier, the other terms Y_2 and Y_3 can be computed in a similar way, with analogous results. Together with (7.10), Y_1 , Y_2 and Y_3 complete the calculation for I_2^{cl} . The evaluation of I_1^{cl} proceeds the same way and, with I_2^{cl} , yield I_{AC}^{cl} . The three other integrals, namely I_B^{cl} , I_{AC}^{op} and I_B^{op} , are handled by the same techniques. The calculations become fairly long, but each step is straightforward if one follows the methods used in the sample calculation detailed above. The next section summarizes the final results.

VIII. SINGLE HEIGHT PROBABILITIES ON THE DISCRETE UHP

In Section VI, explicit formulas were given for the single site probabilities $P_2(m), P_3(m)$ on the UHP, at a site located a distance m from the boundary, chosen to be open or closed. We have shown in the previous section how to evaluate the asymptotic expansion of the four functions, I_{AC}^{cl} , I_B^{cl} , I_{AC}^{op} and I_B^{op} , to second order in m^{-1} . We now put the various pieces together and give the final results for the probabilities. The divergences found in the individual terms, like in (7.58), all cancel out, as they should, leaving finite probabilities.

We obtain for the closed boundary,

$$P_2^{\text{cl}}(m) = P_2 - \frac{1}{8\pi^2 m^2} \left\{ -11 + \frac{34}{\pi} + \frac{4(\pi-2)}{\pi} \left(\gamma + \frac{5}{2} \log 2 \right) + \frac{4(\pi-2)}{\pi} \log m \right\}, \quad (8.1)$$

$$P_3^{\text{cl}}(m) = P_3 - \frac{1}{8\pi^2 m^2} \left\{ \pi + \frac{5}{2} - \frac{44}{\pi} + \frac{2(8-\pi)}{\pi} \left(\gamma + \frac{5}{2} \log 2 \right) + \frac{2(8-\pi)}{\pi} \log m \right\}, \quad (8.2)$$

and for the open boundary,

$$P_2^{\text{op}}(m) = P_2 + \frac{1}{8\pi^2 m^2} \left\{ -9 + \frac{30}{\pi} + \frac{4(\pi-2)}{\pi} \left(\gamma + \frac{5}{2} \log 2 \right) + \frac{4(\pi-2)}{\pi} \log m \right\}, \quad (8.3)$$

$$P_3^{\text{op}}(m) = P_3 + \frac{1}{8\pi^2 m^2} \left\{ \pi + \frac{3}{2} - \frac{36}{\pi} + \frac{2(8-\pi)}{\pi} \left(\gamma + \frac{5}{2} \log 2 \right) + \frac{2(8-\pi)}{\pi} \log m \right\}. \quad (8.4)$$

The first terms, independent of m , are the bulk probabilities, and so can be written in terms of the results from Section IV.

From the above expressions, it is not difficult to see that the probabilities take the form

$$P_i^{\text{cl}}(m) = P_i - \frac{1}{m^2} (a_i + b_i \log m) + \dots, \quad (8.5)$$

$$P_i^{\text{op}}(m) = P_i + \frac{1}{m^2} (a_i + \frac{b_i}{2} + b_i \log m) + \dots, \quad (8.6)$$

with the following exact values for the coefficients a_i and b_i ,

$$a_2 = \frac{\pi-2}{2\pi^3} \left(\gamma + \frac{5}{2} \log 2 \right) - \frac{11\pi-34}{8\pi^3}, \quad b_2 = \frac{\pi-2}{2\pi^3}, \quad (8.7)$$

$$a_3 = \frac{8-\pi}{4\pi^3} \left(\gamma + \frac{5}{2} \log 2 \right) + \frac{2\pi^2+5\pi-88}{16\pi^3}, \quad b_3 = \frac{8-\pi}{4\pi^3}. \quad (8.8)$$

For completeness, we recall that the 1-site probabilities $P_1^{\text{cl}}(m)$ and $P_1^{\text{op}}(m)$ have the same form, with the following coefficients [7],

$$a_1 = \frac{\pi-2}{2\pi^3}, \quad b_1 = 0, \quad (8.9)$$

while those for $P_4^{\text{cl}}(m)$ and $P_4^{\text{op}}(m)$ are obtained by subtraction,

$$a_4 = -(a_1 + a_2 + a_3), \quad b_4 = -(b_1 + b_2 + b_3). \quad (8.10)$$

As we shall see in the next sections, the identity $a_1 = b_2$ is not accidental, but follows from the field assignment for the height 1 and 2 variables, namely the height 2 scaling field is the logarithmic partner of the height 1 field. Similar relations will hold for b_3 and b_4 .

The numerical values of these constants are

$$a_1 = 0.0184091, \quad a_2 = 0.0402789, \quad a_3 = -0.0154395, \quad a_4 = -0.0432485, \quad (8.11)$$

$$b_1 = 0, \quad b_2 = 0.0184091, \quad b_3 = 0.0391728, \quad b_4 = -0.0575818. \quad (8.12)$$

The values of a_2 and b_2 have been announced in [23], though not in an exact form for a_2 . In the same reference, numerical values had also been given for a_3, b_3, a_4 and b_4 , and obtained by fitting numerical simulations of the sandpile model with an Ansatz for the height 3 and 4 conformal fields. The values quoted in [23], namely $a_3 = -0.01243$, $b_3 = 0.03810$, $a_4 = -0.04636$ and $b_4 = -0.05667$ (a_4 and b_4 were obtained from an independent fit, not by subtraction), are in good agreement with the exact values given above.

The forms of (8.5) and (8.6) make it manifest that the probabilities $P_i(m) - P_i$ for $i = 3, 4$ are linear combinations of those for $i = 1, 2$, at order m^{-2} , since they are all linear combinations of the two independent functions m^{-2} and $m^{-2} \log m$,

$$P_3(m) - P_3 = \alpha_3 [P_2(m) - P_2] + \beta_3 [P_1(m) - P_1], \quad (8.13)$$

$$P_4(m) - P_4 = \alpha_4 [P_2(m) - P_2] + \beta_4 [P_1(m) - P_1], \quad (8.14)$$

for the two boundary conditions. The coefficients α_i and β_i satisfy $a_i = \alpha_i a_2 + \beta_i a_1$ and $b_i = \alpha_i b_2$ for $i = 3, 4$, and take the actual values

$$\alpha_3 = \frac{8 - \pi}{2(\pi - 2)} \simeq 2.12791, \quad \beta_3 = \frac{\pi^3 - 5\pi^2 + 12\pi - 48}{4(\pi - 2)^2} \simeq -5.49453, \quad (8.15)$$

$$\alpha_4 = -\frac{\pi + 4}{2(\pi - 2)} \simeq -3.12791, \quad \beta_4 = \frac{32 + 4\pi + \pi^2 - \pi^3}{4(\pi - 2)^2} \simeq 4.49453. \quad (8.16)$$

Remarkably, it follows from these values that the linear relation we have derived above in (4.13) for the probabilities at infinity, actually holds everywhere in the UHP (for large m and at order m^{-2} , that is, in the scaling limit)

$$\frac{48 - 12\pi + 5\pi^2 - \pi^3}{2(\pi - 2)} P_1(m) + (\pi - 8) P_2(m) + 2(\pi - 2) P_3(m) = \frac{(\pi - 2)(\pi - 1)}{\pi}. \quad (8.17)$$

The constant part, corresponding to $m = \infty$, is the relation we had derived at the end of Section IV. It is truly remarkable that the coefficients of the non-constant parts, proportional to $1/m^2$ and $\log m/m^2$, obtained after a long and painful asymptotic analysis, so conspire to fit the same linear relation.

In fact, we argue in the next section that the relations (8.13) and (8.14) actually hold at the level of the fields representing the four height variables, so we expect the last formula to hold in all generality, that is, in any geometry and for any sort of boundary condition. Multisite probabilities would be linearly related in the same way, leaving the probabilities for heights 1 and 2 as the only independent ones (again in the scaling limit). The physical origin of this relation remains to be understood.

IX. CONFORMAL FIELDS

The conformal field theory interpretation of the previous results has been given in [23], which resulted in the field identification of the height variables in the scaling limit. We recall here the salient features of this identification, give computational details that were omitted in [23], and make further comments.

The conformal field theory believed to describe the scaling limit of the sandpile model has central charge $c = -2$. It is non-unitary, and logarithmic [24], meaning that the theory possesses reducible but indecomposable representations of the Virasoro algebra. This characteristic property implies that correlation functions contain logarithms.

We first review the basic ingredients we need to analyze the lattice results given in the previous section, referring to [25] for a more complete description of the $c = -2$ conformal theory (see also [28] and [29] for more general reviews on logarithmic conformal theories).

The 1-site probabilities $P_i(z) = \langle \delta(h(z) - i) \rangle$ are expectation values of the random variables $\delta(h(z) - i)$, computed with respect to the stationary measure of the sandpile model. In the continuum limit, the subtracted random variables $\delta(h(z) - i) - P_i$, normalized to have a zero expectation value on the plane, are expected to converge to conformal fields $h_i(z, \bar{z})$, such that the multipoint field correlators reproduce the scaling limit of the multisite probabilities.

The lattice results show that the four fields h_i have a scaling dimension equal to 2. The height 1 field $h_1(z, \bar{z})$ was the first one to have been studied [6, 7, 8, 9], and turns out to be a primary scalar field $\phi(z, \bar{z})$ with conformal weights (1,1). This field is a true primary field, with rational multipoint correlators.

It has been argued in [23] that the other three fields $h_2(z, \bar{z})$, $h_3(z, \bar{z})$ and $h_4(z, \bar{z})$ are all associated with another field $\psi(z, \bar{z})$, of conformal dimensions (1,1), the logarithmic partner of $\phi(z, \bar{z})$. The fields ϕ and ψ form a rank 2 Jordan block under dilations since their transformations read

$$L_0 \phi = \phi, \quad L_0 \psi = \psi - \frac{1}{2} \phi. \quad (9.1)$$

The precise statement made in [23] was that the lattice calculations for the height 2, as well as the results of the simulations for the heights 3 and 4, now evidenced by the exact results presented above, are all compatible with the following assignments,

$$h_1(z, \bar{z}) = \phi(z, \bar{z}), \quad h_2(z, \bar{z}) = \psi(z, \bar{z}), \quad (9.2)$$

$$h_3(z, \bar{z}) = \alpha_3\psi(z, \bar{z}) + \beta_3\phi(z, \bar{z}), \quad h_4(z, \bar{z}) = \alpha_4\psi(z, \bar{z}) + \beta_4\phi(z, \bar{z}), \quad (9.3)$$

with the coefficients α_i, β_i given in the previous section.

The general form of the 1-point functions of the fields $h_i(z, z^*)$ on the UHP match the dominant terms of the 1-site probabilities $P_i(m) - P_i$, when $z - z^* = 2im$. The normalizations of h_1 and h_2 can be uniquely fixed by comparing with, for instance, the closed boundary results for P_1 and P_2 . However we have to make sure that the same normalizations would be obtained had we chosen to make the comparisons with the open boundary results. This is a highly non-trivial consistency check because much more of the structure of the $c = -2$ theory is needed to prove that indeed the same normalizations would follow.

The probabilities $P_i^{\text{cl}}(m)$ and $P_i^{\text{op}}(m)$ refer to a different boundary condition, and correspondingly the two 1-point functions $\langle h_i(z, z^*) \rangle^{\text{cl}}$ and $\langle h_i(z, z^*) \rangle^{\text{op}}$ are related to each other by the change of boundary condition, itself implemented by the insertion, in the correlator, of a specific boundary field μ [30]. In the present case, we know from [19] that the field which effects a change of boundary condition from closed to open, and vice-versa, is a primary chiral field with conformal weight $h = -1/8$.

It may therefore be used to compute the exact relationship between the open and closed results, and verify that it agrees with the lattice results (8.5) and (8.6). The general form should be retained, but the coefficients of $1/m^2$ and $\log m/m^2$ should be related as $(-a_i, -b_i)^{\text{cl}} \leftrightarrow (a_i + \frac{b_i}{2}, b_i)^{\text{op}}$. This check probes correlators with two fields μ , and therefore the operator product (OPE) of μ with itself. This OPE contains another logarithmic field ω , which itself proves extremely important to make the conformal picture fully consistent with the lattice results.

An even stronger and independent support for the above field identifications will be provided by comparing conformal predictions with actual numerical simulations of the sandpile model. Using again the μ field, one may compute the expectation values $\langle h_i(z, z^*) \rangle$ on the UHP with the negative real axis closed and the positive real axis open. They may then be conformally mapped onto an infinite strip with open and closed boundary conditions on either side of the strip, and eventually compared with the 1-site probability profiles across the strip, measured from numerical simulations on a finite but sufficiently long strip. This is done in the next section, where we will observe a very

good agreement between the two sets of curves.

In order to relate the open and closed boundary expectation values of the fields h_i , we consider the more general situation of an open boundary condition on the real axis with a finite stretch $I = [z_1, z_2]$ which is closed. The corresponding 1-site probabilities $P_i^{\text{op},I}(z)$, which are no longer translation invariant in the horizontal direction, ought to be given in the scaling limit by

$$P_i^{\text{op},I}(z) - P_i = \langle h_i(z, z^*) \rangle_{\text{op},I} = \frac{\langle \mu(z_1) \mu(z_2) h_i(z, z^*) \rangle_{\text{op}}}{\langle \mu(z_1) \mu(z_2) \rangle_{\text{op}}}. \quad (9.4)$$

The notation $\langle \dots \rangle_{\text{op}}$ implies that the boundary condition far out, namely around the point at infinity, is open. Hence the product $\mu(z_1) \mu(z_2)$ really means $\mu^{\text{op,cl}}(z_1) \mu^{\text{cl,op}}(z_2)$, since the closed stretch is in between z_1 and z_2 . The all open or all closed cases is recovered upon taking the limit $z_1, z_2 \rightarrow 0$ or $-z_1, z_2 \rightarrow +\infty$ respectively. While the denominator is simple and can be taken to be $\langle \mu(z_1) \mu(z_2) \rangle_{\text{op}} = z_{12}^{1/4}$, the numerator is more complicated and is computed in the next subsection.

A. Conformal correlation functions

The non-chiral 3-point function is equal to a 4-point chiral correlator, in which two chiral fields h_i are inserted at z and at the mirror image point z^* , namely the left chiral field at z , and the right chiral field at z^* [30]. As h_i is a combination of ϕ and ψ , we have to compute the chiral 4-point functions $\langle \mu \mu \phi \phi \rangle$ and $\langle \mu \mu \psi \psi \rangle$, the latter requiring in any case the former. So we concentrate on $\langle \mu(z_1) \mu(z_2) \psi(z_3) \psi(z_4) \rangle$.

Because the field μ is degenerate at level 2, the chiral 4-point function can be computed in the usual way, by solving first the conformal Ward identities, and then an ordinary second order differential equation. A first complication arises because the field ψ not only is the logarithmic partner of a primary field ϕ , but is also not quasi-primary. Under special conformal transformations (L_1 and \bar{L}_1), it transforms into the fields ρ and $\bar{\rho}$, of conformal weights (0,1) and (1,0) respectively. We will take the OPE of ψ with the left and right stress-energy tensors to be

$$T(z)\psi(w, \bar{w}) = \frac{\rho(w, \bar{w})}{(z-w)^3} + \frac{\psi(w, \bar{w}) - \frac{1}{2}\phi(w, \bar{w})}{(z-w)^2} + \frac{\partial\psi(w, \bar{w})}{z-w} + \dots \quad (9.5)$$

$$\bar{T}(\bar{z})\psi(w, \bar{w}) = \frac{\bar{\rho}(w, \bar{w})}{(\bar{z}-\bar{w})^3} + \frac{\psi(w, \bar{w}) - \frac{1}{2}\phi(w, \bar{w})}{(\bar{z}-\bar{w})^2} + \frac{\bar{\partial}\psi(w, \bar{w})}{\bar{z}-\bar{w}} + \dots \quad (9.6)$$

The factor $-1/2$ in front of ϕ is conventional (when ψ is normalized to be the height 2 variable in the sandpile model, it ensures that ϕ has the right normalization to be the height 1 variable). For more generality, we replace it by λ in what follows.

A second complication comes from the fact that the fields ρ and $\bar{\rho}$ are themselves not fully primary: ρ is a left primary (with left weight 0), but is not quasi-primary under antiholomorphic conformal maps,

$$T(z)\rho(w, \bar{w}) = \frac{\partial\rho(w, \bar{w})}{z-w} + \dots \quad (9.7)$$

$$\bar{T}(\bar{z})\rho(w, \bar{w}) = \frac{\kappa}{(\bar{z}-\bar{w})^3} + \frac{\rho(w, \bar{w})}{(\bar{z}-\bar{w})^2} + \frac{\bar{\partial}\rho(w, \bar{w})}{\bar{z}-\bar{w}} + \dots \quad (9.8)$$

It is the converse situation for $\bar{\rho}$, which is right primary but not left quasi-primary,

$$T(z)\bar{\rho}(w, \bar{w}) = \frac{\kappa}{(z-w)^3} + \frac{\bar{\rho}(w, \bar{w})}{(z-w)^2} + \frac{\partial\bar{\rho}(w, \bar{w})}{z-w} + \dots \quad (9.9)$$

$$\bar{T}(\bar{z})\bar{\rho}(w, \bar{w}) = \frac{\bar{\partial}\bar{\rho}(w, \bar{w})}{\bar{z}-\bar{w}} + \dots \quad (9.10)$$

The coefficients of the cubic terms are equal (to κ), on account of $\bar{L}_1\rho = \bar{L}_1L_1\psi = L_1\bar{L}_1\psi = L_1\bar{\rho}$.

The inhomogeneous transformations of ψ implies that the correlator $\langle\mu\mu\psi(z)\psi(z^*)\rangle$ depends on eight other 4-point functions, in which at least one ψ has been replaced by either ϕ or ρ . (Note that the fields $\psi(z)$ resp. $\psi(z^*)$ are subjected to left resp. right conformal transformations only, so that the chiral ρ and $\bar{\rho}$ behave as primary fields; since $\bar{\rho}$ behaves under right transformations as ρ does under left transformations, we use the same notation ρ for both.) As ρ and ϕ are chiral primary fields, the correlators $\langle\mu\mu\rho\rho\rangle$, $\langle\mu\mu\phi\rho\rangle$, $\langle\mu\mu\rho\phi\rangle$ and $\langle\mu\mu\phi\phi\rangle$ can be computed separately as solutions of a second or first order homogeneous differential equation. Once these are known, the four correlators containing one ψ field can be computed, namely $\langle\mu\mu\rho\psi\rangle$, $\langle\mu\mu\psi\rho\rangle$, $\langle\mu\mu\psi\phi\rangle$ and $\langle\mu\mu\phi\psi\rangle$, which depend on the first four. Finally $\langle\mu\mu\psi\psi\rangle$ can be computed as a solution of a second order inhomogeneous differential equation. More details on the procedure may be found in [28].

As usual, the conformal Ward identities are used to fix the kinematical factors in the correlators, leaving an unknown function of the cross ratio x , which we will take to be $x = \frac{z_{12}z_{34}}{z_{13}z_{24}}$. The Ward identities read ($\langle\dots\rangle$ is any one of the nine correlators)

$$\left\{ \sum_i \partial_i \right\} \langle\dots\rangle = 0, \quad (9.11)$$

$$\left\{ \sum_i (z_i \partial_i + h_i) + \hat{\delta}_i \right\} \langle\dots\rangle = 0, \quad (9.12)$$

$$\left\{ \sum_i (z_i^2 \partial_i + 2h_i z_i) + 2z_i \hat{\delta}_i + \hat{\varepsilon}_i \right\} \langle\dots\rangle = 0. \quad (9.13)$$

The operator $\hat{\delta}$ and $\hat{\varepsilon}$ take into account the inhomogeneous parts in the conformal transformations of ψ under L_0 and L_1 : $\hat{\delta}\psi = \lambda\phi$ and $\hat{\varepsilon}\psi = \rho$, whereas $\hat{\delta}$ and $\hat{\varepsilon}$ annihilate all the other fields.

All nine correlators contain a μ field and as a consequence of its degeneracy at level 2, they satisfy a second order partial differential equation,

$$\left\{ 2\partial_1^2 - \sum_{i=2}^4 \left[\frac{\partial_i}{z_1 - z_i} + \frac{h_i + \hat{\delta}_i}{(z_1 - z_i)^2} + \frac{\hat{\varepsilon}_i}{(z_1 - z_i)^3} \right] \right\} \langle \dots \rangle = 0. \quad (9.14)$$

A correlator which contains a ϕ satisfies a different second order differential equation, since ϕ is also degenerate at level 2. If the field ϕ is at z_a , it reads

$$\left\{ \frac{1}{2}\partial_a^2 - \sum_{i \neq a} \left[\frac{\partial_i}{z_a - z_i} + \frac{h_i + \hat{\delta}_i}{(z_a - z_i)^2} + \frac{\hat{\varepsilon}_i}{(z_a - z_i)^3} \right] \right\} \langle \dots \rangle = 0. \quad (9.15)$$

As they may be of interest for other calculations, we give some details about the derivation of the relevant 4-point correlators. The easiest correlators are those without ψ . As their calculation is standard, we merely give the results,

$$\langle \mu(1)\mu(2)\rho(3)\rho(4) \rangle = z_{12}^{1/4} F_{\rho\rho}(x), \quad F_{\rho\rho} = A_1 + A_2 \log \frac{1 - \sqrt{1-x}}{1 + \sqrt{1-x}}, \quad (9.16)$$

$$\langle \mu(1)\mu(2)\phi(3)\phi(4) \rangle = \frac{z_{12}^{1/4}}{z_{34}^2} F_{\phi\phi}(x), \quad F_{\phi\phi} = B \frac{x-2}{\sqrt{1-x}}, \quad (9.17)$$

$$\langle \mu(1)\mu(2)\phi(3)\rho(4) \rangle = \frac{z_{12}^{5/4}}{z_{13}z_{23}} F_{\phi\rho}(x), \quad F_{\phi\rho} = C \frac{\sqrt{1-x}}{x}, \quad (9.18)$$

$$\langle \mu(1)\mu(2)\rho(3)\phi(4) \rangle = \frac{z_{12}^{5/4}}{z_{14}z_{24}} F_{\rho\phi}(x), \quad F_{\rho\phi} = D \frac{\sqrt{1-x}}{x}. \quad (9.19)$$

The five coefficients A_1, A_2, B, C and D are integration constants.

The conformal Ward identities satisfied by the correlator $\langle \mu\mu\psi\rho \rangle$ require that it be of the following general form,

$$\langle \mu(1)\mu(2)\psi(3)\rho(4) \rangle = \frac{z_{12}^{5/4}}{z_{13}z_{23}} \left[F_{\psi\rho} - \lambda F_{\phi\rho} \log \left(\frac{z_{13}z_{23}}{z_{12}} \right) + \frac{z_{23}}{z_{12}} F_{\rho\rho} \right]. \quad (9.20)$$

When one inserts this form into (9.14), one finds that the unknown function $F_{\psi\rho}$ satisfies an inhomogeneous ordinary differential equation,

$$x(1-x)F_{\psi\rho}'' + \left(3 - \frac{7x}{2}\right)F_{\psi\rho}' + \frac{1-x}{x}F_{\psi\rho} = 2(1-x)F_{\rho\rho}' + \frac{1-x}{2x}F_{\rho\rho} + \lambda F_{\phi\rho}, \quad (9.21)$$

where we have used the equations satisfied by $F_{\rho\rho}$ and $F_{\phi\rho}$ to simplify the right-hand side. The general solution involves two additional arbitrary coefficients,

$$\begin{aligned} F_{\psi\rho}(x) &= E_1 \frac{\sqrt{1-x}}{x} + E_2 \left\{ \frac{2}{x} + \frac{\sqrt{1-x}}{x} \log \frac{1 - \sqrt{1-x}}{1 + \sqrt{1-x}} \right\} - \frac{2\lambda C}{3} \frac{\sqrt{1-x}}{x} \log x \\ &+ \frac{A_1}{2} - A_2 \left\{ -\frac{\sqrt{1-x}}{x} + \frac{2}{3} \frac{\sqrt{1-x}}{x} \log x - \frac{1}{2} \log \frac{1 - \sqrt{1-x}}{1 + \sqrt{1-x}} \right\}. \end{aligned} \quad (9.22)$$

The 4-point function $\langle \mu\mu\rho\psi \rangle$ is related to the previous one by the permutation $3 \leftrightarrow 4$, which induces on x the transformation $x \rightarrow \frac{x}{x-1}$. One thus obtains

$$\langle \mu(1)\mu(2)\rho(3)\psi(4) \rangle = \frac{z_{12}^{5/4}}{z_{14}z_{24}} \left[F_{\rho\psi} - \lambda F_{\rho\phi} \log \left(\frac{z_{14}z_{24}}{z_{12}} \right) + \frac{z_{24}}{z_{12}} F_{\rho\rho} \right], \quad (9.23)$$

and

$$\begin{aligned} F_{\rho\psi}(x) &= F_1 \frac{\sqrt{1-x}}{x} + F_2 \left\{ \frac{2(1-x)}{x} + \frac{\sqrt{1-x}}{x} \log \frac{1-\sqrt{1-x}}{1+\sqrt{1-x}} \right\} + \frac{2\lambda D}{3} \frac{\sqrt{1-x}}{x} \log \frac{1-x}{x} \\ &+ \frac{A_1}{2} - A_2 \left\{ \frac{\sqrt{1-x}}{x} + \frac{2}{3} \frac{\sqrt{1-x}}{x} \log \frac{1-x}{x} - \frac{1}{2} \log \frac{1-\sqrt{1-x}}{1+\sqrt{1-x}} \right\}. \end{aligned} \quad (9.24)$$

The next case is the 4-point function $\langle \mu\mu\psi\phi \rangle$. From the Ward identities, its general form is

$$\langle \mu(1)\mu(2)\psi(3)\phi(4) \rangle = \frac{z_{12}^{1/4}}{z_{34}^2} \left[F_{\psi\phi} - \lambda F_{\phi\phi} \log \left(\frac{z_{13}z_{23}}{z_{12}} \right) - \frac{x}{x-1} \frac{z_{34}}{z_{24}} F_{\rho\phi} \right]. \quad (9.25)$$

When it is inserted into (9.14) and (9.15), one finds that $F_{\psi\phi}$ satisfies two second order ordinary differential equations. By combining them, one obtains a first order equation, namely

$$2(1-x)(2-x)F'_{\psi\phi} - xF_{\psi\phi} = -\frac{4(4-6x+3x^2-x^3)}{3x(2-x)}\lambda F_{\phi\phi} + \frac{2}{3}(4-5x+x^2)F_{\rho\phi}. \quad (9.26)$$

The general solution reads

$$F_{\psi\phi}(x) = G \frac{x-2}{\sqrt{1-x}} - \frac{(4\lambda B - D)}{3} \sqrt{1-x} - \frac{2\lambda B + D}{3} \frac{x-2}{\sqrt{1-x}} \log x. \quad (9.27)$$

Similarly, one finds

$$\langle \mu(1)\mu(2)\phi(3)\psi(4) \rangle = \frac{z_{12}^{1/4}}{z_{34}^2} \left[F_{\phi\psi} - \lambda F_{\phi\phi} \log \left(\frac{z_{14}z_{24}}{z_{12}} \right) + x \frac{z_{34}}{z_{23}} F_{\phi\rho} \right], \quad (9.28)$$

with

$$F_{\phi\psi}(x) = H \frac{x-2}{\sqrt{1-x}} - \frac{(4\lambda B + C)}{3\sqrt{1-x}} + \frac{2\lambda B - C}{3} \frac{x-2}{\sqrt{1-x}} \log \frac{1-x}{x}. \quad (9.29)$$

We finally come to the last correlator $\langle \mu\mu\psi\psi \rangle$. From the Ansatz

$$\begin{aligned} \langle \mu(1)\mu(2)\psi(3)\psi(4) \rangle &= \frac{z_{12}^{1/4}}{z_{34}^2} \left[F_{\psi\psi} - \lambda F_{\phi\psi} f_1(z_i) - \lambda F_{\psi\phi} f_2(z_i) - F_{\rho\psi} f_3(z_i) - F_{\psi\rho} f_4(z_i) \right. \\ &\quad \left. + \lambda^2 F_{\phi\phi} f_5(z_i) + \lambda F_{\phi\rho} f_6(z_i) + \lambda F_{\rho\phi} f_7(z_i) + F_{\rho\rho} f_8(z_i) \right], \end{aligned} \quad (9.30)$$

we find that the Ward identities are satisfied for the following choice of the functions f_j :

$$f_1(z_i) = \log \left(\frac{z_{13}z_{23}}{z_{12}} \right), \quad f_2(z_i) = \log \left(\frac{z_{14}z_{24}}{z_{12}} \right), \quad f_3(z_i) = \frac{x}{x-1} \frac{z_{34}}{z_{24}}, \quad f_4(z_i) = -x \frac{z_{34}}{z_{23}}, \quad (9.31)$$

$$f_5(z_i) = f_1(z_i)f_2(z_i), \quad f_6(z_i) = f_1(z_i)f_4(z_i), \quad f_7(z_i) = f_2(z_i)f_3(z_i), \quad f_8(z_i) = \frac{z_{34}^2}{z_{13}z_{14}}. \quad (9.32)$$

Inserting this form in (9.14) yields an ordinary differential equation for $F_{\psi\psi}$,

$$\begin{aligned}
x(1-x)F_{\psi\psi}'' + \left(1 - \frac{3x}{2}\right)F_{\psi\psi}' - \frac{x}{2(1-x)}F_{\psi\psi} &= -\frac{x}{2-x}\lambda F_{\phi\psi} - \frac{x}{(1-x)(2-x)}\lambda F_{\psi\phi} \\
-\frac{x}{2}F_{\rho\psi} - \frac{x}{2(1-x)^2}F_{\psi\rho} + \frac{2(4-4x+5x^2)}{3x(2-x)^2}\lambda^2 F_{\phi\phi} \\
+ \frac{2(4-3x)}{3(1-x)(2-x)}\lambda F_{\phi\rho} - \frac{2(4-x)}{3(2-x)}\lambda F_{\rho\phi} - \frac{x(6-6x+x^2)}{2(1-x)^2}F_{\rho\rho} - \frac{2x^2(2-x)}{1-x}F_{\rho\rho}', \quad (9.33)
\end{aligned}$$

in terms of the eight functions derived earlier.

The general solution to this equation would be fairly complicated to write down and is in any case not needed. We are primarily interested in the above correlators when the two μ fields form a pair $\mu^{\text{op,cl}}(z_1)\mu^{\text{cl,op}}(z_2)$. When z_1 goes to z_2 , the operator product expansion closes on fields which live on an open boundary. As shown in [21], it reads

$$\mu^{\text{op,cl}}(z_1)\mu^{\text{cl,op}}(z_2) = z_{12}^{1/4} \mathbb{I} + \dots \quad (9.34)$$

Therefore the limit $z_{12} \rightarrow 0$ cannot produce any logarithmic singularity, whatever the other fields in the correlators are. Imposing this condition on the first eight correlators, brings five constraints on the coefficients, namely

$$A_2 = 0, \quad C = -D = -\lambda B, \quad E_2 = -F_2 = \frac{\lambda^2 B}{3}. \quad (9.35)$$

These relations reduce the number of arbitrary constants in the right-hand side of (9.33) from 11 to 6, namely A_1 , B , E_1 , F_1 , G and H . The most general function $F_{\psi\psi}$ contains the general solution of its homogeneous equation, and also six functions which solve the inhomogeneous equation, each one corresponding to one of the six coefficients remaining in the r.h.s. of (9.33),

$$F_{\psi\psi} = F_{\psi\psi}|_{\text{homog}} + F_{\psi\psi}|_{A_1} + F_{\psi\psi}|_B + F_{\psi\psi}|_{E_1} + F_{\psi\psi}|_{F_1} + F_{\psi\psi}|_G + F_{\psi\psi}|_H. \quad (9.36)$$

These seven functions are given explicitly by

$$F_{\psi\psi}|_{\text{homog}} = I_1 \frac{x-2}{\sqrt{1-x}} + I_2 \left\{ \frac{x-2}{\sqrt{1-x}} \log \frac{1-\sqrt{1-x}}{1+\sqrt{1-x}} - 2 \right\}, \quad (9.37)$$

$$F_{\psi\psi}|_{A_1} = \frac{4-4x-3x^2}{4(1-x)}, \quad (9.38)$$

$$F_{\psi\psi}|_{E_1} = -\frac{1}{3\sqrt{1-x}} \left\{ 1 + (x-2) \log \frac{1-x}{x} \right\}, \quad F_{\psi\psi}|_{F_1} = \frac{\sqrt{1-x}}{3} - \frac{1}{3} \frac{x-2}{\sqrt{1-x}} \log x, \quad (9.39)$$

$$\lambda^{-1} F_{\psi\psi}|_G = \frac{1}{3\sqrt{1-x}} \left\{ 2 - 3x + 2(x-2) \log \frac{1-x}{x} \right\}, \quad (9.40)$$

$$\lambda^{-1} F_{\psi\psi}|_H = \frac{1}{3\sqrt{1-x}} \left\{ x + 2 - 2(x-2) \log x \right\}, \quad (9.41)$$

$$\begin{aligned}
\lambda^{-2} F_{\psi\psi} \Big|_B &= \frac{2 - 16 \log 2}{9} - \frac{2 - 2x + x^2}{3(1-x)} - \frac{4}{9} \frac{x-2}{\sqrt{1-x}} \left\{ \text{Li}_2\left(\frac{1-\sqrt{1-x}}{1+\sqrt{1-x}}\right) + \text{Li}_2\left(-\frac{1-\sqrt{1-x}}{1+\sqrt{1-x}}\right) \right\} \\
&- \frac{2}{9} \log \frac{1-x}{x^2} + \frac{10}{9} \left\{ \frac{\log x}{\sqrt{1-x}} + \sqrt{1-x} \log \frac{x}{x-1} \right\} + \frac{8}{9} \frac{x-2}{\sqrt{1-x}} \log x \log \frac{x}{x-1} \\
&- \frac{1}{9} \left\{ 4 + \frac{x-2}{\sqrt{1-x}} \log \left(\frac{1-x}{x^2} \frac{1-\sqrt{1-x}}{1+\sqrt{1-x}} \right) \right\} \log \frac{1-\sqrt{1-x}}{1+\sqrt{1-x}}, \tag{9.42}
\end{aligned}$$

where the polylogarithmic function $\text{Li}_2(z) = \sum_{k=1}^{\infty} \frac{z^k}{k^2}$ is regular at the origin.

Imposing now that the correlator $\langle \mu\mu\psi\psi \rangle$ itself is free of logarithmic singularity at $z_{12} = 0$, and moreover that $\lim_{z_{12} \rightarrow 0} z_{12}^{-1/4} \langle \mu(1)\mu(2)\psi(3)\psi(4) \rangle$ depends on z_{34} only, leads to five new conditions on the coefficients,

$$B = 0, \quad E_1 = -F_1 = -A_1, \quad H = G, \quad I_2 = \frac{2}{3}(A_1 - \lambda G), \tag{9.43}$$

leaving only three free parameters, A_1, G and I_1 . The explicit solution is

$$\begin{aligned}
\langle \mu(z_1)\mu(z_2)\psi(z_3)\psi(z_4) \rangle &= \frac{z_{12}^{1/4}}{z_{34}^2} \left\{ \left(I_1 - \frac{A_1}{3} - \frac{2\lambda G}{3} \right) \frac{x-2}{\sqrt{1-x}} + \frac{A_1}{4} \frac{4-4x-3x^2}{1-x} \right. \\
&- \frac{2}{3} (A_1 - \lambda G) \frac{x-2}{\sqrt{1-x}} \log \frac{(1+\sqrt{1-x})^2}{\sqrt{1-x}} - \frac{4}{3} (A_1 - \lambda G) - 2\lambda G \frac{x-2}{\sqrt{1-x}} \log |z_{34}| \\
&\left. + A_1 \left(\frac{1}{z_{24}\sqrt{1-x}} - \frac{\sqrt{1-x}}{z_{23}} \right) z_{34} + \frac{A_1}{2} \left(\frac{x}{z_{23}} - \frac{x}{(x-1)z_{24}} + \frac{2z_{34}}{z_{13}z_{14}} \right) z_{34} \right\}. \tag{9.44}
\end{aligned}$$

We have required that the correlator be regular when $z_1, z_2 \rightarrow 0$, namely when the boundary is all open. The other extreme regime corresponds to an all closed boundary, obtained by letting $-z_1, z_2 \rightarrow +\infty$. In this limit, the correlator should reproduce the 1-site probabilities in presence of a closed boundary and thus should also be regular. This is the case provided

$$A_1 = \lambda G. \tag{9.45}$$

At this stage, the correlator $\langle \mu\mu\psi(z, z^*) \rangle = \langle \mu\mu\psi(z)\psi(z^*) \rangle$ physically relevant to our situation depends on the two arbitrary coefficients A_1 and I_1 , and reads explicitly,

$$\begin{aligned}
\langle \mu(z_1)\mu(z_2)\psi(z_3, z_4) \rangle &= \frac{z_{12}^{1/4}}{z_{34}^2} \left\{ (I_1 - A_1) \frac{x-2}{\sqrt{1-x}} + \frac{A_1}{4} \frac{4-4x-3x^2}{1-x} - 2A_1 \frac{x-2}{\sqrt{1-x}} \log |z_{34}| \right. \\
&\left. + A_1 \left(\frac{1}{z_{24}\sqrt{1-x}} - \frac{\sqrt{1-x}}{z_{23}} \right) z_{34} + \frac{A_1}{2} \left(\frac{x}{z_{23}} - \frac{x}{(x-1)z_{24}} + \frac{2z_{34}}{z_{13}z_{14}} \right) z_{34} \right\}. \tag{9.46}
\end{aligned}$$

Anticipating a little bit, we trade the coefficients A_1 and I_1 for two other coefficients a_2 and b_2 ,

$$A_1 = -b_2, \quad I_1 = 2a_2 - b_2 \left(\frac{1}{2} + 2 \log 2 \right). \tag{9.47}$$

In terms of those, the correlator becomes

$$\begin{aligned} \langle \mu(z_1)\mu(z_2)\psi(z_3, z_4) \rangle &= \frac{z_{12}^{1/4}}{z_{34}^2} \frac{x-2}{\sqrt{1-x}} \left\{ 2b_2 \log \left| \frac{z_{34}}{2} \right| + 2a_2 + \frac{b_2}{2} - \frac{b_2}{4} \frac{x-2}{\sqrt{1-x}} \right. \\ &\quad \left. + b_2 \frac{z_{34}^2}{z_{13}z_{24}} \left[\frac{1}{x-2} + \frac{1}{2\sqrt{1-x}} \right] \right\}. \end{aligned} \quad (9.48)$$

The other correlator we need involves the non-chiral field $\phi(z, z^*) = \frac{1}{\lambda} L_0\psi(z, z^*) = \frac{1}{\lambda} \bar{L}_0\psi(z, z^*)$, which becomes $\phi(z, z^*) = \phi(z)\psi(z^*) = \psi(z)\phi(z^*)$ in terms of chiral fields. The relevant correlator is thus given by (9.25) or (9.28) with $B = C = 0$ and $H = G = \frac{A_1}{\lambda} = -\frac{b_2}{\lambda}$, namely

$$\langle \mu(z_1)\mu(z_2)\phi(z_3, z_4) \rangle = -\frac{b_2}{\lambda} \frac{z_{12}^{1/4}}{z_{34}^2} \frac{x-2}{\sqrt{1-x}}. \quad (9.49)$$

When we will come to the comparison of the conformal predictions with the numerical simulations, we will also need two other correlators, namely $\langle \mu(z_1)\mu(z_2)\rho(z_3, z_4) \rangle$ and $\langle \mu(z_1)\mu(z_2)\bar{\rho}(z_3, z_4) \rangle$. In terms of a pair of chiral fields, $\rho(z, z^*) = L_1\psi(z, z^*)$ is identified with $\rho(z)\psi(z^*)$. The corresponding correlator is given in (9.23) and reads (we use the values of the constants found above, and $A_1 = -b_2$)

$$\langle \mu(z_1)\mu(z_2)\rho(z_3, z_4) \rangle = -b_2 z_{12}^{1/4} \left\{ \frac{z_{12}}{z_{14}z_{24}} \frac{\sqrt{1-x}}{x} + \frac{1}{2z_{14}} + \frac{1}{2z_{24}} \right\}. \quad (9.50)$$

Similarly, identifying the field $\bar{\rho}(z, z^*) = \bar{L}_1\psi(z, z^*)$ with $\psi(z)\rho(z^*)$, the correlator in (9.20) yields

$$\langle \mu(z_1)\mu(z_2)\bar{\rho}(z_3, z_4) \rangle = -b_2 z_{12}^{1/4} \left\{ -\frac{z_{12}}{z_{13}z_{23}} \frac{\sqrt{1-x}}{x} + \frac{1}{2z_{13}} + \frac{1}{2z_{23}} \right\}. \quad (9.51)$$

The value of κ in the transformations of ρ and $\bar{\rho}$ can also be fixed. The field $\kappa\mathbb{I} = \bar{L}_1\rho(z, z^*)$ should be associated with $\rho(z)\rho(z^*)$, so that the correlator (9.16) yields

$$\kappa \langle \mu(z_1)\mu(z_2) \rangle = -b_2 z_{12}^{1/4}, \quad (9.52)$$

and $\kappa = -b_2$.

B. Closed versus open UHP probabilities

Let us now come back to the 1-site probabilities on the UHP to see how they are related when the boundary is either fully open or fully closed. We set $\lambda = -\frac{1}{2}$ in the expressions of the previous subsection.

We first consider the height 1 probabilities, already discussed in [21]. According to (9.4), the identification $h_1(z, z^*) = \phi(z, z^*)$ and (9.49), the probability $P_1^{\text{op}, I}(z)$ is equal to ($z_4 = z_3^* = z^*$)

$$P_1^{\text{op}, I}(z) - P_1 = z_{12}^{-1/4} \langle \mu(z_1)\mu(z_2)\phi(z, z^*) \rangle = \frac{2b_2}{(z-z^*)^2} \frac{x-2}{\sqrt{1-x}}. \quad (9.53)$$

When z_1 and z_2 go to 0, the cross ratio $x = \frac{(z_1 - z_2)(z - z^*)}{(z_1 - z)(z_2 - z^*)}$ goes to 0, while $\sqrt{1 - x}$ goes to +1. In this limit, $P_1^{\text{op},I}(z) - P_1$ must go to the open boundary result. This fixes $b_2 = a_1 = \frac{P_1}{4}$, so that

$$\lim_{z_1, z_2 \rightarrow 0} P_1^{\text{op},I}(z) - P_1 = P_1^{\text{op}}(m) - P_1 = \frac{a_1}{m^2}, \quad (z - z^* = 2im). \quad (9.54)$$

If now $-z_1, z_2$ go to $+\infty$, the cross ratio still goes to 0 but $\sqrt{1 - x}$ goes to -1 because $1 - x$ circles around zero when $-z_1 = z_2$ take the values from 0 to $+\infty$. Therefore we obtain the expected change of sign,

$$\lim_{-z_1, z_2 \rightarrow +\infty} P_1^{\text{op},I}(z) - P_1 = P_1^{\text{cl}}(m) - P_1 = -\frac{a_1}{m^2}. \quad (9.55)$$

The probability $P_2^{\text{op},I}(z)$ that the site at z has height 2 in presence of an open boundary except on the interval $I = [z_1, z_2]$ which is closed, is equal to the correlator (9.48) divided by $z_{12}^{1/4}$ (there was a misprint in the last term of the formula (8) of [23])

$$\begin{aligned} P_2^{\text{op},I}(z) - P_2 &= \frac{1}{(z - z^*)^2} \frac{x - 2}{\sqrt{1 - x}} \left\{ 2b_2 \log \left| \frac{z - z^*}{2} \right| + 2a_2 + \frac{b_2}{2} - \frac{b_2}{4} \frac{x - 2}{\sqrt{1 - x}} \right. \\ &\quad \left. + b_2 \frac{(z - z^*)^2}{(z_1 - z)(z_2 - z^*)} \left[\frac{1}{x - 2} + \frac{1}{2\sqrt{1 - x}} \right] \right\}, \end{aligned} \quad (9.56)$$

with $x = \frac{(z_1 - z_2)(z - z^*)}{(z_1 - z)(z_2 - z^*)}$ as before (although x is a complex number, $x^* = \frac{x}{x-1}$, the probability is real).

Upon taking z_1 and z_2 to 0, the expression reduces to

$$\lim_{z_1, z_2 \rightarrow 0} P_2^{\text{op},I}(z) - P_2 = \frac{1}{m^2} \left[a_2 + \frac{b_2}{2} + b_2 \log m \right] = P_2^{\text{op}}(m) - P_2, \quad (9.57)$$

which confirms that the two coefficients a_2, b_2 are those derived in the lattice calculations, and given in (8.7). It is now an easy check to see that the other limit $-z_1, z_2 \rightarrow +\infty$, bearing in mind the monodromy factor of $\sqrt{1 - x}$, yields exactly the result for the closed boundary, namely

$$\lim_{-z_1, z_2 \rightarrow +\infty} P_2^{\text{op},I}(z) - P_2 = -\frac{1}{m^2} [a_2 + b_2 \log m] = P_2^{\text{cl}}(m) - P_2. \quad (9.58)$$

The same limits also hold for the height 3 and 4 probabilities. The relations (8.13) and (8.14) expressing $P_3(m)$ and $P_4(m)$ as linear combinations of $P_1(m)$ and $P_2(m)$ suggest that the fields $h_3(z)$ and $h_4(z)$ are given by the same linear combinations of $h_1(z)$ and $h_2(z)$, as in (9.3). Then the formula (9.56) holds for $P_i^{\text{op},I}(z)$, $i = 1, 2, 3, 4$, provided the coefficient a_2, b_2 are replaced by a_i, b_i , given in Section VIII. Consequently the open and closed probabilities $P_i^{\text{op}}(m)$ and $P_i^{\text{cl}}(m)$, for $i = 3$ and $i = 4$, are correctly related to each other by the insertions of μ fields.

So the lattice results for the open and closed boundary conditions are exactly compatible with the effect of a change of boundary condition computed in the conformal setting. The formula (9.56)

is however far more general, and gives access to a probability that looks at present very hard to obtain from lattice calculations.

Beyond the two extreme cases of an all open or all closed boundary, this formula may be confronted with numerical simulations in an intermediate situation. Before doing this, we return to the pure closed boundary with a further comment.

Relying on the operator product expansion (9.34), we have imposed that the correlator $\langle \mu(1)\mu(2)\psi(3)\psi(4) \rangle$ should not produce logarithmic singularities in the limit $z_1, z_2 \rightarrow 0$. On physical grounds, we have then required the same regular behaviour in the limit $-z_1, z_2 \rightarrow +\infty$ since the 4-point correlator reduces to the closed boundary probabilities. In that limit, the two fields μ come close to each other at infinity, so that the operator product expansion may again be invoked. However the relevant expansion is not the same as in the other limit, because it is now the open stretch which is reduced to nothing, in such a way that the expansion must close on fields which live on a closed boundary. The proper operator product expansion reads [21]

$$\mu^{\text{cl,op}}(z_1)\mu^{\text{op,cl}}(z_2) = z_{12}^{1/4} [\omega_N(z_2) - \frac{1}{\pi} \mathbb{I} \log z_{12}] + \dots \quad (9.59)$$

where the boundary field ω_N has conformal weight 0, and forms with the identity, a rank two Jordan block under dilations. The interpretation of $\omega(z)$ in the sandpile model is that it introduces dissipation at z [21].

The insertion of the previous expansion in the 4-point function yields in the limit

$$\langle \psi(z, z^*) \rangle_{\text{cl}} = \lim_{-z_1, z_2 \rightarrow +\infty} \left\{ \langle \omega_N(z_2)\psi(z)\psi(z^*) \rangle - \frac{\log z_{12}}{\pi} \langle \psi(z)\psi(z^*) \rangle \right\}. \quad (9.60)$$

The absence of logarithmic singularity then implies that the chiral 2-point function $\langle \psi(z)\psi(z^*) \rangle$, appropriate for the closed boundary, vanishes identically, but also that

$$\langle \psi(z, z^*) \rangle_{\text{cl}} = \langle \omega_N(\infty)\psi(z)\psi(z^*) \rangle. \quad (9.61)$$

Though strange at first sight, this relation has a natural and physical origin. Probabilities on infinite lattices are limits of probabilities calculated on finite lattices. The sandpile model is not well-defined if the lattice does not have dissipative sites. In the model considered here, dissipation takes place at the open boundary sites, namely at those sites which are connected to the sink, itself located all around the lattice. In the case of the UHP, three boundaries have been sent off to infinity. When the remaining boundary (the real axis) is open, the sandpile model is well-defined without introducing further dissipation on the other three boundaries. When it is closed, dissipation has to be introduced on the other three boundaries by connecting them to the sink.

The sink is, with the boundaries, subsequently sent to infinity, which is where the dissipation is eventually located. This is exactly what the field $\omega_N(\infty)$ does: it inserts at infinity the dissipation needed to make the sandpile model well-defined.

A similar relation holds for the ϕ field, describing the height 1 variable,

$$\langle \phi(z, z^*) \rangle_{\text{cl}} = \langle \omega_N(\infty) \phi(z) \phi(z^*) \rangle. \quad (9.62)$$

The insertion of ω_N prevents $\langle \phi(z, z^*) \rangle_{\text{cl}} \sim P_1^{\text{cl}}(m)$ from being identically zero, since the chiral 2-point function of ϕ vanishes.

X. FINITE SIZE CORRECTIONS VERSUS SIMULATIONS

The simplest case after the pure open and pure closed boundary condition is when the boundary is half closed and half open. It is also a case which is relevant for a comparison with numerical simulations.

We take the boundary of the UHP to be closed on the negative side of the real axis, and open on the positive side. It clearly corresponds to taking $z_1 = -\infty$ and $z_2 = 0$. From (9.56), we obtain for $i = 1, 2, 3, 4$,

$$P_i^{\text{cl}|\text{op}}(z) - P_i = -\frac{z + z^*}{|z|(z - z^*)^2} \left\{ 2b_i \log \left| \frac{z - z^*}{2} \right| + 2a_i + \frac{b_i}{2} + \frac{b_i}{4} \frac{z + z^*}{|z|} \right\}. \quad (10.1)$$

The conformal map $w = \frac{L}{\pi} \log z$ transforms the upper half plane to an infinite strip of width L . The negative and positive real axis are mapped respectively to the line $\Im w = L$ and $\Im w = 0$, which are therefore respectively closed and open.

In order to transform the probabilities from the UHP to the strip, we need the conformal transformation law of the logarithmic field ψ (the field ϕ is primary). The integration of the infinitesimal conformal transformations (9.5) and (9.6) yields

$$\begin{aligned} \psi_{\text{strip}}(w, \bar{w}) = & |z'(w)|^2 \left\{ \psi_{\text{uhp}}(z, \bar{z}) - \frac{1}{2} \log |z'(w)|^2 \phi_{\text{uhp}}(z, \bar{z}) \right. \\ & \left. + \frac{z''(w)}{2z'^2(w)} \rho_{\text{uhp}}(z, \bar{z}) + \frac{\bar{z}''(\bar{w})}{2\bar{z}'^2(\bar{w})} \bar{\rho}_{\text{uhp}}(z, \bar{z}) + \kappa \left| \frac{z''(w)}{2z'^2(w)} \right|^2 \right\}, \end{aligned} \quad (10.2)$$

where the last piece comes from the transformations² of ρ and $\bar{\rho}$.

² The inhomogeneous terms in the non-chiral transformation laws of ρ and $\bar{\rho}$ have been overlooked in [23], resulting in a number of missing terms in the equations (10-12) and (14) of that reference. In particular the equation (14) of [23] misses a constant term proportional to $1/L^2$, see the equation (10.6) in the present article. This however makes no numerical difference.

Taking the expectation value, one obtains the corresponding 1-site probabilities on the infinite strip in terms of those on the UHP and the expectation values of $\rho, \bar{\rho}$. For the height 1 probability, the relation is

$$P_1^{\text{strip}}(w) - P_1 = |z'(w)|^2 [P_1^{\text{cl|op}}(z) - P_1], \quad (10.3)$$

whereas for the height 2 probability,

$$P_2^{\text{strip}}(w) - P_2 = |z'(w)|^2 \left\{ [P_2^{\text{cl|op}}(z) - P_2] - \frac{1}{2} \log |z'(w)|^2 [P_1^{\text{cl|op}}(z) - P_1] \right. \\ \left. + \frac{z''(w)}{2z'^2(w)} \langle \rho(z, z^*) \rangle_{\text{cl|op}} + \left(\frac{z''(w)}{2z'^2(w)} \right)^* \langle \bar{\rho}(z, z^*) \rangle_{\text{cl|op}} + \kappa \left| \frac{z''(w)}{2z'^2(w)} \right|^2 \langle \mathbb{I} \rangle_{\text{cl|op}} \right\}. \quad (10.4)$$

The height 3 and 4 probabilities are simply obtained by linear combinations (see (9.3)). In these formulas, the expectation values refer to the UHP with the boundary condition closed on the negative axis and open on the positive axis, *i.e.* $z_1 \rightarrow -\infty$ and $z_2 \rightarrow 0$. From (9.50) and (9.51), these are given by

$$\langle \rho(z, z^*) \rangle_{\text{cl|op}} = b_2 \left\{ -\frac{\sqrt{z/z^*}}{z - z^*} + \frac{1}{2z^*} \right\}, \quad \langle \bar{\rho}(z, z^*) \rangle_{\text{cl|op}} = b_2 \left\{ \frac{\sqrt{z^*/z}}{z - z^*} + \frac{1}{2z} \right\}, \quad (10.5)$$

and $\langle \mathbb{I} \rangle_{\text{cl|op}} = 1$.

Putting everything together and setting $w = u + iv$, we find the following 1-site probabilities on the strip, for $i = 1, 2, 3, 4$, as functions of v only,

$$P_i^{\text{strip}}(w) - P_i = \left(\frac{\pi}{L} \right)^2 \frac{\cos(\pi v/L)}{\sin^2(\pi v/L)} \left\{ a_i + \frac{b_i}{4} \left[1 + \cos\left(\frac{\pi v}{L}\right) \right] + b_i \log\left(\frac{L}{\pi} \sin\left(\frac{\pi v}{L}\right)\right) \right\} + \frac{b_i \pi^2}{4L^2}. \quad (10.6)$$

Should the field identifications proposed earlier be correct, these formulas represent the scaling limit of the probability that a site of an infinite strip, located at a distance v from the open boundary and $L - v$ from a closed boundary, has a height equal to i .

We have run numerical simulations on strips of width N and height M for various values of M and N (details about these simulations have been given in [23]). For ratios $\frac{M}{N}$ large enough, we expect that the results on a finite height strip be very close to those on an infinite strip, so that the numerical simulations should be reliable enough to be compared with the exact scaling limit (10.6), provided by the conformal approach. For simplicity, we chose the boundary conditions on the two sides separated by M to be open —exactly what boundary conditions are imposed there should make no difference—, and the other two were open and closed. The two sets of plots, the numerical results and the conformal formulas, in each case for the four heights, are shown in Fig. 16 (as explained in [23], the width L in the continuum and the width N of the lattice should be related by $L = N + \frac{1}{2}$). The simulation data are the same as in the figures of [23], but the conformal

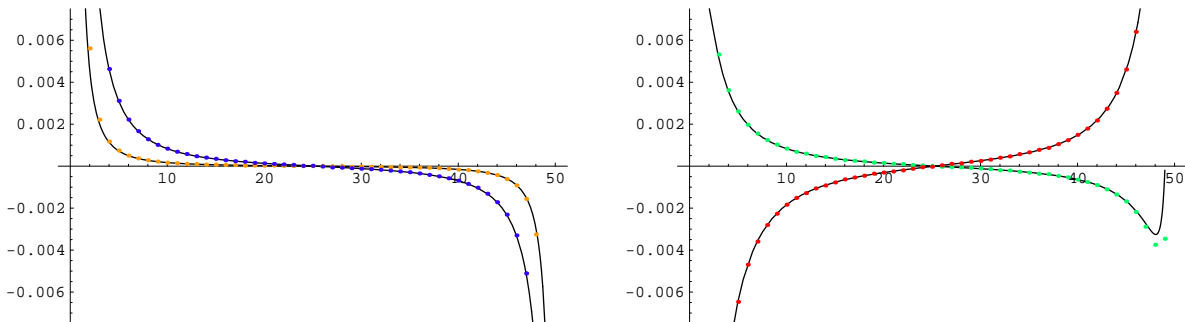


FIG. 16: Subtracted probabilities to find a height 1 (orange), 2 (in blue), 3 (green) or 4 (red) at a site lying along the short medial line of a rectangle $M \times N$, and going from an open boundary (left end of the graph) to a closed boundary (right end). The dots correspond to data obtained from numerical simulations, with $M = 200$ and $N = 50$, while the solid curves represent the conformal predictions (10.6), with $L = N + \frac{1}{2}$, for the limit $M = +\infty$.

curves are plotted here with the exact coefficients a_i, b_i , derived from the lattice calculations, rather than with fitted coefficients.

The agreement is very satisfactory for the four heights. In the previous section, we had shown that our proposal for the field identifications were fully compatible with the lattice results for homogeneous boundary conditions. Here we have an independent and direct confirmation.

XI. NATURE OF THE LOGARITHMIC FIELD ψ

The previous sections contain two major results: first, the computation of the 1-site probabilities for having a height 2, 3 or 4 on the UHP, and second, the identification of the scaling limit of the corresponding height variables with a logarithmic field ψ , belonging to a logarithmic conformal field theory with $c = -2$. There exists a well-known free field realization of a local logarithmic theory with $c = -2$, so that a natural question is whether our field ψ can be realized in this free field theory. Our answer to that question will be negative.

A. Comparison of correlations

The free field theory defined by the following action

$$S = \frac{1}{\pi} \int \partial\theta\bar{\partial}\tilde{\theta}, \quad (11.1)$$

where $\theta, \tilde{\theta}$ are anticommuting scalar fields, is a logarithmic conformal field theory, with central charge $c = -2$, and is a realization of the so-called triplet theory [24, 25, 26, 31, 32]. Zero (constant) modes, if any, play a special role, due to their grassmannian nature. Because the action does not depend on them, their integration “eats up” one pair of $\theta, \tilde{\theta}$ fields in the expectation values if there is such a pair, and yields identically zero if not. Apart from this peculiarity, correlators of local functionals of θ and $\tilde{\theta}$ can be computed in the usual way from Wick’s theorem.

Correlation functions are usually normalized by the partition function, with the result that $\langle \mathbb{I} \rangle = 1$. When the fields $\theta, \tilde{\theta}$ have zero modes, the partition function vanishes identically, so that this normalization is not possible. A convenient alternative choice is to set $\langle \omega(z, \bar{z}) \rangle = 1$, where $\omega = \alpha_0 : \theta \tilde{\theta} : + \beta_0$ is a dimension zero scalar field, which forms with the identity \mathbb{I} a rank two Jordan cell,

$$L_0 \omega = -\frac{\alpha_0}{2} \mathbb{I}. \quad (11.2)$$

On the other hand, when there are no zero modes, the usual normalization $\langle \mathbb{I} \rangle = 1$ can be chosen.

In [21], the bulk field ω and the boundary field ω_N describing the insertion of isolated dissipation at a bulk site and at a site of a closed boundary respectively, have expectation value equal to 1, $\langle \omega(z, \bar{z}) \rangle_{\text{plane}} = \langle \omega_N(x) \rangle_{\text{cl}} = 1$. They can be realized in terms of the free fermions as

$$\omega = \frac{1}{2\pi} : \theta \tilde{\theta} : + \frac{1}{2\pi} (\gamma + \frac{3}{2} \log 2) + 1, \quad \omega_N = \frac{1}{2\pi} : \theta \tilde{\theta} : + \frac{2}{\pi} \log 2. \quad (11.3)$$

Their transformations under dilations are $L_0 \omega = -\frac{1}{4\pi} \mathbb{I}$ and $L_0 \omega_N = -\frac{1}{\pi} \mathbb{I}$.

On the infinite plane, the fields $\theta, \tilde{\theta}$ have zero modes, ξ and $\tilde{\xi}$. The above normalization implies

$$\langle \mathbb{I} \rangle = 0, \quad \langle \theta(z, \bar{z}) \tilde{\theta}(w, \bar{w}) \rangle = \langle \xi \tilde{\xi} \rangle = 2\pi. \quad (11.4)$$

Higher correlators (and OPEs) are computed using the following elementary Wick contraction,

$$\underbrace{\theta(z, \bar{z}) \tilde{\theta}(w, \bar{w})}_{\text{Wick contraction}} = -\log |z - w|. \quad (11.5)$$

For instance, the 4-point function on the plane takes the form [26]

$$\langle \theta(z_1) \tilde{\theta}(z_2) \theta(z_3) \tilde{\theta}(z_4) \rangle = 2\pi [\log |z_1 - z_2| + \log |z_3 - z_4| - \log |z_1 - z_4| - \log |z_2 - z_3|]. \quad (11.6)$$

On the UHP with closed (Neumann) boundary condition on the real axis, namely $\partial\theta - \bar{\partial}\theta = \partial\tilde{\theta} - \bar{\partial}\tilde{\theta} = 0$ on \mathbb{R} , the fields also have zero modes. Thus the relations (11.4) still hold, while the Wick contraction appropriate to the closed boundary condition is

$$\underbrace{\theta(z, \bar{z}) \tilde{\theta}(w, \bar{w})}_{\text{Wick contraction}} = -\log |(z - w)(z - \bar{w})|. \quad (\text{closed on } \mathbb{R}) \quad (11.7)$$

If the open (Dirichlet) boundary condition is imposed, $\theta = \tilde{\theta} = 0$ on \mathbb{R} , the fields no longer have zero modes. In this case, one has $\langle \mathbb{I} \rangle_{\text{op}} = 1$ and the 2-point function $\langle \theta(z) \tilde{\theta}(w) \rangle_{\text{op}}$ is simply given by a Wick contraction, equal to

$$\underbrace{\theta(z, \bar{z}) \tilde{\theta}(w, \bar{w})}_{\text{Wick contraction}} = -\log \left| \frac{z-w}{z-\bar{w}} \right|. \quad (\text{open on } \mathbb{R}) \quad (11.8)$$

The same is true for the mixed boundary condition we have considered earlier, namely closed on \mathbb{R}_- and open on \mathbb{R}_+ . The fields do not have zero modes, and the relevant Wick contraction reads (the phases of \sqrt{z} , \sqrt{w} are between 0 and $\pi/2$)

$$\underbrace{\theta(z, \bar{z}) \tilde{\theta}(w, \bar{w})}_{\text{Wick contraction}} = -\log \left| \frac{(\sqrt{z}-\sqrt{w})(\sqrt{z}+\sqrt{\bar{w}})}{(\sqrt{z}+\sqrt{w})(\sqrt{z}-\sqrt{\bar{w}})} \right|. \quad (\text{closed on } \mathbb{R}_-, \text{ open on } \mathbb{R}_+) \quad (11.9)$$

Let us now come back to the 1-point functions on the UHP we have computed earlier for the height variables, to see what they are in the free fermionic theory.

The scaling field ϕ corresponding to the height 1 variable has been much studied. It is a primary field with conformal weights (1,1), realized in the free theory as [8]

$$\phi(z, \bar{z}) = -P_1 : \partial \theta \bar{\partial} \tilde{\theta} + \bar{\partial} \theta \partial \tilde{\theta} : = -P_1 \partial \bar{\partial} : \theta \tilde{\theta} : . \quad (11.10)$$

In order to compute the expectation value of ϕ on the UHP, one may use the OPE to make a point splitting,

$$: \theta \tilde{\theta} : = \lim_{w \rightarrow z} [\theta(z) \tilde{\theta}(w) + \log |z-w|], \quad (11.11)$$

and then evaluate Wick contractions.

For an open or a mixed boundary condition, the 1-point function of ϕ is equal to

$$\langle \phi(z, z^*) \rangle_{\text{op}} = \langle \phi(z, z^*) \rangle_{\text{cl|op}} = -P_1 \partial \bar{\partial} \lim_{w \rightarrow z} \underbrace{[\theta(z) \tilde{\theta}(w) + \log |z-w|]}_{\text{Wick contraction}}. \quad (11.12)$$

For the closed boundary condition, the boundary dissipation field $\omega_N(\infty)$ is to be inserted, but is eaten up by the path integration over the zero modes (the piece in ω_N proportional to the identity does not contribute since ϕ contains derivative fields only). Once the zero modes are integrated out, one simply compute Wick contractions for what remains, so that the previous formula is also valid for the closed boundary.

Using Eqs. (11.7)-(11.9), one easily obtains

$$\langle \omega_N(\infty) \phi(z, z^*) \rangle_{\text{cl}} = \frac{P_1}{(z-z^*)^2}, \quad \langle \phi(z, z^*) \rangle_{\text{op}} = -\frac{P_1}{(z-z^*)^2}, \quad (11.13)$$

$$\langle \phi(z, z^*) \rangle_{\text{cl|op}} = -\frac{P_1}{2} \frac{z+z^*}{|z|(z-z^*)^2}, \quad (11.14)$$

in agreement with our earlier results, Eqs. (9.54), (9.55) and (10.1) with $a_1 = P_1/4$ and $b_1 = 0$.

The scaling fields corresponding to the heights 2, 3 and 4 involve the logarithmic partner of the primary field ϕ . In the fermionic theory, the logarithmic partner of ϕ is proportional to

$$\psi_\theta(z, \bar{z}) = : \theta \tilde{\theta} (\partial \theta \bar{\partial} \tilde{\theta} + \bar{\partial} \theta \partial \tilde{\theta}) : + I \partial \bar{\partial} : \theta \tilde{\theta} : = : \theta \tilde{\theta} \partial \bar{\partial} \theta \tilde{\theta} : + I \partial \bar{\partial} : \theta \tilde{\theta} :, \quad (11.15)$$

and may contain an arbitrary multiple I of its primary partner. The expectation value of this term is given by the expressions we have just established.

The same point splitting procedure as for ϕ can be applied to ψ_θ , for instance,

$$\psi_\theta(z) = - \lim_{w \rightarrow z} [\theta \partial \theta(z) \tilde{\theta} \bar{\partial} \tilde{\theta}(w) + \theta \bar{\partial} \theta(z) \tilde{\theta} \partial \tilde{\theta}(w) - \text{singular terms}]. \quad (11.16)$$

The subtraction terms are such that the 1-point function $\langle \psi_\theta(z, z^*) \rangle$ is equal to the limit $w \rightarrow z$ of the point splitted fields $\langle \theta \partial \theta(z) \tilde{\theta} \bar{\partial} \tilde{\theta}(w) + \theta \bar{\partial} \theta(z) \tilde{\theta} \partial \tilde{\theta}(w) \rangle$, in which one removes the singular part in each Wick contraction.

Again for an open boundary or a mixed one, the 1-point function follows from Wick contracting the point-splitted fields, resulting in

$$\begin{aligned} \langle \psi_\theta(z, z^*) \rangle_{\text{op}} &= \langle \psi_\theta(z, z^*) \rangle_{\text{cl|op}} = \lim_{w \rightarrow z} \left\{ \left[\theta(z) \tilde{\theta}(w) + \log |z - w| \right] \partial \theta(z) \bar{\partial} \tilde{\theta}(w) \right. \\ &\quad \left. - \left[\theta(z) \bar{\partial} \tilde{\theta}(w) - \frac{1}{2(z^* - w^*)} \right] \left[\partial \theta(z) \tilde{\theta}(w) + \frac{1}{2(z - w)} \right] + \text{c.c.} \right\}. \end{aligned} \quad (11.17)$$

For the closed boundary, the insertion of $\omega_N(\infty) = \frac{1}{2\pi} : \theta \tilde{\theta} : + \frac{2}{\pi} \mathbb{I} \log 2$ brings two contributions. One comes from the identity piece, and reduces to the calculation we made above for the field ϕ . If we remember that the integration over the zero modes equals 2π , one obtains that this first contribution is

$$\frac{2}{\pi} \log 2 \langle \psi_\theta(z, z^*) \rangle_{\text{cl}} = - \frac{4 \log 2}{(z - z^*)^2}. \quad (11.18)$$

The second contribution from the $: \theta \tilde{\theta} :$ piece produces logarithmically divergent terms, because after the integration of the two zero modes, one θ (or $\tilde{\theta}$) in $\omega_N(\infty)$ may be contracted with a $\tilde{\theta}$ (or θ) in ψ_θ . On the other hand a regularized, finite answer is obtained if we decide to integrate the two zero modes contained in the $: \theta \tilde{\theta} :$ piece of $\omega_N(\infty)$, since this leaves us with contractions of $\theta, \tilde{\theta}$ within ψ_θ . This regularized expectation value is then given by the same formula as for the open or mixed boundary, Eq. (11.17), and yields, by using the appropriate Wick contraction,

$$\langle \frac{: \theta \tilde{\theta} :}{2\pi} \psi_\theta \rangle_{\text{cl,reg}} = \frac{1}{(z - z^*)^2} \left\{ \frac{1}{2} + \log |z - z^*| \right\}. \quad (11.19)$$

Computing the required Wick contractions for the open and mixed boundaries, and adding the contribution from the term $I \partial \bar{\partial} : \theta \tilde{\theta} :$, we obtain the 1-point function of ψ_θ on the UHP for the three boundary conditions,

$$\langle \psi_\theta(z, z^*) \rangle_{\text{op}} = \frac{1}{(z - z^*)^2} \left\{ I + \frac{1}{2} + \log |z - z^*| \right\}, \quad (11.20)$$

$$\langle \omega_N(\infty) \psi_\theta(z, z^*) \rangle_{\text{cl,reg}} = \frac{1}{(z - z^*)^2} \left\{ -I - 4 \log 2 + \frac{1}{2} + \log |z - z^*| \right\}, \quad (11.21)$$

$$\langle \psi_\theta(z, z^*) \rangle_{\text{cl|op}} = \frac{z + z^*}{|z|(z - z^*)^2} \left\{ \frac{I}{2} + \frac{1}{2} \log \left| \frac{4z(z - z^*)}{(\sqrt{z} + \sqrt{z^*})^2} \right| - \frac{(z - z^*)^2 - 4|z|^2}{8|z|(z + z^*)} \right\}. \quad (11.22)$$

We see that the first two expectation values of ψ_θ are not related as they are for the field ψ associated with the height variables $h \geq 2$. In particular, they do not show the characteristic change of sign of the logarithmic term. Moreover, the third one $\langle \psi_\theta(z, z^*) \rangle_{\text{cl|op}}$ does not have the form obtained in (10.1) for $\langle \psi(z, z^*) \rangle_{\text{cl|op}}$. This suggests that the fields ψ and ψ_θ are distinct fields, and that ψ has no realization in the free fermionic theory.

A further check of this statement is as follows. The two fields ψ and ψ_θ are different, but they have the same abstract conformal transformations. Namely, the OPEs with the stress-energy tensors (9.5) and (9.6) are formally the same for ψ and ψ_θ . Consequently, the correlation functions $\langle \mu(z_1) \mu(z_2) \psi(z, z^*) \rangle$ and $\langle \mu(z_1) \mu(z_2) \psi_\theta(z, z^*) \rangle$ satisfy the same differential equations, so that $\langle \mu(z_1) \mu(z_2) \psi_\theta(z, z^*) \rangle$ must be of the same general form (9.44), as derived in Section IX.A.

The general solution (9.44) involved three arbitrary parameters, A_1, G and I_1 . For the ψ corresponding to the heights 2, 3 and 4, we had required that the limit $-z_1, z_2 \rightarrow \infty$, in which the boundary becomes fully closed, does not produce the logarithmic singularity $\langle \psi(z, z^*) \rangle \log z_{12}$ coming from the identity channel in the OPE $\mu(z_1) \mu(z_2)$,

$$\lim_{-z_1, z_2 \rightarrow +\infty} z_{12}^{-1/4} \langle \mu^{\text{op,cl}}(z_1) \mu^{\text{cl,op}}(z_2) \psi(z, z^*) \rangle = \lim_{-z_1, z_2 \rightarrow +\infty} \left\{ \langle \omega_N(z_2) \psi(z, z^*) \rangle - \frac{\log z_{12}}{\pi} \langle \psi(z, z^*) \rangle \right\}. \quad (11.23)$$

This had implied $\langle \psi(z, z^*) \rangle = 0$, and the relation $A_1 = \lambda G$. This condition cannot be imposed for ψ_θ because the expectation value $\langle \psi_\theta(z, z^*) \rangle$ is not zero on the UHP.

Thus for ψ_θ , the limit in (11.23) does produce a logarithmic singularity, but this singularity is in any case discarded since, according to our prescription of inserting a field $\omega_N(\infty)$ for the closed boundary, we are only interested in the ω_N channel of the OPE, namely the first term in (11.23). As it turns out, the limit (11.23) also produces the divergent terms $\log |z_1 - z|$ and $\log |z_2 - z^*|$, which correspond to the divergencies discussed above in terms of the free fermions. The rest, which forms the regularized expectation value, should be a function of $z - z^*$, which, in order to conform

with the results for $\langle \omega_N(\infty) \psi_\theta(z, z^*) \rangle_{\text{cl}}$ and $\langle \psi_\theta(z, z^*) \rangle_{\text{op}}$ established above, ought to contain a term $\log |z - z^*|$ with the same sign as for the open boundary (corresponding to the limit $z_1, z_2 \rightarrow 0$). It is not difficult to see that this condition imposes the relation $A_1 = -2\lambda G$, reducing the general solution (9.44) to

$$\begin{aligned} \langle \mu(z_1) \mu(z_2) \psi_\theta(z_3, z_4) \rangle &= \frac{z_{12}^{1/4}}{z_{34}^2} \left\{ I_1 \frac{x-2}{\sqrt{1-x}} + \frac{A_1}{4} \frac{4-4x-3x^2}{1-x} - A_1 \frac{x-2}{\sqrt{1-x}} \log \left| \frac{(1+\sqrt{1-x})^2}{z_{34}\sqrt{1-x}} \right| \right. \\ &\quad \left. + A_1 \left(\frac{1}{z_{24}\sqrt{1-x}} - \frac{\sqrt{1-x}}{z_{23}} \right) z_{34} + \frac{A_1}{2} \left(\frac{x}{z_{23}} - \frac{x}{(x-1)z_{24}} + \frac{2z_{34}}{z_{13}z_{14}} \right) z_{34} - 2A_1 \right\}. \end{aligned} \quad (11.24)$$

The limit $z_1, z_2 \rightarrow 0$ yields, after the division by $z_{12}^{1/4}$, the expectation value of ψ_θ in front of an open boundary,

$$\langle \psi_\theta(z, z^*) \rangle_{\text{op}} = \frac{-1}{(z-z^*)^2} \left[2(I_1 - 2A_1 \log 2) + A_1 + A_1 \log |z - z^*|^2 \right]. \quad (11.25)$$

The limit $-z_1, z_2 \rightarrow +\infty$, after discarding the singular terms $\log \frac{z_{12}}{z_{13}z_{24}}$ and dividing by $z_{12}^{1/4}$, yields the regularized expectation value in front of a closed boundary,

$$\langle \psi_\theta(z, z^*) \rangle_{\text{cl,reg}} = \frac{-1}{(z-z^*)^2} \left[-2(I_1 - 2A_1 \log 2) - 8A_1 \log 2 + A_1 + A_1 \log |z - z^*|^2 \right]. \quad (11.26)$$

Both expressions coincide with the results (11.20) and (11.21) obtained in the fermionic free theory if we choose $A_1 = -\frac{1}{2}$ and $I = -2(I_1 - 2A_1 \log 2)$.

Moreover, the limit $z_1 \rightarrow -\infty$ and $z_2 \rightarrow 0$ yields the expectation value of ψ_θ in front of a half-closed half-open boundary,

$$\langle \psi_\theta(z, z^*) \rangle_{\text{cl|op}} = -\frac{z+z^*}{|z|(z-z^*)^2} \left\{ A_1 \log \left| \frac{4z(z-z^*)}{(\sqrt{z}+\sqrt{z^*})^2} \right| - A_1 \frac{(z-z^*)^2 - 4|z|^2}{4|z|(z+z^*)} + I_1 - 2A_1 \log 2 \right\}, \quad (11.27)$$

which, remarkably, exactly matches the form (11.22) obtained in the $\theta, \tilde{\theta}$ theory, for the same values of A_1 and I . Again we conclude that the logarithmic field ψ_θ in the fermionic theory and the field ψ describing the height variables $h > 1$ correspond to two distinct fields.

B. Representation theory

In the previous subsection, we have shown that the field ψ describing the heights $h \geq 2$ in the sandpile model has no realization in terms of free fermions. On the other hand, the fields ϕ and ω corresponding to the height 1 variable and to the insertion of dissipation in the bulk, do have such a realization. Likewise the fields ρ and $\bar{\rho}$ appearing in the conformal transformations of ψ can also be realized in the free fermionic theory. So all the fields we need except the ψ can be realized

in terms of $\theta, \tilde{\theta}$. This peculiar situation can be understood from a representation theory point of view. Indeed the conformal transformations typical of these fields allow for an infinite number of inequivalent representations [33]. We show here that the two fields ψ and ψ_θ in fact belong to inequivalent representations.

Let us first examine the situation in the free fermionic theory. For the sake of clarity, we attach a suffix θ to the fields constructed out from θ and $\tilde{\theta}$. So we take $\psi_\theta = \theta\tilde{\theta}(\partial\theta\bar{\partial}\tilde{\theta} + \bar{\partial}\theta\partial\tilde{\theta})$ and its primary partner $\phi_\theta = \partial\theta\bar{\partial}\tilde{\theta} + \bar{\partial}\theta\partial\tilde{\theta}$. The Wick contraction of θ and $\tilde{\theta}$, $\theta(z, \bar{z})\tilde{\theta}(w, \bar{w}) = -\log|z-w|$, implies the normalization of the stress-energy tensor, $T_\theta = 2\partial\theta\partial\tilde{\theta}$.

From the OPE of ψ_θ with T , we obtain

$$L_0\psi_\theta = \psi_\theta - \frac{1}{2}\phi_\theta, \quad L_1\psi_\theta = \rho_\theta, \quad (11.28)$$

with $\rho_\theta = \frac{1}{2}(\theta\bar{\partial}\tilde{\theta} - \tilde{\theta}\bar{\partial}\theta)$ a field of weight $(0, 1)$. There is a second field $\bar{\rho}_\theta = \frac{1}{2}(\theta\partial\tilde{\theta} - \tilde{\theta}\partial\theta) = \bar{L}_1\psi_\theta$ arising from the right conformal transformations of ψ_θ . All these fields belong to a reducible but indecomposable representation \mathcal{R} , which is however a representation of an extended algebra [25].

Clearly the two fields ρ_θ and ϕ_θ are not independent but satisfy

$$L_{-1}\rho_\theta = \frac{1}{2}\phi_\theta. \quad (11.29)$$

The keypoint of this section is to show that, although a relation between ρ_θ and ϕ_θ is to be expected in general, the value of the coefficient $\frac{1}{2}$ is particular to the triplet theory, of which the symplectic fermion theory is a realization.

In Section IX, we have computed the correlator $\langle\mu(z_1)\mu(z_2)\psi(z_3, z_4)\rangle$ where ψ is a field with the same conformal transformation as ψ_θ . The general form of this correlator has been obtained on the sole basis of the conformal transformations of the fields involved, namely (the first relation had been written $L_0\psi = \psi + \lambda\phi$ but λ was taken to be equal to $-\frac{1}{2}$ later on)

$$L_0\psi = \psi - \frac{1}{2}\phi, \quad L_1\psi = \rho, \quad \bar{L}_1\psi = \bar{\rho}, \quad (11.30)$$

$$L_0\rho = 0, \quad L_1\rho = 0, \quad \bar{L}_0\rho = \rho, \quad \bar{L}_1\rho = \kappa\mathbb{I}, \quad (11.31)$$

and similar relations for $\bar{\rho}$ (moreover L_{-1} and \bar{L}_{-1} act by differentiations). The important fact in these calculations is that we have not used the identification of $L_{-1}\rho$ with a multiple of ϕ .

The general solution for $\langle\mu(z_1)\mu(z_2)\psi(z_3, z_4)\rangle$ is given in (9.44). It depends on three arbitrary coefficients, A_1, G, I_1 . The derived three-point correlators $\langle\mu(z_1)\mu(z_2)\rho(z_3, z_4)\rangle$ and $\langle\mu(z_1)\mu(z_2)\phi(z_3, z_4)\rangle$ are given in (9.23) and (9.28) respectively, where we can use the values of

the coefficients as given in (9.35) and (9.43). One obtains

$$\langle \mu(z_1)\mu(z_2)\rho(z_3, z_4) \rangle = \frac{z_{12}^{5/4}}{z_{14}z_{24}} \left\{ A_1 \frac{\sqrt{1-x}}{x} + \frac{A_1}{2} + A_1 \frac{z_{24}}{z_{12}} \right\}, \quad (11.32)$$

$$\langle \mu(z_1)\mu(z_2)\phi(z_3, z_4) \rangle = G \frac{z_{12}^{1/4}}{z_{34}^2} \frac{x-2}{\sqrt{1-x}}. \quad (11.33)$$

To see whether $L_{-1}\rho$ can be consistently identified with ϕ , we simply compute the partial derivative ∂_3 of the first correlator to obtain

$$\partial_3 \langle \mu(z_1)\mu(z_2)\rho(z_3, z_4) \rangle = \frac{A_1}{2} \frac{z_{12}^{1/4}}{z_{34}^2} \frac{x-2}{\sqrt{1-x}}. \quad (11.34)$$

A simple comparison with (11.33) implies that the general solution allows the following identification

$$L_{-1}\rho = \beta\phi \quad \text{with} \quad \beta = \frac{A_1}{2G}. \quad (11.35)$$

In the interpretation of the height 2,3 and 4 variables of the sandpile model in terms of the ψ field, we have set $A_1 = \lambda G = -\frac{G}{2}$ in order to avoid a logarithmic singularity when the two μ fields are sent off to infinity (see (9.45)). This gives

$$\beta_{ASM} = -\frac{1}{4}. \quad (11.36)$$

In the previous subsection, where we made contact with the fermionic theory, we argued that the correct choice to reproduce the fermion correlators is $A_1 = -2\lambda G = G$. This then gives

$$\beta_\theta = \frac{1}{2}, \quad (11.37)$$

in agreement with the above relation (11.29) obtained from straight calculations.

Since the normalizations of ρ and ϕ are completely fixed by that of ψ , the parameter β cannot be scaled away, and this implies that different values of β label inequivalent conformal representations [33]. So there is a one-parameter family of inequivalent Virasoro representations from which a field ψ transforming as above can be chosen. The specific ψ that is relevant to the sandpile model belongs to the representation with $\beta = -\frac{1}{4}$, while the one realized in the free fermion theory corresponds to $\beta = \frac{1}{2}$. Because the coefficient G can be traded for β , the general solution of $\langle \mu(z_1)\mu(z_2)\psi_\beta(z_3, z_4) \rangle$ for a fixed given value of β , depends on two arbitrary coefficients A_1, I_1 , as expected (one for the norm of ψ , the other for the multiple of ϕ that can be freely added to it).

This explains why our general correlators involving $\rho, \bar{\rho}$ and ϕ (and ω) are separately consistent with what these fields would be in the fermionic theory. But when we bring in the ψ , it automatically adjusts the relative normalization of ρ and ϕ in a way that is not consistent with the fermionic picture, except if the parameter β is fine-tuned, and taken equal to $\frac{1}{2}$.

XII. BULK CORRELATIONS OF HEIGHT VARIABLES

In this last Section, we build on the knowledge we have of the scaling description to assess further properties of the lattice height variables in the sandpile model. We will focus on the 2-site correlations for height variables on the plane, and deduce their large distance limits. On the lattice, these correlations have never been computed, so that the formulas which follow can be considered as predictions, or conjectures.

If $P_{ij}(z_{12})$ denotes the joint probability that the height at z_1 be i and the height at z_2 be j , the 2-site correlations are given by $P_{ij}(z_{12}) - P_i P_j$ for $i, j = 1, 2, 3, 4$. In the scaling regime, when the distance z_{12} is large, these correlations should be equal to expectation values of pairs of fields $h_i(z_1, \bar{z}_1)h_j(z_2, \bar{z}_2)$. However the plane has no boundary where sand can leave the system, so that the prescription we used earlier requires to insert a bulk dissipation field $\omega(\infty)$ at infinity. Thus one should have, in the scaling limit, that

$$P_{ij}(z_{12}) - P_i P_j = \langle h_i(z_1, \bar{z}_1)h_j(z_2, \bar{z}_2)\omega(\infty) \rangle, \quad |z_{12}| \gg 1. \quad (12.1)$$

As the four height variables $h_i(z, \bar{z})$ are linear combinations of the fields ϕ and ψ , we clearly need to compute the (non-chiral) 3-point functions $\langle \psi\psi\omega \rangle$, $\langle \phi\psi\omega \rangle$ and $\langle \phi\phi\omega \rangle$. We concentrate on the first one, and let first the ω field be inserted at z_3 .

The general form of $\langle \psi(z_1, \bar{z}_1)\psi(z_2, \bar{z}_2)\omega(z_3, \bar{z}_3) \rangle$ can be computed from the Ward identities, but the nested procedure as we used it in Section IX, is rather cumbersome. Instead it is simpler to use the finite Möbius transformations directly, by seeing the insertion points z_1, z_2, z_3 as the images of a fixed triplet, say $w_1 = -1, w_2 = +1, w_3 = 0$.

The conformal transformation $w \rightarrow z$ of the plane onto itself which brings $(w_1, w_2, w_3) = (-1, +1, 0)$ onto three arbitrary points (z_1, z_2, z_3) is

$$w(z) = -\frac{z_{12}(z - z_3)}{z_{23}(z - z_1) + z_{13}(z - z_2)}, \quad (12.2)$$

under which the conformal transformations of ψ and ω read

$$\begin{aligned} \psi(z, \bar{z}) &= |w'(z)|^2 \left\{ \psi(w, \bar{w}) - \frac{1}{2} \log |w'(z)|^2 \phi(w, \bar{w}) \right. \\ &\quad \left. + \frac{w''(z)}{2w'^2(z)} \rho(w, \bar{w}) + \frac{\bar{w}''(\bar{z})}{2\bar{w}'^2(\bar{z})} \bar{\rho}(w, \bar{w}) + \kappa \left| \frac{w''(z)}{2w'^2(z)} \right|^2 \right\}, \end{aligned} \quad (12.3)$$

$$\omega(z, \bar{z}) = \omega(w, \bar{w}) - \frac{1}{4\pi} \log |w'(z)|^2. \quad (12.4)$$

It is straightforward to compute the various derivatives, and express $\psi(z_1, \bar{z}_1)$ as a linear combination of $\psi(-1, -1), \phi(-1, -1), \rho(-1, -1), \bar{\rho}(-1, -1)$ and the identity, and similarly

for $\psi(z_2, \bar{z}_2)$ and $\omega(z_3, \bar{z}_3)$. Inserting these expressions into the 3-point function yields $\langle \psi(z_1, \bar{z}_1)\psi(z_2, \bar{z}_2)\omega(z_3, \bar{z}_3) \rangle$ in terms of fifty constants, given by various correlators of fields inserted at $-1, +1, 0$. In the limit $z_3 \rightarrow \infty$ however, most of these fifty constants combine or drop out. Specifically, when $z_3 \rightarrow \infty$, the transformations of the fields read

$$\psi(z_1, \bar{z}_1) = \frac{4}{|z_{12}|^2} \left\{ \psi(-1) + \log \left| \frac{z_{12}}{2} \right| \left[\phi(-1) - \rho(-1) - \bar{\rho}(-1) - \kappa \right] \right\}, \quad (12.5)$$

$$\psi(z_2, \bar{z}_2) = \frac{4}{|z_{12}|^2} \left\{ \psi(1) + \log \left| \frac{z_{12}}{2} \right| \left[\phi(1) + \rho(1) + \bar{\rho}(1) + \kappa \right] \right\}, \quad (12.6)$$

$$\omega(z_3, \bar{z}_3) = \omega(0) - \frac{1}{2\pi} \log \left| \frac{z_{12}}{2z_{13}z_{23}} \right|. \quad (12.7)$$

Using these, one sees that the 3-point function retains a logarithmic singularity in the limit $z_3 \rightarrow \infty$, unless the following identities hold (among others)

$$\langle \psi(z_1, \bar{z}_1)\psi(z_2, \bar{z}_2) \rangle = \langle \phi(z_1, \bar{z}_1)\psi(z_2, \bar{z}_2) \rangle = \langle \phi(z_1, \bar{z}_1)\phi(z_2, \bar{z}_2) \rangle = 0. \quad (12.8)$$

The 3-point function then takes the form

$$\begin{aligned} \langle \psi(z_1, \bar{z}_1)\psi(z_2, \bar{z}_2)\omega(\infty) \rangle &= \frac{16}{|z_{12}|^4} \left\langle \left[\psi(-1) + \log \left| \frac{z_{12}}{2} \right| \left[\phi(-1) - \rho(-1) - \bar{\rho}(-1) - \kappa \right] \right] \right. \\ &\quad \left. \left[\psi(1) + \log \left| \frac{z_{12}}{2} \right| \left[\phi(1) + \rho(1) + \bar{\rho}(1) + \kappa \right] \right] \omega(0) \right\rangle \end{aligned} \quad (12.9)$$

$$\equiv \frac{1}{|z_{12}|^4} \left\{ C + 2B \log |z_{12}| + A \log^2 |z_{12}| \right\}, \quad (12.10)$$

where the coefficients A and B are given by

$$A = 16 \langle \phi(-1)\phi(1)\omega(0) \rangle, \quad (12.11)$$

$$B = 16 \langle \phi(-1)[\psi(1) - \phi(1) \log 2 + \rho(1) + \bar{\rho}(1)]\omega(0) \rangle. \quad (12.12)$$

The same procedure with one ψ replaced by a ϕ , or the two ψ 's replaced by ϕ 's, yields

$$\begin{aligned} \langle \phi(z_1, \bar{z}_1)\psi(z_2, \bar{z}_2)\omega(\infty) \rangle &= \frac{16}{|z_{12}|^4} \left\langle \phi(-1) \left[\psi(1) + \log \left| \frac{z_{12}}{2} \right| \left[\phi(1) + \rho(1) + \bar{\rho}(1) \right] \right] \omega(0) \right\rangle \\ &= \frac{1}{|z_{12}|^4} \left\{ B + A \log |z_{12}| \right\}, \end{aligned} \quad (12.13)$$

and

$$\langle \phi(z_1, \bar{z}_1)\phi(z_2, \bar{z}_2)\omega(\infty) \rangle = \frac{16}{|z_{12}|^4} \langle \phi(-1)\phi(1)\omega(0) \rangle = \frac{A}{|z_{12}|^4}. \quad (12.14)$$

From these results and the way the height variables are expressed in terms of ϕ and ψ , namely $h_i(z, \bar{z}) = \alpha_i \psi(z, \bar{z}) + \beta_i \phi(z, \bar{z})$, one easily obtains the scaling form of the 2-site correlations,

$$\begin{aligned} P_{ij}(z_{12}) - P_i P_j &= \frac{1}{|z_{12}|^4} \left\{ \alpha_i \alpha_j C + (\alpha_i \beta_j + \beta_i \alpha_j) B + \beta_i \beta_j A \right. \\ &\quad \left. + [2\alpha_i \alpha_j B + (\alpha_i \beta_j + \beta_i \alpha_j) A] \log |z_{12}| + \alpha_i \alpha_j A \log^2 |z_{12}| \right\}. \end{aligned} \quad (12.15)$$

The value of A is related, through (12.14), to the correlation of the two height 1 variables on the plane, whose dominant term was computed in [6],

$$P_{11}(r) = P_1^2 - \frac{P_1^2}{2r^4} + \dots \quad (12.16)$$

This fixes the constant $A = -P_1^2/2$. The other two constants B and C cannot be determined purely from conformal theoretic arguments, and require further input from lattice calculations.

The value of A alone however determines the dominant terms of all correlations, and yields

$$P_{1i}(r) - P_1P_i \simeq -\frac{\alpha_i P_1^2}{2r^4} \log r, \quad P_{ij}(r) - P_iP_j \simeq -\frac{\alpha_i \alpha_j P_1^2}{2r^4} \log^2 r, \quad i, j = 2, 3, 4, \quad (12.17)$$

where the values of α_i have been given in Section VIII, namely $\alpha_2 = 1$, $\alpha_3 = 2.12791$ and $\alpha_4 = -3.12791$. The heights are found to be anticorrelated except the height 4 variable, which has a positive correlation with the other three (but is anticorrelated with itself).

In order to check these behaviours and to assess the values of B and C , we have run further numerical simulations of the model. The main problem here is that the correlation term $\sim r^{-4}$ in the joint probabilities $P_{ij}(r)$ is largely subdominant with respect to the trivial constant piece P_iP_j . It means that we cannot test these scaling behaviours in the regime where they are supposed to hold ($r \gg 1$), since that would require a huge numerical precision on the data. We have nevertheless tested the scaling formulas for small and intermediate values of r ($r \leq 20$), and found very good agreement, in some cases for as small distances as $r = 2$. Also the fitted values of B, C are consistent for all fits.

We have run the simulations on a cylindrical lattice, of height $L = 50$ and perimeter $P = 200$. We have sampled a total of 3.5×10^9 recurrent configurations, and for each configuration, we have measured the heights on the six circles located at mid-height. On each circle, and for each value of r between 2 and 20, we have recorded all pairs of heights which are r sites apart, and subsequently computed the occurrence probabilities $P_{ij}(r)$. Thus r is a distance which was always directed along the perimeter of the cylinder.

Once the joint probabilities $P_{ij}(r)$ are obtained, we fit them (leaving out the data for $r = 2, 3$) to the form given by (12.15), that is, a constant contribution P_iP_j and terms $\log^k r/r^4$, for $k = 0, 1, 2$ depending on the values of i, j . Then, using the exact values of the coefficients α_i and β_i , the values of P_iP_j, A, B and C could be extracted (note that, as a further check, we did not use the known value of P_iP_j and A). As expected, better results are obtained for larger values of i, j . The results for P_{13}, P_{33}, P_{34} and P_{44} , as well as the fitted curves, are shown in Fig. 17.

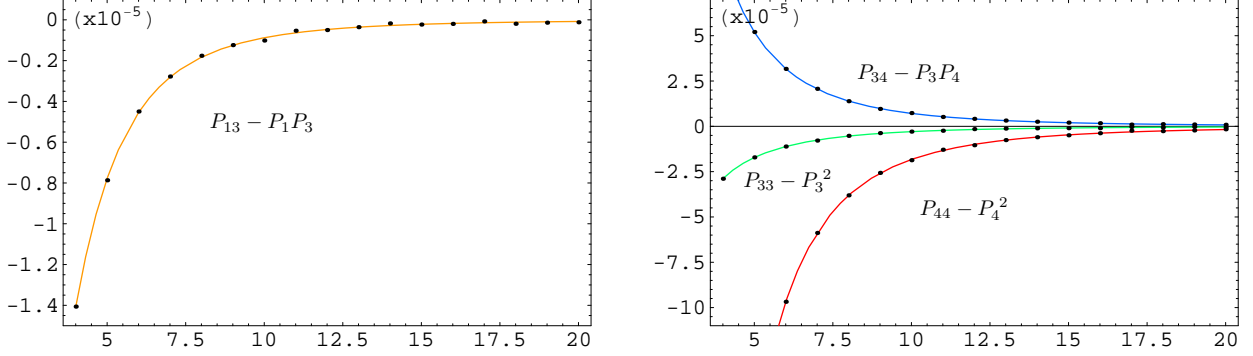


FIG. 17: Two-site correlations of height variables on a cylindrical lattice (height $L = 50$, perimeter $P = 200$), measured along the perimetrical circles located at mid-height. The abscissa represents the separation distance, in lattice sites. The dots correspond to data obtained from numerical simulations, and the solid curves represent the fitted functions, given in (12.15).

As a first qualitative check, we see that the signs of the correlations are as predicted, namely negative, except for the height 4 with a strictly smaller height (P_{34} here).

As mentioned above, the agreement is excellent, and is so, somewhat unexpectedly, down to very small values of r ($r = 4$ and even smaller). For $P_{13}(r)$, the fitted values of the subtraction term P_1P_3 and of A and B were found to be (no $\log^2 r$ term was included in this case)

$$P_1P_3 = 0.02261, \quad A = -0.002648, \quad B = -0.004861. \quad (12.18)$$

The first two are consistent with the exact values $P_1P_3|_{\text{exact}} = 0.02255$ and $A_{\text{exact}} = -0.002711$.

The fits of $P_{33}(r), P_{34}(r), P_{44}(r)$ yield the following values,

$$P_3P_3 = 0.09410, \quad A = -0.002821, \quad B = -0.004718, \quad C = -0.008883, \quad (12.19)$$

$$P_3P_4 = 0.1366, \quad A = -0.002517, \quad B = -0.004329, \quad C = -0.008773, \quad (12.20)$$

$$P_4P_4 = 0.1982, \quad A = -0.002699, \quad B = -0.004065, \quad C = -0.009608. \quad (12.21)$$

Again the values of the subtraction terms compare well with the exact values, $P_3^2|_{\text{exact}} = 0.09381$, $P_3P_4|_{\text{exact}} = 0.1367$, $P_4^2|_{\text{exact}} = 0.1991$, and the fitted values for A are also comparable to the exact value quoted above. The values of B and C obtained from these four (or three) independent fits are all close to each other, from which we infer that the exact values should be around

$$B \sim -0.0045, \quad C \sim -0.009. \quad (12.22)$$

As far as we can see, these values can only be confirmed by exact calculations of correlations on the lattice.

XIII. CONCLUSIONS

Let us first summarize our main results. As a preliminary but crucial step, we have carried out the calculation of the 1-point probabilities of the four height variables on the lattice upper-half plane. This was long and technical, but gave us an exact formula for their scaling term m^{-2} , where m is the distance to the boundary. As 1-point functions on the upper-half plane are 2-point correlators, this enabled us to obtain our second main result, namely, the field identification of the four bulk height variables in the scaling limit, in terms of conformal fields of a $c = -2$ logarithmic conformal theory. The picture that emerges is that the height 1 variable turns out to be a primary field, whereas the heights 2, 3 and 4 are all proportional to the logarithmic partner of this primary field (in a rank 2 Jordan cell).

This should constitute a major step towards the exact solution of the Abelian sandpile model, since, if the conformal picture we propose is confirmed, it basically solves the aspects of the model concerned with the height variables, which are the most natural microscopic variables. (Indeed the simpler problem of identifying the scaling fields corresponding to the boundary height variables on open and closed boundaries was solved in [12, 13].) It however does not solve the part of the model which is related to other non-local variables, like avalanche observables, whose exact solution remains a challenge.

Before getting there, we believe that a number of issues deserve further investigations, which lie in the context of the present article, and from which the sandpile model but also logarithmic conformal field theory in general could benefit.

One of them concerns the unexpected nature of the logarithmic field describing the heights 2, 3 and 4. We have argued that it has no realization in the free symplectic fermion field theory, widely considered as the canonical local realization of a $c = -2$ conformal theory. One certainly would like to know to what extent the sandpile realization and the symplectic fermion realization differ, and what the specific properties of the theory realized by the sandpile model are.

Acknowledgments

We would like to thank Matthias Gaberdiel for very useful and encouraging discussions. The hospitality of the ETH Zürich is also gratefully acknowledged. M.J. was supported by a Southern Illinois University Edwardsville Summer Research Fellowship. P.R. is financially supported by the

Belgian Fonds National de la Recherche Scientifique.

- [1] P. Bak, *How Nature Works*, Oxford University Press 1997.
- [2] H. J. Jensen, *Self-Organized Criticality*, Cambridge Lectures Notes in Physics 10, Cambridge University Press 1998.
- [3] D. Dhar, *Studying Self-Organized Criticality with Exactly Solved Models*, [cond-mat/9909009](#).
- [4] P. Bak, C. Tang, K. Wiesenfeld, Phys. Rev. Lett. 59, 381 (1987).
- [5] D. Dhar, Phys. Rev. Lett. 64, 1613 (1990); Phys. Rev. Lett. 64, 2837 (1990).
- [6] S. N. Majumdar and D. Dhar, J. Phys. A: Math. Gen. 24, L357 (1991).
- [7] J. G. Brankov, E. V. Ivashkevich, and V. B. Priezzhev, J. Phys. I France 3, 1729 (1993).
- [8] S. Mahieu, P. Ruelle, Phys. Rev. E 64, 066130 (2001).
- [9] M. Jeng, Phys. Rev. E 71, 016140 (2005).
- [10] V. B. Priezzhev, J. Stat. Phys. 74, 955 (1994).
- [11] E. V. Ivashkevich, J. Phys. A: Math. Gen. 27, 3643 (1994).
- [12] M. Jeng, Phys. Rev. E 71, 036153 (2005).
- [13] G. Piroux and P. Ruelle, J. Phys. A: Math. Gen. 38, 1451 (2005).
- [14] E. V. Ivashkevich, D. V. Ktitarov and V. B. Priezzhev, Physica A 209, 347 (1994).
- [15] D. Dhar and S. S. Manna, Phys. Rev. E 54, 2684 (1994).
- [16] E. V. Ivashkevich, D. V. Ktitarov and V. B. Priezzhev, J. Phys. A: Math. Gen. 27, L585 (1994).
- [17] V. B. Priezzhev, E. V. Ivashkevich and D. V. Ktitarov, Phys. Rev. Lett. 76, 2093 (1996).
- [18] D. V. Ktitarov and V. B. Priezzhev, Phys. Rev. E 58, 2883 (1998).
- [19] P. Ruelle, Phys. Lett. B 539, 172 (2002).
- [20] M. Jeng, Phys. Rev. E 69, 051302 (2004).
- [21] G. Piroux and P. Ruelle, J. Stat. Mech., P10005 (2004).
- [22] S. N. Majumdar and D. Dhar, Physica A 185, 129 (1992).
- [23] G. Piroux and P. Ruelle, Phys. Lett. B 607, 188 (2005).
- [24] V. Gurarie, Nucl. Phys. B 410, 535 (1993).
- [25] M. R. Gaberdiel and H. G. Kausch, Phys. Lett. B 386, 131 (1996); Nucl. Phys. B 538, 631 (1999).
- [26] H. G. Kausch, Nucl. Phys. B 583, 513 (2000).
- [27] F. Spitzer, *Principles of Random Walk*, 2nd ed. (Springer-Verlag, New York, 1976).
- [28] M. Flohr, Int. J. Mod. Phys. A 18, 4497 (2003).
- [29] M. R. Gaberdiel, Int. J. Mod. Phys. A 18, 4593 (2003).
- [30] J. L. Cardy, Nucl. Phys. B 324, 581 (1989).
- [31] V. Gurarie, M. Flohr and C. Nayak, Nucl. Phys. B 498, 513 (1997).
- [32] M. R. Gaberdiel and I. Runkel, *The logarithmic triplet theory with boundary*, [hep-th/0608184](#).

- [33] M. R. Gaberdiel and H. G. Kausch, Nucl.Phys. B 477, 293 (1996).